Zeitschrift: IABSE reports = Rapports AIPC = IVBH Berichte
Band: 54 (1987)

Rubrik: Session 4: Static loading (applications)

SESSION 4

August 27, 1987 (afternoon)

Static Loading (Applications)

Chargement statique (applications)

Statische Belastung (Anwendungen)

Chairman: A.R. Ingraffea, USA

Invited Lecturers: P.G. Bergan, A. Arnesen, Norway;
N.S. Ottosen, Sweden
Large-Scale Analysis of Gravity Platforms

D.R.J. Owen, N. Bicanic, UK;
A.Y. Thannon, Iraq
Ultimate Load Analysis of Eccentrically Stiffened Shell Structures

Leere Seite
Blank page
Page vide

Large-Scale Analysis of Gravity Platforms

Analyse des plates-formes de gravité

Berechnung von Betonplattformen grosser Abmessungen

A. ARNESEN
Principal Res. Eng.
A.S. Veritas Research
Hoevik, Norway

P.G. BERGAN
President
A.S. Veritas Research
Hoevik, Norway

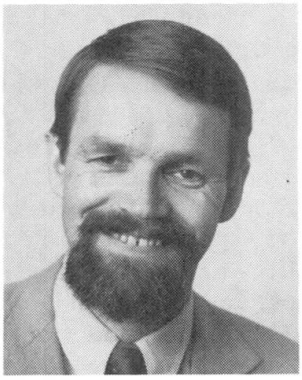

N.S. OTTOSEN
Assoc. Professor
Lund Inst. of
Techn.
Lund, Sweden

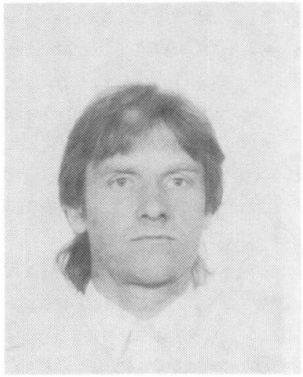

SUMMARY

The paper describes a coordinated effort to establish efficient and reliable methods and procedures for the analysis of large-scale gravity platforms placed in deep waters. Alternative concepts for concrete platforms and their characteristics are described. Constitutive models for inelastic behaviour of reinforced concrete are presented, and their applicability in connection with practical, large-scale analyses are discussed. Special emphasis is placed on realistic crack modelling of concrete. Finally, various computational aspects related to integrated, large-scale nonlinear static and dynamic finite element analyses are considered with particular reference to soil-structure interaction.

RÉSUMÉ

L'article décrit un effort coordonné pour établir des méthodes efficaces et sûres et des procédures pour l' analyse de grandes plates-formes de gravité, en eau profonde. D'autres concepts pour les plates-formes en béton et leurs caractéristiques sont décrits. Les modèles constitutifs du comportement inélastique du béton armé sont présentés et leurs applications, en relation avec des analyses pratiques et à large échelle, sont discutées. Une attention particulière est portée sur la modélisation réaliste des fissures du béton. L'article considère enfin différents aspects de calcul à l'ordinateur pour intégrer des études par éléments finis statiques et dynamiques tenant compte, en particulier, de l'interaction sol-structure.

ZUSAMMENFASSUNG

Der Beitrag beschreibt eine gemeinsame Anstrengung zur Erarbeitung von erfolgversprechenden und zuverlässigen Methoden und Berechnungsverfahren für grosse Schwergewichtsplattformen im tiefen Wasser. Alternative Konzepte für Betonplattformen und ihre charakteristischen Eigenschaften werden beschrieben. Materialgesetze für das unelastische Verhalten von Stahlbeton, ihre Anwendbarkeit auf Konstruktionen grosser Abmessungen und vor allem ein realistisches Rissmodell werden behandelt. Schliesslich werden verschiedene Berechnungsgesichtspunkte im Zusammenhang mit integrierten grossmassstäblichen nicht-linearen statischen und dynamischen Finite-Elemente-Analysen mit besonderer Berücksichtigung der Boden-Bauwerk-Interaktion behandelt.

1. INTRODUCTION

Up till now, about 20 concrete platforms for oil and gas production in the North Sea have been built or are under construction. The largest is the Gullfaks C platform, which is to be placed (1988) at 217 meters of water. However, concrete platforms for even deeper water are under planning, such as for the TROLL field, where the water depth is 300-350 meters. One of the proposed platforms for the Troll field, the T-300 platform, is 470 meters high, require 250.000 m^3 of concrete, 60.000 tons of reinforcement and has a foundation area of 26.200 m^2. Completed and fully equipped it represents a value of approximately 3.5-4.0 billion USD. Description of some of these platforms may be found in [1,2,3].

Most of the previous concrete platforms have been designed on the basis of linear finite element analyses (with up to one million degrees of freedom) combined with cross-sectional checks against cracking and failure [4,5,6]. However, these procedures become insufficient as new platforms are to be placed in hostile waters with up to 350 meters depth, and in locations with very poor soil conditions where settlements could be more than 5 meters. Such situations calls for sophisticated design methods involving inelastic material modelling, and nonlinear static and dynamic finite element analyses, [7,8,9]. Considering the complexity of linear analysis of such structures it is evident that nonlinear analysis becomes quite a challenge. However, it is clear that a full-fledged nonlinear analysis of these problems cannot be carried out even with the most powerful computers available. The approach to be adopted must therefore be one of using nonlinear modelling where required and to combine this with simpler models elsewhere. Theoretical refinements and sophistication in the material modelling has to be weighed against what can be provided in terms of material parameters in practice. Reliability of a model is more important than sophistication per se.

The present paper addresses some of these problems in general terms and focuses on application to large-scale concrete platforms in particular.

2. DEEP WATER GRAVITY PLATFORMS

The experience from nearly 15 years with concrete oil production platforms in the North Sea has led to great confidence in this type of structures. Gravity platforms are kept in place by their own weight without piling and are hence the basis for their name. Typically, they consist of a multi- cylindrical, large volume caisson part which rests on the sea floor. From this three or more shafts extend beyond the water surface and support a steel deck on which the production equipment is placed, see Fig. 1. The caisson may serve as reservoir for storing oil, and the shafts may be used for drilling purposes as well as for production equipment. The slim shafts minimize the impact of the wave loading while the caissons and the large foundation area provide high structural stability.

Concrete platforms have a number of favourable features for offshore oil and gas production, such as; large deck areas on which heavy payloads can be accommodated, concrete minimizes costly inspection and maintenance work and they are well suited to sustain exhausting environmental conditions. These features become increasingly important as oil and gas production goes into deeper water. For the Troll field, the functional requirements have resulted in a need for a large platform in terms of oil production capacity, with an operational topside weight of 60.000 tons [10]. The environmental conditions at this field are extremely hostile with an estimated 100 years wave of 30.5 meters and with very poor soil conditions, consisting of very soft normal consolidated clay. This has great implications on the foundation design of the structure. The challenge posed by the soil are illustrated in Fig. 2, where the shear strength profile of the Troll field is compared with some other fields in the North Sea [11].

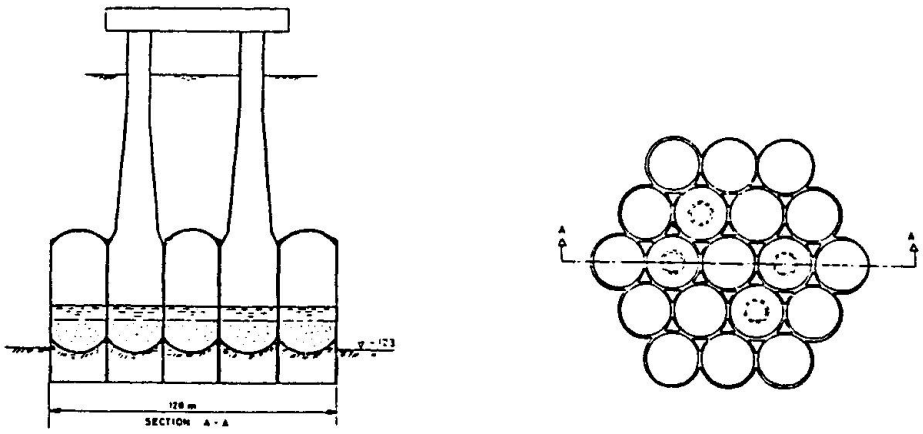

Fig. 1. Condeep concrete platform [3]

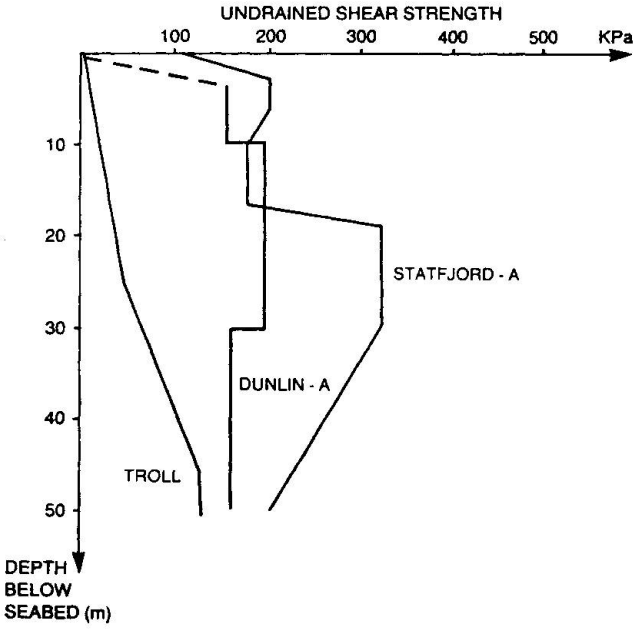

Fig. 2. Shear strength profiles of various fields in the North Sea [11]

The greatest uncertainties with respect to the soil problem lie in the determination of parameters in the response of the soil, to cyclic loading and in dynamic soil-structure interaction. The deep water and the soft supporting soil increase the dynamic effects of the wave loading. The loading effects are not only dependent upon the wave description and wave loading process alone, but also on the stiffness of the soil and damping of the structure-water-soil system. The fundamental period of deep water platforms may exceed the range of 4-6 seconds, approaching the typical period of high energy waves. This may in turn lead to significant dynamic amplification effects.

Soft soil conditions require special considerations in order to ensure sufficient safety against soil stability failure, to limit settlements and to assess the dynamic properties of the structure. Long skirts or piles underneath the platform penetrating into stiffer soil layers have been proposed for the Troll platform in order to give sufficient support for the structure. The long skirts, which may be of 20-30 meters length, are rather flexible; soil-structure interaction effects certainly have to be considered for the overall stiffness as well as for the dynamic response [13]. Nonlinear simulations are necessary in

order to verify various safety aspects of the soil-structure systems such as risk of failure, large inelastic deformation and progressive collapse. The design considerations involve extreme loading conditions due to wave loading, earthquake loading and accidental loads, combined with permanent loads and hydrostatic pressure loading of the submerged structure.

A variety of concrete platforms have been proposed for deep water; some of them are shown in Fig. 3. The Condeep SP and the Målfrid concepts shown in Figs. 3a and 3b, represent deep water versions of the commonly used Condeep concept, see Fig. 1. The T-300 and the Astrid platforms shown in Figs. 3c and 3d, are mono-shaft concepts especially designed for deep water installations. All of the concepts shown in Fig. 3 are equipped with long skirts underneath the platforms.

3. MODELLING OF REINFORCED CONCRETE

The complicated loading states and histories on deep water platforms, which include nonproportional loads, large hydrostatic pressure, as well as loading/unloading/reloading phenomena, place severe requirements on the constitutive models used. This implies that rather complicated constitutive models have to be resorted to in order to describe the inelastic behaviour and the extreme strength.

3.1 Failure criteria

The general constitutive models for concrete are normally based on the state of failure for concrete, i.e. the peak strength for a homogenously loaded concrete specimen. Two alternative failure criteria expressed in terms of all three stress invariants are adopted in the present study; they are the Ottosen model [14] and the Willam-Warnke model [15]. A CEB report [16] as well as a state-of-the-art report by ASCE [17] support the choice of these models.

The failure criteria provide no indication of the type of failure, i.e. whether the failure is of the crushing (shearing) type or of the cracking type. Thus, an additional failure mode criterion has to be provided. It is assumed [18] that cracking occurs if the stress state violates the failure criterion in addition to that the maximum principal stress exceeds half the uniaxial tensile strength of the concrete. The crack plane is assumed to be normal to the direction of the maximum principal stress.

3.2 Tensile cracking

Accurate analysis of failure of concrete structures normally depends greatly on the modelling of the tension cracking process. Due to the discrete, localized nature of cracks, correct crack modelling is a difficult topic because it implies that discontinuities in the displacement field should be accounted for [19]. However, the extreme complexity of deep water platforms does not lend itself to discrecte crack modelling, in fact, a total model would have to include millions of freedoms in order to account for discrete cracking in a satisfactory way. Instead, the smeared crack technique, originally proposed by Rashid [20], is adopted here.

In its original form, the smeared crack approach assumes the slope of the softening branch to be a material property. Special studies have demonstrated that this leads to the well known lack of objectivity [21]. Moreover, this original approach cannot model the structural size effect, which can easily be demonstrated experimentally for structures loaded primarily in tension [21,22].

In view of this, it is worth while focusing on the major improvements in crack modelling provided by the fictitious crack model [23] and the crack band model [24]. While the fictitious crack model is a two-parameter model (tensile strength, fracture energy), the crack band model is a three-parameter model (tensile strength, fracture energy, size of process zone). These models are able

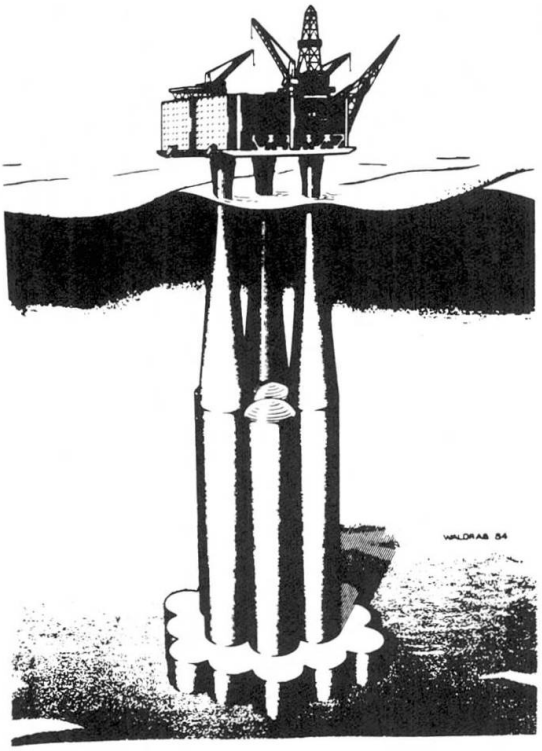

FIG. 3a CONDEEP SP3 [1]

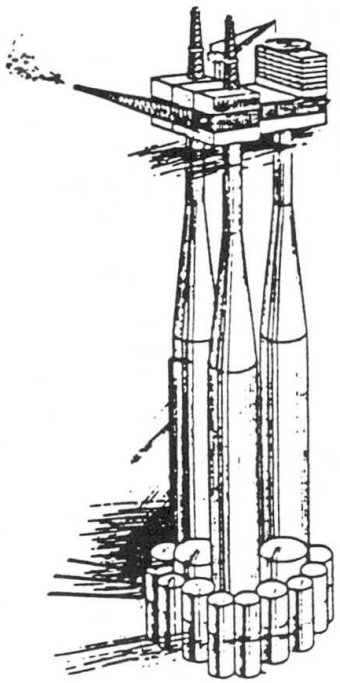

FIG. 3b MÅLFRID [2]

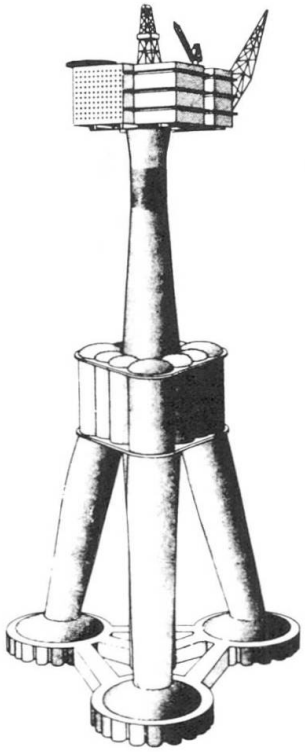

FIG. 3c T-300 [1]

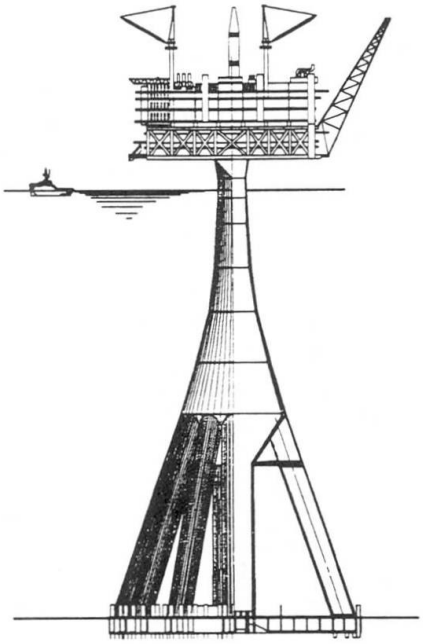

FIG. 3d ASTRID [12]

FIG. 3 Deep water concrete platforms

to describe all the essential phenomena related to crack modelling, but the use of these models in large-scale computer analyses raises some questions. In particular the crack band theory is directly applicable to a smeared cracking approach, and its use has been extensively verified for one particular type of element [24]. However, similar verifications for other element types are not yet available, in particular for cases in which the direction of cracking is not parallel to an element side. The fictitious crack model is in its original form a discrete approach, and, thus, it cannot be used for large-scale finite element te calculations. A smeared version of the fictitious crack model was proposed in [25] for uniaxial elements and in [26,27,28] for general elements. In references [26,27,28], even the shear behaviour of smeared cracked elements was accounted for in a way similar to the fictitious crack model.

The present cracking procedure is based on the concept proposed in [26,27,28], in which the dissipated fracture energy, as well as the shear mechanism, is objective with respect to element mesh size and form.

The crack opening w^n normal to the plane of crack is assumed to be given by

$$w^n = (\sigma_t - \sigma)/N \quad \text{where} \quad w^n \geq 0 \tag{1}$$

where σ_t is the uniaxial tensile strength, σ is the stress normal to the plane of crack and N is a material parameter. It can be shown that [26]

$$N = -E/\lambda \quad \text{where} \quad \lambda = 2G_cE/\sigma_t^2 \tag{2}$$

where the material parameter λ is a characteristic length of the material and G_c is the fracture energy.

For a shear displacement, w^s, parallel to the plane of crack, the following simple relation is assumed

$$w^s = w^n\tau/G_s \tag{3}$$

where τ is the shear stress in the crack and G_s is the slip modulus which may be determined from experiments. A comparison between the simple form (3) and experimental data for G_s = 3.8 MPa shows very close agreement, see [27,28].

A key point to this crack formulation is the introduction of the socalled equivalent length, L_{eq}, which is a purely geometrical quantity dependent on the element mesh size and shape as well as the orientation of the crack. As an example, the definition of the equivalent length L_{eq} is illustrated in Fig. 4 for the constant strain triangle and the isoparametric 8-node membrane element with 2x2 Gauss point integration. It appears that L_{eq} is simply the maximum length internal of the element in the direction normal to the crack. In the case of isoparametric element the equivalent crack length is based on the subdomain belonging to the integration point considered, see Fig. 4.

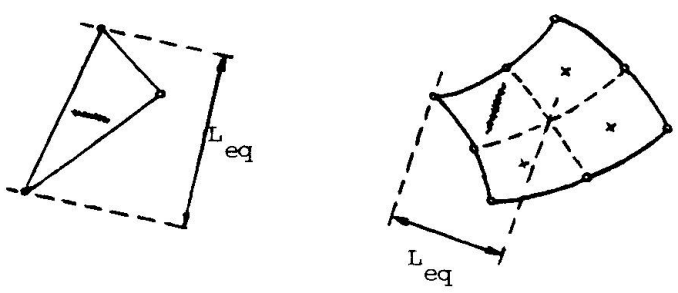

Fig. 4 Definition of equivalent length L_{eq}

For plane stress conditions the observations above lead to the following constitutive relation [26,27,28], where the x-axis is normal to the plane of the crack

$$\begin{bmatrix} \sigma_x \\ \sigma_y \\ \tau_{xy} \end{bmatrix} = \frac{E}{\alpha} \begin{bmatrix} 1 & \nu & 0 \\ \nu & 1-\frac{\lambda}{L_{eq}} & 0 \\ 0 & 0 & \alpha \frac{G_{eff}}{E} \end{bmatrix} \begin{bmatrix} \varepsilon_x \\ \varepsilon_y \\ \gamma_{xy} \end{bmatrix} - \frac{\frac{\lambda}{L_{eq}} \sigma_t}{\alpha} \begin{bmatrix} 1 \\ \nu \\ 0 \end{bmatrix} \tag{4}$$

where

$$\alpha = 1-\nu^2 - \frac{\lambda}{L_{eq}} \qquad \text{where} \qquad \lambda \geq L_{eq} \tag{5}$$

and the effective shear modulus, G_{eff} is given by

$$G_{eff} = \frac{G}{1 + \frac{G}{G_s} \frac{w^n}{L_{eq}}} \tag{6}$$

Note that G_{eff} is dependent on the crack opening, w^n, as well as on the equivalent length L_{eq} in such a way that G_{eff} decreases with increasing crack opening. It is seen that G_{eff} depends on the equivalent length in such a manner that the shear displacement of a cracked structure is independent on the size of the cracked element. This feature is of utmost importance and it has not been considered in previous crack models.

As an illustration of the application of this concept [27,28] consider the concrete specimen in Fig. 5 loaded by an increased elongation to complete separation. The following material parameters are assumed: $E = 2{,}1 \cdot 10^4$ MPa, $\nu = 0.2$, $\sigma_t = 3.3$ MPa, $G_s = 3.8$ MPa and $G_c = 130$ N/m

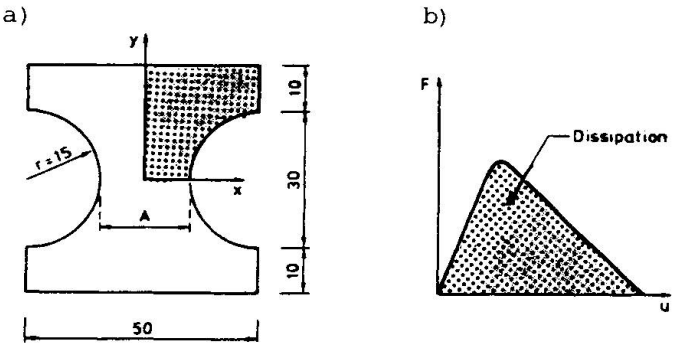

Fig. 5 Concrete tension specimen, A = cross sectional area

Due to symmetry, only one quarter of the tension specimen is considered. The purpose of the calculations is to verify that the adopted smeared crack approach is objective in the sence that the total cracking energy dissipated approaches the correct value. By definition, the total dissipated energy is AG_c, where G_c is the prescribed fracture energy per unit area $G_c = 130$ N/m and A is the cross sectional area of the specimen, see Fig. 5a. An outline of the total force – total elongation diagram is shown in Fig. 5b.

The specimen was analyzed using isoparametric 8-node elements with 2x2 Gauss integration points. The finite element meshes and the corresponding calculated force-elongation diagrams are shown in Fig. 6 and 7, respectively.

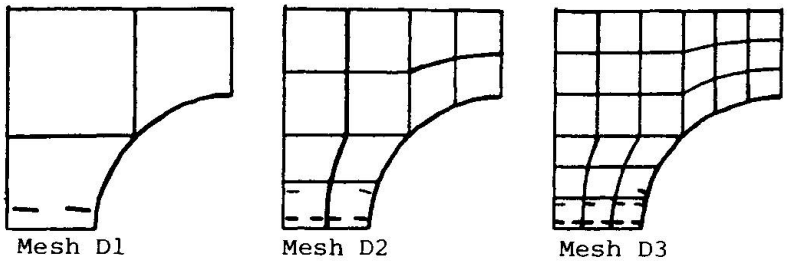

Fig. 6 Finite element meshes and crack patterns

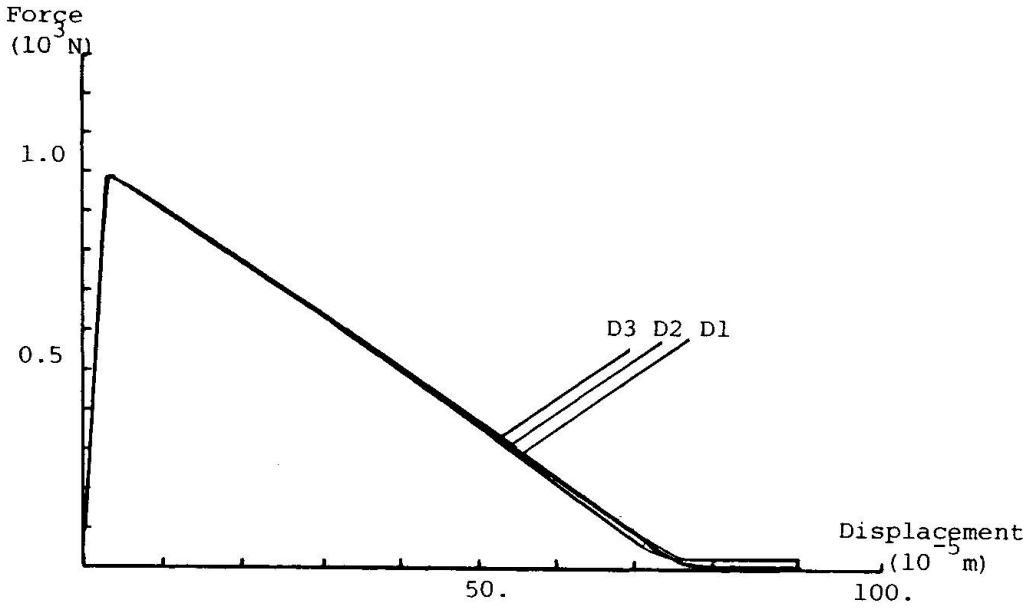

Fig. 7 Calculated force-displacement curves for meshes shown in Fig. 6

It appears from Fig. 7 that the result is almost independent of the element mesh size and; for the most detailed mesh, the calculated fracture energy is $G_{c,calc}$ = 129.1 N/m as compared with the exact (input) value, G_c = 130 N/m.

A more demanding situation is shown in Fig. 8 where the same type of element is tested for rather distorted meshes.

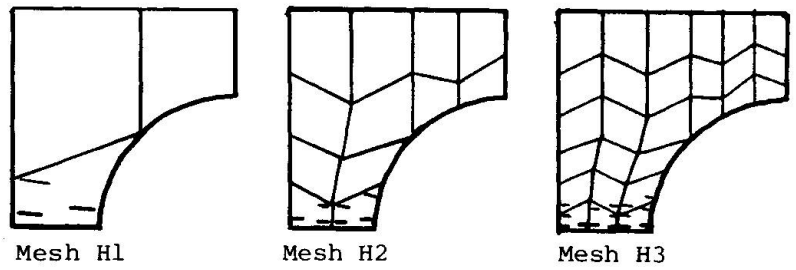

Fig. 8 Distorted finite element meshes and crack patterns

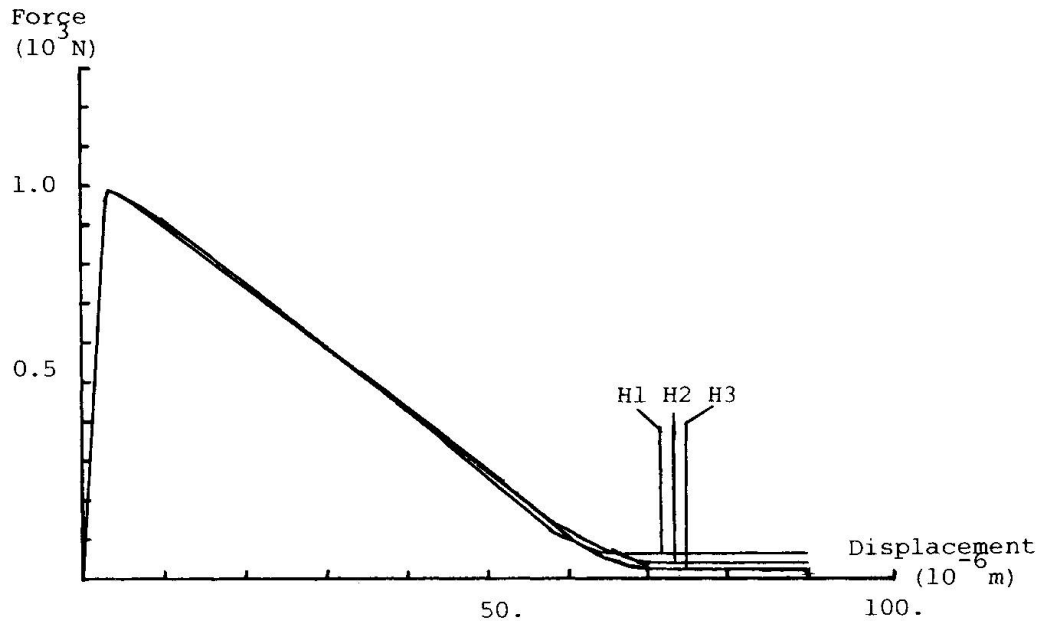

Fig. 9 Calculated force-displacement curves for meshes shown in Fig. 8

Fig. 9 shows the results to be almost independent of the element mesh size. For the most detailed mesh, the calculated fracture energy is $G_{c,calc}$ = 114.2 N/m compared with the exact (input) value, G_c = 130 N/m. It is seen, however, that the force-displacement curves do not converge exactly to the zero value as they should. This is because of the distorted element meshes cannot reproduce the true crack pattern quite correctly, and hence shear stresses along the cracks contribute to a small load bearing capacity which is observed in Fig. 9.

3.3 Stress-strain models

The general three-dimensioned stress-strain behaviour of concrete is very complex, and it is characterized by effects like strain-hardening, strain-softening, dilatation, coupling effects between hydrostatic loading and deviatoric response and vice versa, elastic-plastic coupling and different behaviour in loading and unloading. It may therefore not be surprising that a general consensus does not exist as to the proper choice of stress-strain models applicable for general load paths. A wide range of constitutive models for concrete has been suggested in the literature, such as nonlinear elastic models, endochronic models, plastic-fracturing models and plasticity models.

Plasticity models are especially powerful, because realistic loading/unloading/reloading criteria may be formulated and the incremental stress-strain law may be derived directly. Moreover, the introduction of a yield surface makes plasticity models conceptually simple, as it becomes possible, a priori, to evaluate the qualitative behaviour of the models. The failure surface, which can be demonstrated experimentally, may be introduced explicitly in the model and utilized as yield surface.

The nonassociated plasticity model proposed by Han & Chen [29] is of particular interest. The yield surface is a closed surface in the stress space and, through a mixed kinematic-isotropic hardening formulation, the yield surface changes so that it becomes identical to the failure surface at peak-stresses. The yield potential surface is of the Drucker-Prager type. The model has been extensively verified by comparing its predictions with a wide range of stress histories including tensile loading as well as uniaxial, biaxial and triaxial compressive loadings. Also softening effects are accounted for. A main drawback of a nonassociated formulation is that the tangential stiffness matrix becomes non-symmetric.

3.4 Creep and shrinkage

Creep of concrete depends not only on the stress history, but also on the ageing of the concrete as well as on the histories of temperature and humidity. Hence, the determination of the time-dependent behaviour of concrete is a formidable task that calls for simplifications. Such simplications should be in order for analysis of offshore structures as large creep strains are not expected due to the moderate temperatures and because the concrete is always rather old when exposed to the main loads. Moreover, as the mechanical loading mainly is caused by gravity and hydrostatic pressure, the stress changes over time are moderate.

The proportional relationship between creep strains and stresses is experimentally well established, as long as the sustained stress is below half the short-term strength for uniaxial compressive conditions. Moreover, Poisson's ratio under creep can be assumed to be equal to Poisson's ratio during short-term loading. These observations suggest that the socalled effective E-modulus method is sufficiently accurate for simulation of creep.

Shrinkage of concrete offshore platforms can normally be ignored for two reasons. First, these structures are composed of very massive and thick-walled concrete sections and, second, they are exposed to stable, humid conditions.

3.5 Reinforcement

The reinforcement has a completely different behaviour from concrete, and a separate treatment of the two materials and their interaction is necessary. A perfect bond between concrete and steel is assumed in this study, and for the representation of the reinforcement the socalled smeared concept [30] and embedded concept [31] are considered.

The smeared concept assumes that the reinforcement are uniformly distributed over the concrete element and the stiffness of the reinforcement is superimposed in a straightforward manner. The method is simple and it only requires a small amount of input data. Hence it is well suited for global analyses of concrete platforms when the overall behaviour of the structure is of main interest and no detailed information of stress distribution is required.

The smeared concept is not suited for dealing with inhomogenous reinforcement arrangement and arbitrary location of the bars within the concrete elements. The embedded concept, however, in which the reinforcement can be located arbitrarily within the concrete elements, has not such disadvantages. In localized analyses of sectional parts of the structure in which detailed information of the stress distribution, crack pattern, slip and bond failure is of primar interest, the embedded concept is superior to the smeared concept. The embedded concept implies, however, that the stiffness of each bar has to be determined in a straightforward, but rather cumbersome way. To avoid this problem, noting that a finite element model may include thousands of bars, an automatic search routine is under consideration. Knowing the end points of each bar or each layer of bars, the stiffness contribution may automatically be calculated using a geometrical search routine that determines the intersection between the bars and the concrete elements.

Only the axial stiffness of the bars need be considered and the stress-strain behaviour is modelled by a mixed kinematic-isotropic hardening rule. In this way reversed loadings due to dynamic excitation can be accounted for.

4. INTEGRATED SOIL-STRUCTURE ANALYSIS

The usual type of linear analysis of concrete offshore platforms involves two major idealizations with respect to soil-structure interaction: 1) the foundation of the structure is assumed to be rigid and 2) the skirts and the soil in between are assumed to be rigid. For deep water platforms equipped with flexible

skirts penetrating into very soft soil, however, it is necessary to account for the flexibility of the foundation, the skirts and the soil in between, for the evaluation of the dynamic response of the structure [32].

4.1 Dynamic soil-structure interaction analysis

Two main classes of methods are used for dynamic soil-structure interaction analysis: 1) frequency domain analysis and 2) time domain analysis [33]. The most common approach is frequency domain analyses which allows for the possibility of dividing the problem into substructures and introducing frequency dependent energy radiation at the boundaries. However, in order to account for nonlinear effects the solution has to be carried out in the time domain. Time domain soil-structure interaction methods may be categorized in three groups [34]; complete methods, boundary methods and volume methods.

The complete method assumes no superposition or substructuring and the problem is solved as a full-fledged nonlinear analysis. For soil-structure systems exhibiting extensive nonlinear behaviour this approach is necessary, however, costs and computer storage requirements related to such analyses normally limit the size of the problem that may be solved.

For earthquake analysis, the normal procedure is to divide the problem into a free field- or scattering problem and an interaction problem [33]. It is assumed that the total displacements of the soil consists of a free field contribution and an interaction contribution. In the free field analysis the excavated part of the soil may either be included (volume method) or excluded (boundary method). For nonlinear earthquake problems the boundary method is most suitable and is adopted here. The interaction contribution may account for nonlinearities in the structure and in the near field soil. This implies, however, that the excavation includes such a large part of the near field soil that the behaviour along the boundary of the excavation is predominately linear.

4.2 Modelling techniques

A full three dimensional model with solid finite elements is generally required to obtain satisfactory description of the nonlinear soil- structure problem. However, the nonlinearities in the soil will normally be confined to regions close to the structure and nonlinear material behaviour in the structure itself will normally be limited to critical sections in highly stressed areas. A significant reduction of the problem size may be obtained by limiting the nonlinear modelling to regions where substantial nonlinearities take place and by applying linear modelling elsewhere. Some techniques that may be utilized are:

1) Near field – far field modelling of the soil [34], see Fig. 10a. The near field, comprising regions of nonlinear behaviour, is modelled with solid elements. At a distance from the structure where the soil behaviour is linear and tends to behave like an axisymmetric system with nonaxisymmetric loads, the far field can be modelled by means of harmonic expansions of axisymmetric finite elements. At the interface, the displacements of the solid elements are expanded in Fourier series in order to match the corresponding displacement field of the axisymmetric elements.

2) Dynamic substructuring, see Fig. 10b. Dynamic substructuring implies that the total system is partitioned into linear and nonlinear regions and thereafter the number of degrees of freedom are reduced. Applying conventional implicit time integration schemes, the dynamic equilibrium equation can be replaced by an equivalent quasi-static incremental equilibrium expression [35] leading to an effective stiffness matrix and an effective load vector. A linear system, in which the effective stiffness matrix will be constant, lends itself to use of static condensation techniques, while a full nonlinear analysis implies that all terms have to be updated during the calculation.

3) Ritz-functions. Reduction of the number of freedoms may also be obtained by applying the concepts of component mode synthesis [33]. The displacements in the linear region are assumed to be constructed for a set of Ritz-vectors. This is done by considering the linear region fixed at the boundaries while the motion in the interior is described by a selected set of Ritz-vectors. This is combined with the overall solution for the nonlinear regions. A crucial point is the selection of Ritz vectors. To obtain reliable results these should be determined with due consideration of the inertia forces associated with the internal degrees of freedom. An alternative procedure is to use some of the lowest eigenvectors, however, this requires a significantly higher computational effort. Lanczos vectors may also be used.

4) Combination of solid elements and beam elements. Linear and moderate nonlinear regions of the structure may be represented by beam elements while regions with extensive nonlinearities (cracking, cruching and yielding of the concrete and reinforcement) are represented by nonlinear solid elements. This may be a viable approach when detailed knowledge of stress distribution in the beam element regions is not required. The global loads and the corresponding deformation state of the structure will in this way be accounted for in the solid element solution of the localized nonlinear regions.

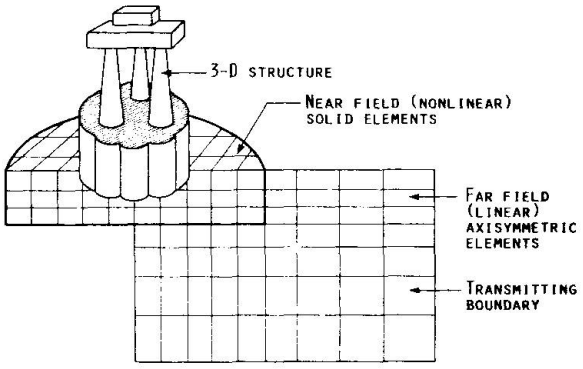

FIG. 10a. Far field-near field modelling

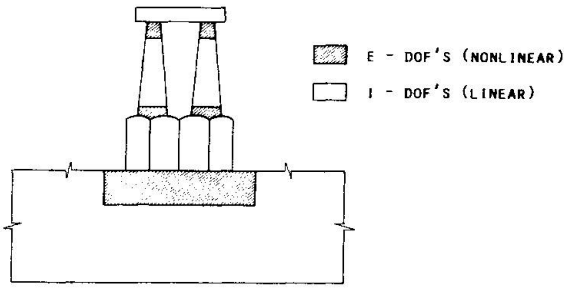

FIG. 10b. Substructuring into linear and nonlinear regions

5. CONCLUSIONS

Design of concrete gravity platforms placed in deep hostile water and in location with very poor soil conditions, calls upon reliable methods and procedures accounting for nonlinearities in the soil, the structure and the soil-structure interaction system. Constitutive models for inelastic behaviour of reinforced concrete have been discussed in connection to their applicability to large-scale nonlinear analysis of deep water gravity platforms. Particular emphasis has been given to a realistic modelling of crack development in concrete. Various computational aspects related to soil-structure interaction have been discussed.

ACKNOWLEDGEMENT

The authors would like to thank Mr. O. Dahlblom, graduate student of Lund Institute of Technology, for carrying out the numerical testing of present concrete cracking model. Our thanks are also extended to other members of the project team of "Integrated Analysis of Gravity Platforms", in particular Dr. G. Svanø and Professor T.H. Søreide, for valuable discussions regarding large-scale finite element analysis of concrete offshore platforms.

REFERENCES

1. ERIKSEN K., JAKOBSEN B., MOKSNES J. and SCHETLEIN I.O., The Evolution of the Concrete Structure, Offshore Northern Seas (ONS), Advanced Projects Conference, Stavanger, Norway, 19-21 November 1985.

2. STOKKE K., New Generation Deep Water Structures, Offshore Northern Seas (ONS), Advanced Projects Conference, Stavanger, Norway, 19-21 November 1985

3. EIDE O., Geoteknikk i Nordsjøen ('Geotechnique in the North Sea', in Norwegian), NIF-kurs: Plattformer til havs - samvirke mellom jord og konstruksjon, Trondheim, Norway, 6-8 January 1986.

4. FJUKMOEN Y., Finite Element Analysis of the Condeep Platform A, Block 34/10, Global Analysis, Computas Report 82-6017, 1982, Høvik, Norway.

5. KJEKEN J., NEKSTAD O.J., Gullfaks C, Condeep Type Gravity Platform, Global Analysis, Final Report, Vo. I and II, VERITEC Rep. No. 86-3144, 1986, Høvik, Norway.

6. Målfrid Deepwater Concrete Platform, Veritec Marine Technology Journal, June 1985.

7. BERGAN P.G., NYGÅRD M.K., SANDSMARK N., Technical Needs in Computational Mechanices for the Offshore Oil Industry, Proceedings, Symposium on Future Directions of Computational Mechanics", ASME, Winter Annual Meeting, December 10-11, 1986, Anaheim, California.

8. ARNESEN A., BERGAN P.G and SØRENSEN S.I, Nonlinear Analysis of Reinforced Concrete Structures, Computers and Structures, Vol. 12, pp. 571-579, 1980.

9. BERGAN P.G, FISKVATN A. and SØRENSEN S.I, Nonlinear Analysis and Design of Offshore Structures, ACI-ASCE Symposium on Nonlinear Design of Concrete Structures, Waterloo, Canada, Aug. 1979. Published in Study No. 14, edited by M.Z. Cohn, Solid Mechanics Division, University of Waterloo Press, Waterloo, Ontario, Canada, 1980.

10. FAY C.E, Platform Alternatives for the Troll Field, Proc. of 4th Int. BOSS Conf., Delft, The Netherlands, 1985.

11. LEIJTEN S., Factors Affecting Choice of Design of Foundations of Fixed Platform Concepts for Troll, NIF-kurs: Plattformer til havs - samvirke mellom jord og konstruksjon, Trondheim, Norway, 6-8 January 1986.

12. VAN DER POT B.J.G, The Evolution of the Concrete Structure, Offshore Northern Seas (ONS), Advanced Projects Conference, Stavanger, Norway, 19-21 November 1985.

13. SØREIDE T.H., AMDAHL J. and ARNESEN A., Nonlinear Integrated Soil/Structure Analysis of Gravity Platforms, NIF-kurs: Plattformer til havs - samvirke mellom jord og konstruksjon, Trondheim, Norway, 6-8 January 1986.

14. OTTOSEN N.S, A Failure Criterion for Concrete, Journal of the Engineering Mechanics Division, ASCE, Vol 103, No. EM4, pp 527-535, August 1977

15. WILLAM K.J and WARNKE E.P, Constitutive Model for the Triaxial Behaviour of Concrete, Int. Association of Bridge and Structural Engineers, Seminar on "Concrete Structures Subjected to Triaxial Stresses", Paper III-1, Bergamo, Italy, May 17-19 1974.

16. EIBL J. et at., Concrete under Multiaxial States of Stress - Constitutive Equations for Practical Design, Comite Euro-International du Beton, Bulletin No. 156, June 1983.

17. Constitutive Relations and Failure Theories, Chapter 2 in "Finite Element Analysis of Reinforced Concrete", ASCE, New York, 1982.

18. OTTOSEN N.S., Nonlinear Finite Element Analysis of Concrete Structures, Risø National Laboratory, Roskilde, Denmark, Risø-R-411, May 1980.

19. BERGAN P.G., Some Aspects of Interpolation and Integration in Nonlinear Finite Element Analysis of Concrete Structures, Proc. Int. Conference on Computer Aided Analysis and Design of Concrete Structures, Split, Yugoslavia, Sept. 17-21, 1984, Eds. F. Damjanic et al., Pineridge Press, pp. 301-316, 1984.

20. RASHID Y.R., Ultimate Strength Analysis of Reinforced Concrete Pressure Vessels, Nuclear Engineering and Design, Vol. 7, No. 4, pp 334-344, April 1968.

21. BAZANT Z.P. and CEDOLIN L., Blunt Crack Band Propagation in Finite Element Analysis, Journal of the Engineering Mechanics Division, ASCE, Vol. 105 No. EM2, pp 297-315, April 1979

22. PETERSON P.E., Crack Growth and Development of Fracture Zones in Plain Concrete and Similar Materials, Report TVBM-1006, Div. of Building Materials, Lund Institute of Technology, Sweden, 1981.

23. HILLERBORG A., MODEER M. and PETERSON P.E., Analysis of Crack Formation and Crack Growth in Concrete by Means of Fracture Mechanics and Finite Elements, Cement and Concrete Research, Vol. 6, 1976, pp 773-782.

24. BAZANT Z.P and OH B.H., Crack Band Theory for Fracture of Concrete, Materials and Structures, RILEM, Vol. 16, 1983, pp 155-177.

25. OTTOSEN N.S., Thermodynamical Consequences of Strain Softening in Tension, Jour. of Engineering Mechanics, ASCE, Vol. 112, No EM11, pp 1152-1164, November 1986.

26. OTTOSEN N.S., DAHLBLOM O., Smeared Crack Analysis Using a Nonlinear Fracture Model for Concrete, Proc. at Third Int. Conf. on Num. Meth. for Nonlinear Problems, Dubrovnik, Yugoslavia, September 15-18, 1986.

27. DAHLBLOM O., OTTOSEN N.S., Smeared Crack Analysis Using the Fictitious Crack Model, Submitted to Journal of Engineering Mechanics, ASCE, 1987

28. DAHLBLOM O., Constitutive Modelling and Finite Element Analysis of Concrete Structures Considering Environmental Influence, Div. of Structural Mechanics, Rep. TVSM-1004, Lund Institute of Technology, Sweden 1987

29. HAN D.J. and CHEN W.F., Constitutive Modelling in Analysis of Concrete Structures, Report No. CE-STR-84-19, School of Civil Engineering, Purdue University, Indiana, USA, May 1984.

30. CERVENKA V. and GERSTLE K.H., Inelastic Analysis of Reinforced Concrete Panels: Theory, Int. Association for Bridge and Structural Engineering Publications, Zürich, Switzerland, Vol. 31-II, 1971, pp 31-45.

31. TINGLEFF O., A Method for Simulating Concentrated Forced and Local Reinforcement in Stress Computations, in "The Mathematics of Finite Elements and Applications", Edited by Whitman, J.P., Academic Press, New York, 1973, pp 463-470.

32. KVALSTAD T.J., Effect av usikre last- og jorddata (The effect of uncertain load- and soil data, in Norwegian), NIF-kurs; Platformer til havs - samvirke mellom jord og konstruksjon, 4-8 januar 1986, Trondheim, Norway.

33. WOLF J.P., Dynamic Soil-Structure Interaction, Prentice-Hall Inc., Englewood Cliffs, New Jersey, 1985

34. BAYO E.and WILSON E.L., Numerical Techniques for the Evaluation of Soil-Structure Interaction Effects in the Time Domain, Report No. UCB/EERC-83/04 Earthquake Engineering Research Center, University of California, Berkeley, 1983.

35. CLOUGH R.W. and WILSON E.L., Dynamic Analysis of Large Structural Systems with Local Nonlinearities, Computer Methods in Applied Mechanics and Engineering 17/18, 1979, pp 107-129.

Leere Seite
Blank page
Page vide

Ultimate Load Analysis of Eccentrically Stiffened Shell Structures

Calcul à la rupture de structures spatiales raidies

Traglastberechnung von exzentrisch versteiften Schalenkonstruktionen

A.Y. THANNON
Lecturer
University of Mosul
Mosul, Iraq

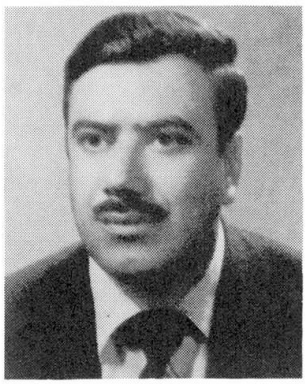

Akram Younis Thannon, born 1941. B.Sc. University of Baghdad, Iraq, 1963. M.Sc. University of Mosul, Iraq, 1978. Worked in design and construction of industrial buildings.

N. BICANIC
Lecturer
University of Wales
Swansea, U.K.

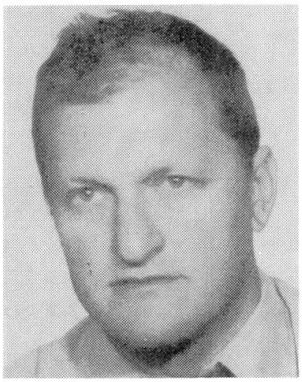

Nenad Bicanic, born 1945. Dipl. Ing. University of Zagreb, Yugoslavia, 1968. Ph.D. University of Wales, 1978. Professor at Faculty of Civil Engineering in Zagreb. He joined the Department in Swansea in 1985.

D.R.J. OWEN
Prof. of Civil Eng.
University of Wales
Swansea, U.K.

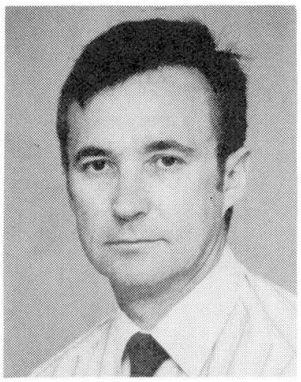

Roger Owen, born 1942. B.Sc., M.Sc., University of Wales. Ph.D. Northwestern University, U.S.A. In 1983 he was awarded the degree of D.Sc. by the University of Wales.

SUMMARY

Numerical solution techniques are presented for simulating the behaviour of reinforced concrete plates and shells stiffened with eccentric beam systems when subjected to short term loading conditions. Degenerate quadratic thick shell elements are employed for the shell and for the beams a curved element formulation is adopted based on beam theory incorporating transverse shear deformation. A through thickness layered representation is used for both the shell and the beam in order to model progressive failure characteristics. Comparison is made with several experimental results.

RÉSUMÉ

Des solutions numériques sont présentées pour la simulation du comportement de plaques et de coques en béton armé raidies avec des systèmes de poutres excentriques, lorsqu'elles sont soumises à des conditions de charges de courte durée. Des éléments de coque épais particuliers sont employés pour la coque tandis qu'une formulation d'éléments courbes est adoptée pour les poutres, sur la base de la théorie des poutres prenant en compte les déformations dues au cisaillement. Une représentation en couches successives est utilisée pour la coque et la poutre afin d'inclure les caractéristiques de la rupture progressive dans le modèle. Une comparaison est faite avec plusieurs résultats expérimentaux.

ZUSAMMENFASSUNG

Numerische Lösungsmethoden werden gezeigt, die das Verhalten von balkenversteiften Stahlbetonplatten und -schalen unter Kurzzeitbelastung simulieren. Entartete quadratische dicke Schalenelemente werden für Schalen verwendet, während für die Balken ein krummliniges Element angewandt wird, das die Schubverzerrung miteinschliesst. Eine über die ganze Dicke reichende Schichtendarstellung wird sowohl für die Schale wie für den Balken gewählt, um fortschreitendes Versagen zu modellieren. Die Ergebnisse werden mit einigen Versuchsresultaten verglichen.

1. INTRODUCTION

The continuing trend towards limit state design of reinforced concrete structures makes increasing demands on the development of adequate computational models for their analysis. The situation is particularly crucial for stiffened shell structures where uncertainties still exist with regards to appropriate element formulation and material modelling under ultimate load conditions. The work presented in this paper represents a further, though small step towards the ultimate goal of a reliable and robust computer code capable of predicting the response of arbitrary stiffened shell structures throughout the entire loading range leading to collapse.

The primary objective of a finite element model developed for global analysis and design purposes is the accurate prediction of the overall deformational and load carrying characteristics of structures together with the corresponding limit loads. The modelling of the complex behaviour of reinforced concrete is frequently simplified in the local context (e.g. crack discontinuities, bond slip) in order to render the problem more tractable and provide numerical solutions within acceptable computational costs. A successful model, however, must be capable of simulating the fundamental nonlinear behaviour up to collapse and must be based on material parameters which can be unambiguously determined from simple tests. The present paper is concerned with developing a numerical approach for modelling the ultimate load response of reinforced concrete shell structures with integral stiffening beams under quasi-static short term loading within these constraints.

The degenerate quadratic thick shell element , employing a layered representation through the thickness, has been successfully employed for the analysis of reinforced concrete plates and shells [1]. Several versions of this element (Lagrangian , Heterosis , Serendipity) have been utilized with various material constitutive models. Most approaches have been based on a dual criterion for yield and crushing in compression expressed in terms of stresses and strains which is complemented with a tension cut-off representation. A smeared or distributed model for cracked concrete is assumed and an average shear modulus is used for cracked zones . Gradual bond deterioration with progressive cracking is simulated by means of a tension stiffening model. Such an approach is again employed in this work as a basis for plate and shell modelling.

The need for a curved beam element to model integral reinforced concrete stiffeners, or even seperate beams, has led to the introduction of various types of elements [2,3] In the present analysis, the curved beam element used by Jirousek [2] for the linear analysis of stiffened shells, is adopted. This element exhibits the required displacement compatibilty with the degenerate quadratic thick shell element. The six degrees of freedom associated with any node are capable of representing torsional and transverse bending behaviour and the element formulation also models transverse shear effects . The constitutive model referred to above must also be modified to allow prediction of the ultimate load behaviour of beam components.

The finite element computational model is summarized and four numerical examples are presented which both illustrate the capabilities of the present code and draw attention to some problems that still exist in the numerical prediction of the ultimate load behaviour of stiffened shell structures.

2. FINITE ELEMENT FORMULATION FOR ECCENTRICALLY STIFFENED PLATES AND SHELLS

2.1 Eccentric curvilinear beam element

2.1.1 Reference, joint and centroidal axes

Fig. 1 illustrates a typical 3 noded curvilinear beam element, with six degrees of freedom comprising three global displacements u_i, v_i, w_i and three global rotations $\alpha_L, \beta_L, \gamma_L$

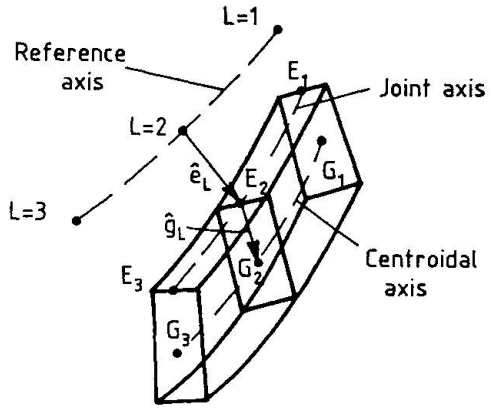

Fig.1 Geometry of the eccentric beam element

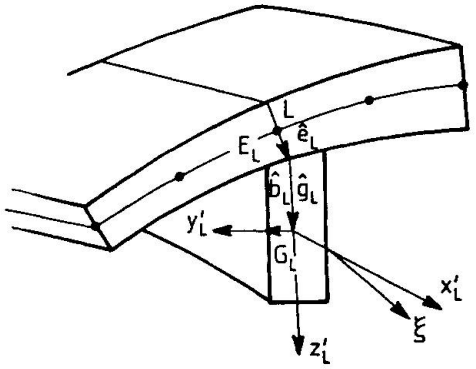

Fig.2 Local coordinate system in a nodal section of the eccentric beam element

The points G1, G2, and G3 are the nodes on the element centroidal axis and ξ is a curvilinear coordinate which varies between (-1,+1). Any point on the element centroidal axis can be defined from

$$\begin{bmatrix} x_G \\ y_G \\ z_G \end{bmatrix} = \sum_{L=1}^{3} N_L(\xi) \begin{bmatrix} x_{GL} \\ y_{GL} \\ z_{GL} \end{bmatrix} \quad \ldots\ldots\ldots\ldots (1)$$

where N_L are the shape functions, and x_{GL}, y_{GL}, z_{GL} are the global cartesian coordinates of the nodes on the element centroidal axis.

When employing such an element in conjuction with a thick shell element to model a stiffened shell, two additional axes have to be introduced, the reference axis, situated at the mid surface of the corresponding thick shell element, and the joint axis on the contact between the beam and the shell, denoted in Fig.1 by points E1,E2 and E3.

Points on the reference axis and on the joint axis can be defined in terms of the corresponding nodal coordinates and the curvilinear coordinate in the same way as points on the centroidal axis are defined in Eq.(1).

The position of the points G_L, E_L with respect to the reference axis can be specified using vectors $\hat{e}_L$, $\hat{g}_L$. Consequently nodal coordinates on the centroidal axis can be expressed in terms of the nodal coordinates on the reference axis as

$$\begin{bmatrix} x_{GL} \\ y_{GL} \\ z_{GL} \end{bmatrix} = \begin{bmatrix} x_L \\ y_L \\ z_L \end{bmatrix} + \hat{e}_L + \hat{g}_L = \begin{bmatrix} x_L \\ y_L \\ z_L \end{bmatrix} + \begin{bmatrix} \Delta x_L \\ \Delta y_L \\ \Delta z_L \end{bmatrix} \quad \ldots\ldots\ldots\ldots (2)$$

The local cartesian coordinates x',y',z' where x' is normal to the plane of the element cross section and y', z' are the principal axes of area of the cross section, are shown in Fig.2 .

The beam cross section at a given ξ should ideally contain point E on the joint axis

$$\begin{bmatrix} x_E \\ y_E \\ z_E \end{bmatrix} = \sum_{L=1}^{3} N_L(\xi) \begin{bmatrix} x_{EL} \\ y_{EL} \\ z_{EL} \end{bmatrix} \quad \text{.....(3)}$$

This requirement cannot be fulfilled in general, if one insists on having the cross section plane rigorously perpendicular to the centroidal axis. It is assumed that the the vector $\hat{b}$ coincides with the direction of the local y'axis so that the cross section plane is approximately normal to the centroidal axis. For intermediate section along the axis it holds that

$$\hat{g}\ (\xi) = \sum_{L=1}^{3} N_L(\xi)\ \hat{g}_L \quad , \quad \hat{b}\ (\xi) = \sum_{L=1}^{3} N_L(\xi)\ \hat{b}_L \quad \text{.....(4)}$$

Using the vectors $\hat{g}$ and $\hat{b}$,the unit vectors in the local coordinate system x,y,z can be computed

$$\hat{i}' = \frac{\hat{a}}{|a|} \quad , \quad \hat{j}' = \frac{\hat{b}}{|b|} \quad , \quad \hat{k}' = \frac{\hat{c}}{|c|} \quad \text{.....(5)}$$

where

$$\hat{a} = \hat{b} \times \hat{g} \quad \text{and} \quad \hat{c} = \hat{a} \times \hat{b} \quad \text{.....(6)}$$

The matrix of the orthogonal transformation from the local to global axes will therefore be given as

$$\Omega\ (\xi) = [\ \hat{i}'(\xi) \quad \hat{j}'(\xi) \quad \hat{k}'(\xi)] \quad \text{.....(7)}$$

2.1.2 Generalized stress-strain relationship.

Assuming that the cross section plane is perpendicular to the centroidal axis, the constitutive equation relating the generalized stress $\underset{\sim}{\sigma}$ (Fig.3) to the generalized strain $\underset{\sim}{\varepsilon}$ will be of the form

$$\underset{\sim}{\sigma} = \underset{\sim}{D}\ \underset{\sim}{\varepsilon} \quad \text{.....(8)}$$

where

$$\underset{\sim}{\sigma} = \begin{bmatrix} N \\ Q_{y'} \\ Q_{z'} \\ M_{y'} \\ M_{z'} \\ T \end{bmatrix} , \quad \underset{\sim}{D} = \begin{bmatrix} EA & & & & & \\ & GA_{y'} & & & 0 & \\ & & GA_{z'} & & & \\ & & & EI_{y'} & & \\ & 0 & & & EI_{z'} & \\ & & & & & GJ \end{bmatrix} , \quad \underset{\sim}{\varepsilon} = \begin{bmatrix} u_{G,x'} \\ v_{G,x'} - \gamma' \\ w_{G,x'} + \beta' \\ \alpha',x' \\ \beta',x' \\ \gamma',x' \end{bmatrix}$$

where , ', denotes the local reference frame and ,x' stands for differentiation with respect to x' .

The cross sectional properties for each layer are

A	cross section area
$A_{y'}$, $A_{z'}$	equivalent shear area
E	modulus of elasticity
G	shear modulus
J	torsional constant
$I_{y'}$,$I_{z'}$	principal moment of inertia

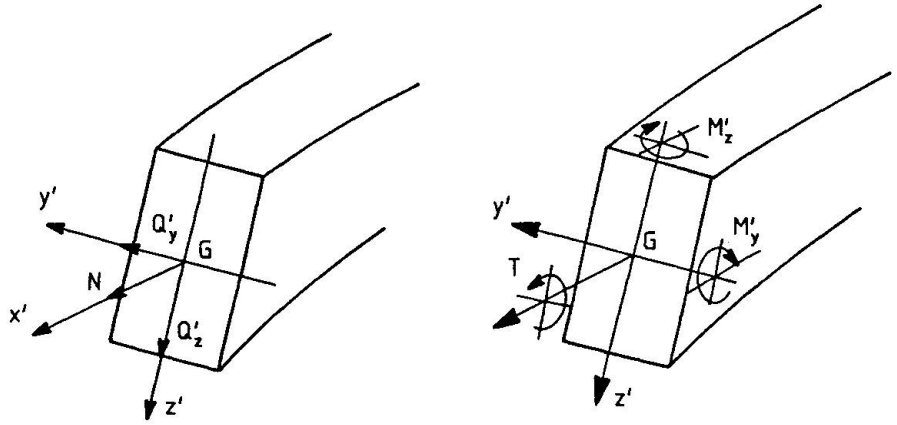

Fig.3 Generalized stress of a curved beam element

The displacements and rotations in the local and global reference system are related through

$$\begin{bmatrix} u'_G \\ v'_G \\ w'_G \end{bmatrix} = \Omega^T \begin{bmatrix} u_G \\ v_G \\ w_G \end{bmatrix} \quad , \quad \begin{bmatrix} \alpha' \\ \beta' \\ \gamma' \end{bmatrix} = \Omega^T \begin{bmatrix} \alpha \\ \beta \\ \gamma \end{bmatrix} \qquad \text{.....(9)}$$

By neglecting the possible small difference between the local axis x' and the tangent to the centroidal axis it follows that

$$\frac{d}{dx'} = \frac{1}{t} \frac{d}{d\xi} \qquad \text{.....(10)}$$

where t is modulus of the vector $\hat{t}$

$$\hat{t}(\xi) = \sum_{L=1}^{3} \frac{dN_L(\xi)}{d\xi} \begin{bmatrix} x_{GL} \\ y_{GL} \\ z_{GL} \end{bmatrix} \qquad \text{.....(11)}$$

2.1.3 Element stiffness matrix

Standard finite element procedures can be followed for computing the stiffness matrix K_G associated with the centroidal axis displacements δ_G

$$K_G = \sum^{Ln} \int_{-1}^{1} B_G^T D B_G \; t \, d\xi \qquad \text{.....(12)}$$

where, Ln is the number of layers through the thickness

The calculation (at the Gauss points) of the strain matrix B_G for each layer follows from

$$\varepsilon = B_G \, \delta_G = \sum_{L=1}^{3} B_{GL} \, \delta_{GL} \qquad \ldots\ldots\ldots\ldots (13)$$

In turn, B_{GL} for each layer can be written by using the definition of the the generalized strain and the transformation matrix Ω as

$$B_{GL} = \begin{bmatrix} \frac{1}{t}\frac{dN_L}{d\xi}\,\Omega^T & \vdots & 0 \\ & \vdots & N_L\,\hat{k}',^T \\ & \vdots & N_L\,\hat{j}',^T \\ \cdots\cdots\cdots\cdots & \vdots & \cdots\cdots\cdots \\ 0 & \vdots & \frac{1}{t}\frac{dN_L}{d\xi}\,\Omega^T \end{bmatrix} \qquad \ldots\ldots\ldots (14)$$

The K matrix associated with the reference axis can be obtained by either transforming K_G matrix or by transforming the strain matrix B from each layer into a strain matrix B_G associated with the reference axis which has been found to be more ecconomical. This latter transformation will be discussed after the formulation of the thick shell element .

2.2 Thick shell element

Formulation of the standard quadratic degenerate shell element (Ahmad's element) is well known [4], and therefore only a brief description of the element will be presented here. Since the element formulation does not allow a direct combination with the beam element described above, the necessary modifications are also summarised.

The degenerate shell element (Fig.4) has five nodal degrees of freedom, i.e three global displacements (u_i, v_i, w_i) and two local rotations (α''_i,β''_i) about the x'' and y'' axes respectively.

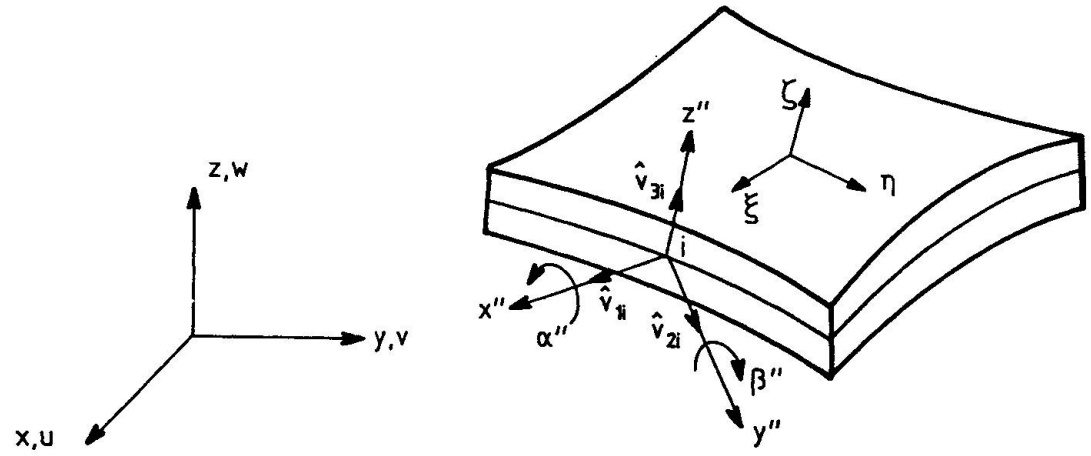

Fig.4 Geometry of a standard thick shell element

The displacement field is assumed to be of the form

$$\begin{bmatrix} u \\ v \\ w \end{bmatrix} = \sum_{i=1}^{n} M_i(\xi,\eta) \begin{bmatrix} u_i \\ v_i \\ w_i \end{bmatrix} + \frac{1}{2} \sum_{i=1}^{n} M_i(\xi,\eta) [-\hat{v}_{2i} \ \hat{v}_{1i}] \begin{bmatrix} \alpha_i'' \\ \beta_i'' \end{bmatrix} \quad ..(15)$$

where x'', y'', z'' are the local coordinate system, $\hat{v}_{1i}$,$\hat{v}_{2i}$,$\hat{v}_{3i}$ are unit vectors and n is the number of nodes.

For the nodes where the shell element is linked to a stiffening beam element, the local rotations (α_L'', β_L'') must be expressed in terms of the global rotations $(\alpha_L, \beta_L, \gamma_L)$

$$\begin{bmatrix} \alpha_L'' \\ \beta_L'' \end{bmatrix} = T_L \begin{bmatrix} \alpha_L \\ \beta_L \\ \gamma_L \end{bmatrix} \quad .....(16)$$

where T_L is a matrix which can be derived from geometric considerations as

$$T_L = \begin{bmatrix} -\hat{v}_{2L}^T \\ \hat{v}_{1L}^T \end{bmatrix} \begin{bmatrix} 0 & v_{3L}^z & -v_{3L}^y \\ -v_{3L}^z & 0 & v_{3L}^x \\ v_{3L}^y & -v_{3L}^z & 0 \end{bmatrix} \quad ...(17)$$

The transformation of the generalized degenerated shell degrees of freedom δ_L'' to δ_L is then given by

$$\begin{bmatrix} u_L \\ v_L \\ w_L \\ \alpha_L'' \\ \beta_L'' \end{bmatrix} = \begin{bmatrix} I & 0 \\ 0 & T_L \end{bmatrix} \begin{bmatrix} u_L \\ v_L \\ w_L \\ \alpha_L \\ \beta_L \\ \gamma_L \end{bmatrix} \quad ...(18)$$

2.3 Beam element combined with the degenerate shell element

To meet the requirements of displacement compatibility along the joint axis, it is assumed that the displacement field of the curved beam element is generated by linking each cross-section to the reference axis by means of a rigid rod vector $\hat{e}_L(\xi)$. It can be shown [2] that

$$\begin{bmatrix} u_{GL} \\ v_{GL} \\ w_{GL} \end{bmatrix} = \begin{bmatrix} u_L \\ v_L \\ w_L \end{bmatrix} + A_L \begin{bmatrix} \alpha_L \\ \beta_L \\ \gamma_L \end{bmatrix} \quad .....(20)$$

where

$$A_L = \begin{bmatrix} 0 & \Delta z_L & -\Delta y_L \\ -\Delta z_L & 0 & \Delta x_L \\ \Delta y_L & -\Delta x_L & 0 \end{bmatrix}$$

The B_{GL} submatrix in Eq. (15) associated with the centroidal axis nodes can be transformed to B_G (associated with the reference axis nodes) by

$$B_L = B_{GL}\, TR_L \qquad \text{.....(21)}$$

where

$$TR_L = \begin{bmatrix} I & \vdots & 0 \\ \cdots & \vdots & \cdots \\ 0 & \vdots & A_L \end{bmatrix}$$

Finally the total stiffness matrix can be assembled following standard finite element procedures.

3. MATERIAL MODELLING

Usually, a simplified formulation of the highly complex behaviour of reinforced concrete is employed [6] and the formulation adopted here has been found very effective despite its simplicity [5].

The compressive behaviour of concrete is modellled using the flow theory of plasticity [8]. Employing Kupfer's results [7], the yield condition for the plate and shell elements is written in stress component form as

$$f(\sigma)=[1.335[(\sigma_x^2+\sigma_y^2-\sigma_x\sigma_y)+ 3(\tau_{xy}^2+\tau_{xz}^2+\tau_{yz}^2)] +0.355\sigma_o(\sigma_x+\sigma_y)]^{1/2} = \sigma_o \qquad \text{.....(22)}$$

This yield condition is a function of only one material parameter ($\sigma_o=f_c'$) which can be obtained relatively easily from experimental data.

The crushing condition is controlled by the state of straining and can be written in terms of total strain components again based on Kupfer's results as

$$1.335[(\varepsilon_x^2+\varepsilon_y^2-\varepsilon_x\varepsilon_y)+ 0.75(\gamma_{xy}^2+\gamma_{xz}^2+\gamma_{yz})] +0.355\ \varepsilon_u(\varepsilon_x+\varepsilon_y) = \varepsilon_u^2 \qquad \text{.....(23)}$$

When ε_u reaches the specified limiting value the concrete is assumed to have lost all its characteristics of strength and stiffness.

For the beam element, the uniaxial behaviour of concrete Fig.5 is adopted.

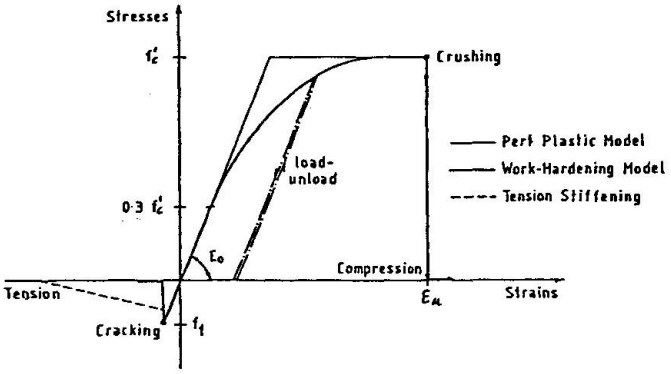

Fig.5 Uniaxial representation of the concrete constitutive model

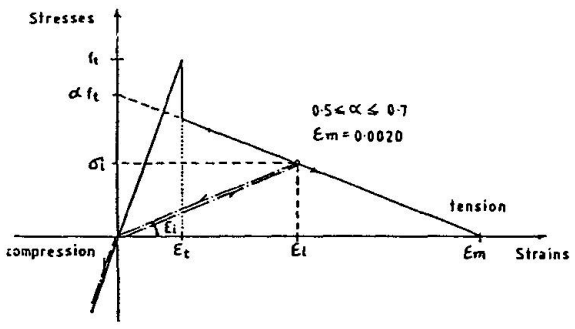

Fig.6 Tension stiffening diagram

The response of concrete under stress is assumed to be linearly elastic until the fracture surface is reached. When the maximum tensile stress is reached, cracks are assumed to form in planes perpendicular to the direction of the maximum principal stress.

After cracking has occured, either a sudden release or gradual relaxation of the normal stress on the cracked plane is adopted according to a tension stiffening diagram as shown in Fig. (6). The modulus of elasticity and the Poisson's ratio are reduced to zero in the direction perpendicular to the crack plane. A reduced shear modulus taken as a function of tensile strain is employed to simulate aggregate interlock.

The behaviour of steel in tension and compression is modelled by considering the reinforcing steel bars as layers of equivalent thickness. Each steel layer has a uniaxial behaviour, i.e resisting only the axial force in the bar direction.

An incremental/iterative numerical solution technique is used in order to trace the response of the structure throughout the loading history. The modified Newton-Raphson method has been employed to avoid frequent calculation and factorization of the tangential stiffness matrix.

4. NUMERICAL EXAMPLES

4.1 Duddeck's two span beam

A simply supported reinforced concrete beam, continuous over two spans tested by Duddeck et al [9] is shown in Fig.7. The material properties as reported by Muller [10] are given in Table 1.

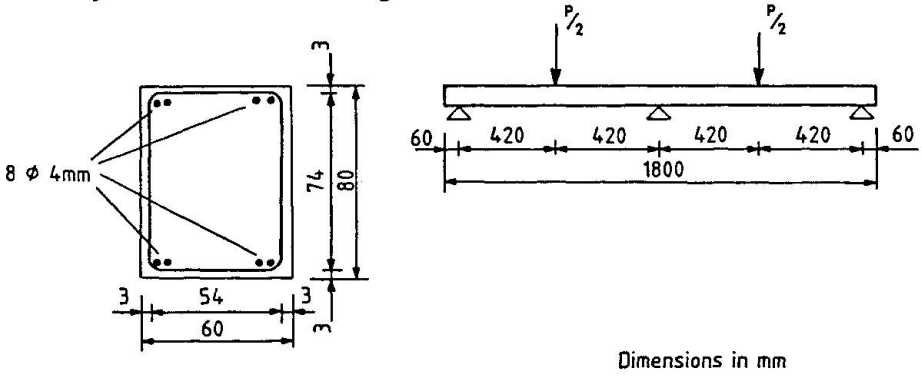

Fig.7 Geometry and details of Duddeck's beam

Table 1 Material properties for Duddeck's beam in (N,mm)

concrete		steel	
Young's Modulus	$E_c = 16660.$	Young's Modulus	$E_s = 196000.0$
Poisson's ratio	$\nu = 0.0$	Young's Modulus	$E_s = 28000.0$
Ult. Comp. St.	$f'_c = 32.0$	Yield Stress	$F_Y = 490.0$
Ult. Tens. St.	$f'_t = 1.67$		
Ult. Comp. Stn.	$\varepsilon_u = .0027$		
Tens. Stiff. Coeff.	$\alpha = 0.5$		
Tens. Stiff. Coeff.	$\varepsilon_m = 0.0015$		

Taking advantage of symmetry only one half of the beam is considered and idealized by 8 beam elements.

Results from the analysis in Fig.8 are in close agreement with experimental observations and data.

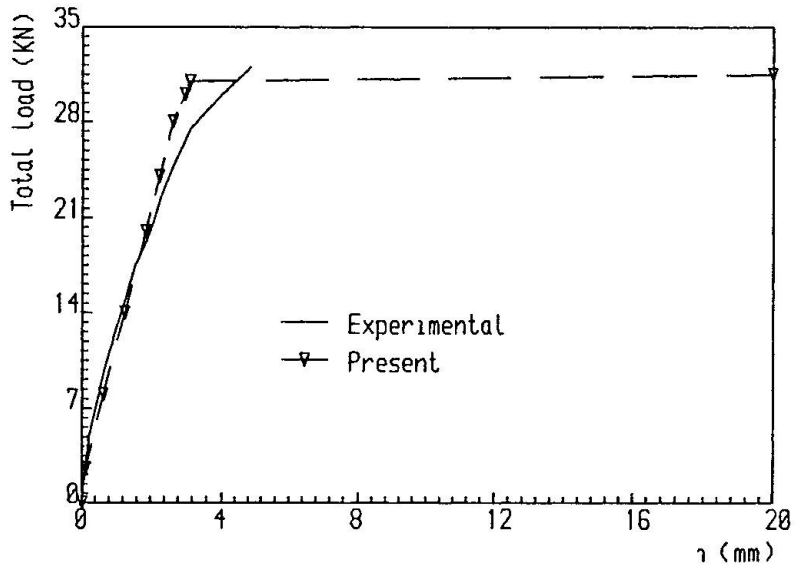

Fig.8 comparison of the load deflection curve for Duddeck's beam.

4.2 Cope and Rao 'T' beam analysis

The reinforced concrete 'T' beam tested by Cope and Rao [11] is chosen to assess the present approach in solving problems involving an assembly of plates and beams. The details of the T beam are shown in Fig.9 , and the relevant material properties are given in Table 2.

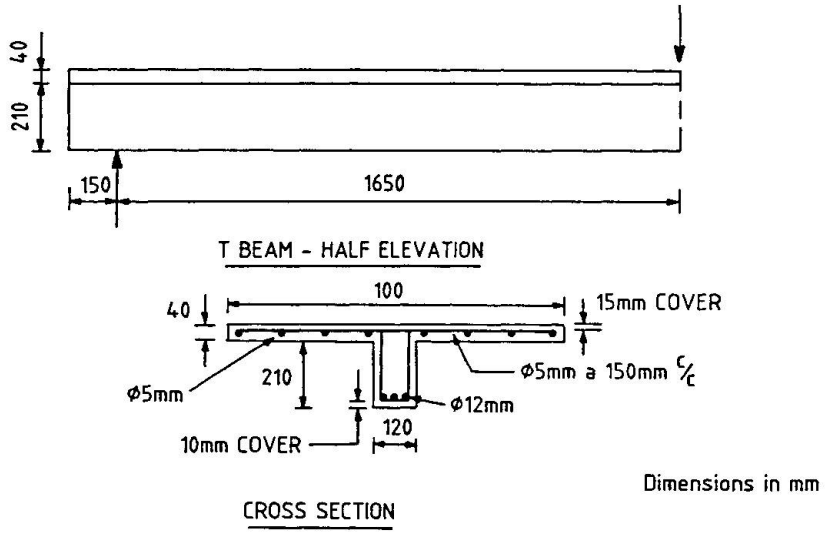

Fig.9 Geometry and details of the Cope/Rao T beam

Table 2 Material properties for Cope/Rao T beam in (N,mm)

concrete		steel	
Young's Modulus	$E_c = 35000.$	Young's Modulus	$E_s = 200000.0$
Poisson's ratio	$\nu = 0.2$	Young's Modulus	$E'_s = 0.00$
Ult. Comp. St.	$f'_c = 48.0$	Yield Stress	$F_Y = 340.0$
Ult. Tens. St.	$f'_t = 4.80$		
Ult. Comp. Stn.	$\varepsilon_u = .003$		
Tens. Stiff. Coeff.	$\alpha = 0.5$		
Tens. Stiff. Coeff.	$\varepsilon_m = 0.0015$		

Using symmetry conditions, one quarter of the T beam is idealized by 12 shell elements and 12 beam elements.

Comparison of the numerical results with those of the experiment in Fig.10 indicates a difference at the initial stage of the response. This difference was also reported by Cope and Rao [11], and can be explained by the existence of micro cracks which reduce the effective tensile strength of the concrete. The close agreement in the later stages up to failure, shows that the present predictive approach is both efficient and adequate. The predicted ultimate load of 36 KN was very close to the experimental load of 40 KN.

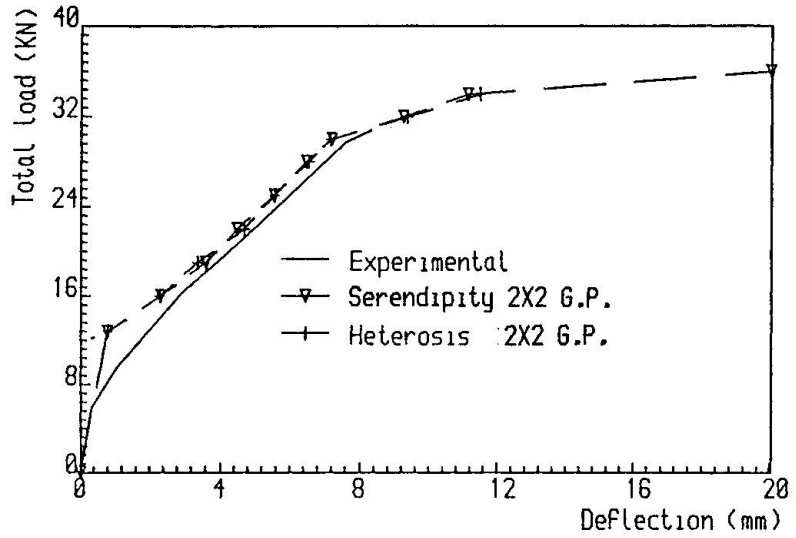

Fig.10 Comparison of load deflection curves for Cope/Rao T beam

4.3 Bouma's cylindrical shell with edge beams

From a series of experimental tests performed on various cylindrical shell roofs [12,13] two tests are chosen for comparison with the present numerical formulation. Fig.11 illustrates the dimensions and reinforcement details of the cylindrical shell and the edge beams. The shell has end diaphragms and is simply supported at the edge of these diaphragms. The shell surface is subjected to uniformly distributed load in the vertical direction with the free edges being subjected to line loading, and both loads are increased in the same ratio during testing.

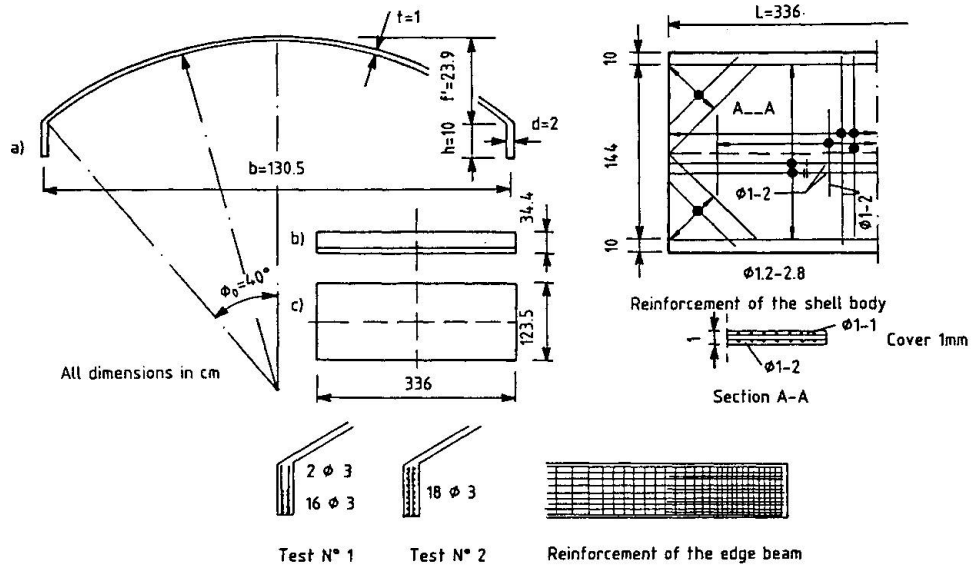

Fig.11 Geometry and details of Bouma's cylindrical shell

For both models, one quarter of the stiffened shell roof has been idealized by 12 shell elements and 4 beam elements, noting the dual symmetry of the problem.

The material properties are assumed to be those indicated in Table 3. The properties are identical to those assumed by both Anerson [13] and Ramm [14] in their analysis of the same shell,which allows comparison with their published predictions.

Table 3 Material properties for Bouma's shells in (N,mm)

concrete		steel	
Young's Modulus	E_c = 30000.	Young's Modulus	E_s = 210000.0
Poisson's ratio	ν = 0.2	Young's Modulus	E_s' = 2000.0
Ult. Comp. St.	f_c' = 30.0	Yield Stress	F_Y = 295.0
Ult. Tens. St.	f_t' = 3.00		
Ult. Comp. Stn.	ε_u = .003	For the edge beam	
Tens. Stiff. Coeff.	α = 0.5		
Tens. Stiff. Coeff.	ε_m = 0.0015	Yield Stress	F_Y = 280.0

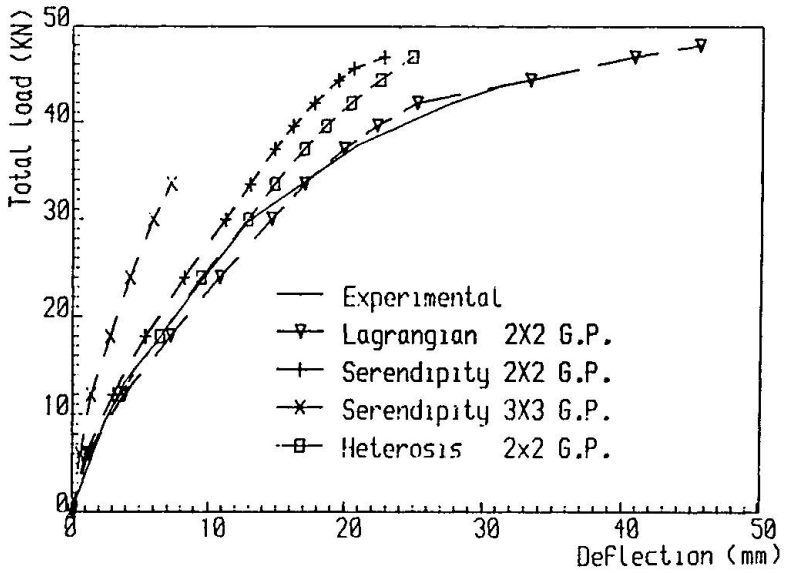

Fig.12 Comparison of load-deflection curves for the middle of the edge beam (Bouma's shell test No.2)

In Fig.12 the numerical results for test No.2 are shown for different types of element and are compared with the test results. The Heterosis element formulation (with reduced integration) shows an excellent agreement with the experimental results up to approximately half the failure load, while the Lagrangian element formulation (with reduced integration) indicates good shell response prediction up to failure load. Full integration leads to a completely 'locked' solution, as expected.

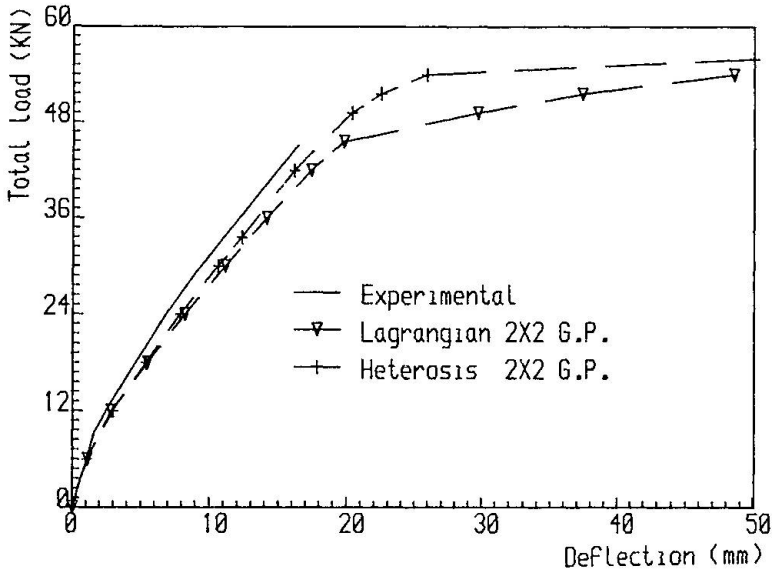

Fig.13 Comparison of load-deflection curves for the middle of the edge beam (Bouma's shell test No.1)

The numerical results for test No.1 are shown in Fig.13. The Heterosis element formulation shows a better agreement with the experimental results than the Lagrangian element formulation.

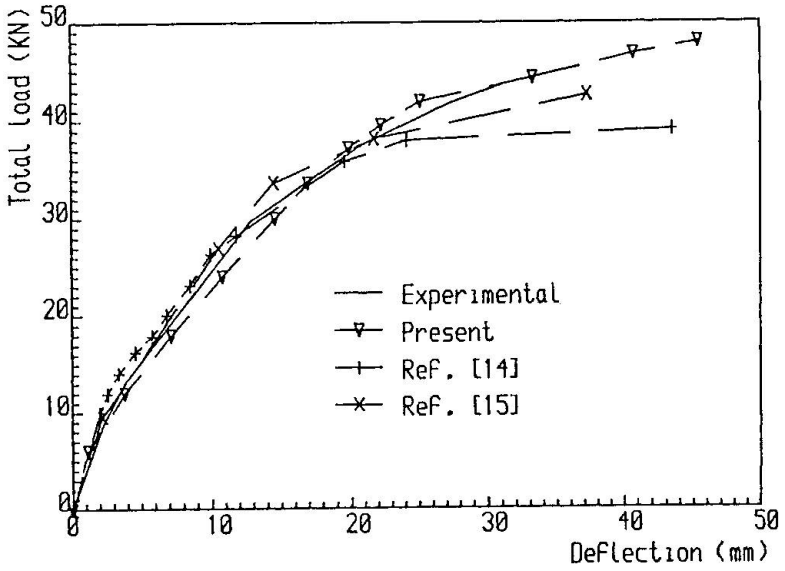

Fig.14 Comparison of load- deflection curves for the middle of the edge beam (Bouma's shell test No.2) with results in Ref. [14,15]

In Fig.14, the numerical results for test No.2 are compared with the predictions from the analyses of Anerson [14] and Ramm [15] and with the experiment results.

It is worth mentioning that in Anerson's analysis the beam was idealized as a shell element connected at it's mid height (inner face) to the shell surface. Ramm [15] also idealized the edge beam as a shell element, and tried 3 different heights of connection point at the middle plane of the beam. The results chosen for comparison here are the best ones reported by Ramm [15]. In addition, both Ramm [15] and Anerson [14] did not mention that the load imposed on the shell during the actual test was composed of two parts, one uniformly distributed on the shell surface and the second being a line load applied to the edge beam, as clearly stated by Bouma et al. [13].

Finally the applicability of the present code is evident from the comparison of the predicted ultimate loads with the experimental values, as shown in Table 4 .

Table 4

	experimental	predicted
Test No.1	53.4 KN	53.0 KN
Test No.2	42.3 KN	46.0 KN

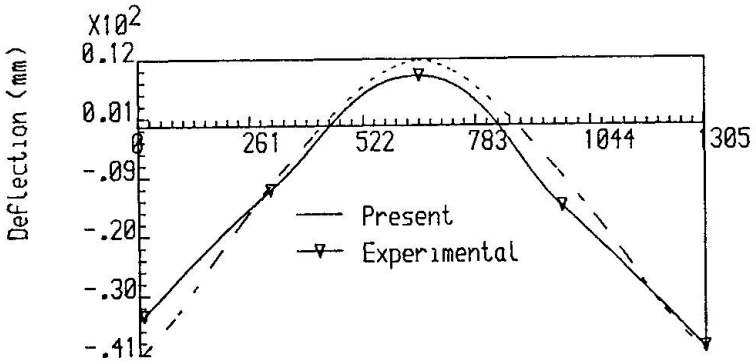

Fig.15 Shell mid section near failure for test No.2

In Fig.15 the shell mid section is shown at different load levels, compared with those measured during test and the very close agreement again illustrates the efficiency of the present approach. The analyses of both Anerson and Ramm did not predict the inward bending of the edge beam and the upward rising of the shell longitudinal centre line.

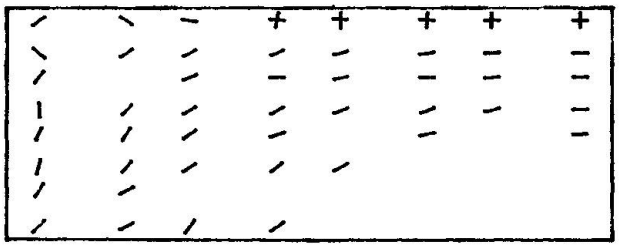

Fig.16 Crack distribution on the upper surface of test No.2

The crack distribution on the upper surface of test No.2 is shown in Fig.16, and is in good agreement with a photograph of the shell taken after failure [12].

5. DISCUSSION AND CONCLUSIONS

A finite element computational model for the ultimate load analysis of stiffened plate and shell structures has been presented and evaluated by application to several problems for which both experimental results and other numerical solutions are available. A good correlation was found between experimental and the present numerical results throughout the entire structural response which demonstrates the effectivness of the solution procedure. The curved beam element, developed to be compatible with degenerate thick shell elements, performed satisfactory and proved to be superior to modelling beam components by additional shell elements.

Further development work is currently being undertaken on the model to include geometric nonlinear effects which have been shown [1] to be significant in the case of unstiffened shells.

Considerable further verification of the solution procedure and associated code is necessary before use in engineering practice can be contemplated.

6. REFERENCES

1. D.R.J. OWEN and J.A. FIGUEIRAS, 'Ultimate load analysis of reinforced concrete plates and shells includung geometrical nonlinear effects', Finite element software for plates and shells, (eds. E. Hinton and D.R.J. Owen), Pineridge press, Swansea, U.K. Sept. 1983.

2. J.JIROUSEK, 'A family of variable section curved beam and thick-shell or membrane-stiffening isoparametric elements', Int.J.num. Meth. Engng, 17,171-186 (1981).

3. G.H. FERGUSON and R.D. CLARK,'A variable thickness curved beam and shell stiffening element with shear deformations',Int.J. num. Meth. Engng, 14 581-592 (1979).

4. S. AHMAD, B.M. IRONS AND O.C. ZEINKEIWICZ, 'Analysis of thick and thin Shell structures by curved elements' Int. J. Num. Engng. 419-451 (1971).

5. J.A. FIGUEIRAS, 'Ultimate load analysis of anisotropic and reinforced concrete plates and shells', Ph.D. Thesis, C/PH/72/83, Department of Civil Engineering, University College of Swansea, U.K. Sept.,1983.

6. W.F. CHEN , 'Plasticity in reinforced concrete', McGraw-Hill book company, New York, 1982.

7. H. KUPFER, K.H. HILSDROF and RUSH, 'Behaviour of concrete under biaxial stresses', Proceedings ACI Vol. 16, No.8, 656-666, 1969

8. D.R.J. OWEN and E. HINTON, 'Finite elements in plasticity, theory and theory and practice', Pineridge Press Ltd. Swansea, U.K. 1980.

9. H.DUDDECK, G. GRIEBENOW, and G. SCHAPER, ' Auszuge aus dem Sechsten Arbeitsbricht zum Forschungsvorhaben Stahlbetonpatten mit nichtlinearen Stoffgesetzen' , Arbeitsbericht Institut fur Statik, TU Braunschweig, 1976.

10. G.MUELLER, 'Numerical problems in nonlinear analysis of reinforced concrete', Report No.UC SESM 77-5, Department of Civil Engineering, University of California, Berkeley, Sept. 1977.

11. R.J COPE and P.V. RAO, ' Nonlinear finite element analysis of concrete slab structures', Proc. Inst. Civil Engng. part 2, 63, 159-197 , 1977.

12. A.C VAN RIEL, W.J. BERANEK and A.C. BOUMA, ' Test on shell roof model roof model of reinforced mortar', Proceedings of 2nd Symposium on concrete shell roof construction, July 1957, Teknisk Ukeblad, Oslo (organized by the Norwegian Engineering Society).

13. A. L. BOUMA, A. C. VAN RIEL, H. VAN KOTEN and W. J. BERANEK, 'Ivestigations on models of eleven cylindrical shells made of reinforced and prestressed concrete', Proceedings of the Symposium on shell research, Delft, Aug. 30 - Sept. 2 1961, (eds. A.M. Haas and A.C. Bouma).

14. A. ANERSEN, 'Analysis of reinforced concrete shells considering material and geometric nonlinearties', Division of structural mechanics, Norwegian Institute of Technology, University of Trondheim, Norway, Report No. 79-1, July 1979.

15. E.RAMM and T.A. KOMPFNER , 'Reinforced concrete shell anlaysis using an inelastic large deformation finite element formulation', Proceeding of the International Conference on computer aided analysis and design of concrete structures, part 1, (eds. F. Damjanic et al.), Pineridge Press, Swansea, U.K. 581-597, 1984.

Application of Finite Element Methods to Design of Reinforced Concrete Structures

Application de méthode des éléments finis au projet des structures en béton armé

Anwendung der Finite Element Methode auf den Entwurf von Stahlbetontragwerken

Junichiro NIWA
Assoc. Prof.
Yamanashi University
Kofu, Japan

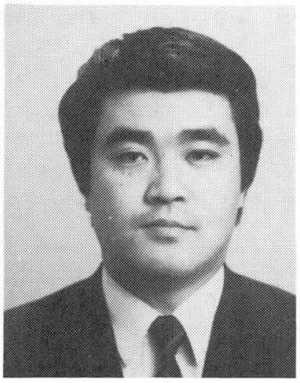

J. Niwa, born 1956, received D.Eng. from the University of Tokyo in 1983. His research interests include the behavior and the design of RC members under shear and torsion. He is a member of IABSE, ACI and JCI.

Shoichi MAEDA
Chief Engineer
Nishimatsu Constr. Co.
Tokyo, Japan

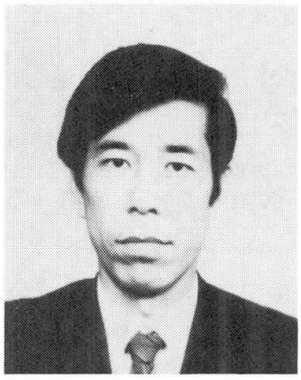

S. Maeda, born 1949, graduated from Osaka University in 1972. He is a chief engineer of the civil engineering design department of Nishimatsu Constr. Co. He is a member of JCI.

Hiroshi NOGUCHI
Assoc. Prof.
Chiba University
Chiba, Japan

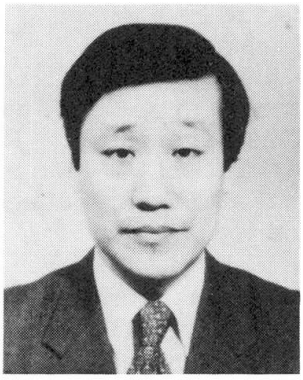

H. Noguchi, born 1947, received D.Eng. from the University of Tokyo in 1976. His research interests include the application of FEM and the seismic design of RC structures. He is a member of IABSE, ASCE, ACI and JCI.

SUMMARY

The Japan Concrete Institute had established the Committee on Finite Element Analysis of Reinforced Concrete Structures. One of the final aims of this committee is to propose guidelines for the application of FEM analyses to design. As a first step, the committee circulated a questionnaire on design examples using FEM analyses. Based on results of the questionnaire, this paper outlines the present situation and subjects to be treated in Japan.

RÉSUMÉ

L'Institut Japonais du Béton a mis sur pied un comité pour l'analyse des structures en béton armé au moyen des éléments finis. Un des objectifs finaux de ce comité est de proposer des directives pour l'application de la méthode des éléments finis au calcul du projet. Dans une première phase, le comité a réalisé un questionnaire sur des exemples de projet à calculer au moyen de la méthode des éléments finis. Sur la base des résultats du questionnaire, l'article explique la situation actuelle et les sujets à étudier au Japon.

ZUSAMMENFASSUNG

Der Japanische Betonverein hat einen Ausschuss für FE-Berechnungen im Massivbau eingesetzt. Eines der Ziele ist, Richtlinien für die Anwendung von FE-Berechnungen beim Entwurf vorzuschlagen. Als erster Schritt wurde ein Fragebogen verschickt über Beispiele von FE-Entwurfsberechnungen. Auf der Grundlage dieses Fragebogens stellt dieser Beitrag die gegenwärtige Situation und noch ausstehende Fragen in Japan dar.

1. INTRODUCTION

Recently according to the widespread adoption and advancement of computers, opportunities for the use of finite element method (FEM) analyses have been rapidly increasing in the fields of both the design and analytical research of reinforced concrete (RC) structures. The following reasons can be indicated as the background of this tendency.

In the field of design, it has always been difficult to apply conventional design procedures to large scale or special structures. Because of the relatively recent occurrence of these structures, there are very few preceding design examples. Therefore, it is not easy to convert them into simple structural members such as beams, columns, plates and frames. Secondly, the number of cases that demand precise examination of local stress conditions in a structure has increased remarkably. Lastly, a method of finite element analysis for thermal cracks in a massive concrete structure has been rapidly developed.

In the field of analytical research, the application of FEM analyses instead of the former experimental approach to derive or refine design equations of RC structures has increased. This is because FEM analyses can accurately compute the flow of internal forces and stress distributions in structures. Fig.1 shows the relationship between FEM analyses and RC structures from the point of view of applied fields.

The present situation and future prospects of FEM in the research field have already been reported by Aoyama and Noguchi[1]. A few practical examples of specific RC structures designed by FEM were presented by Ikeda and Tsubaki[2]. However, there are very few reports that discuss the present situation regarding the application of FEM analyses to design.

The Japan Concrete Institute (JCI) had established the Committee on Finite Element Analysis of Reinforced Concrete Structures (chairman H.Noguchi). One of the aims of this committee is to propose guidelines for the application of finite element analyses to the design of RC structures.

As the first step, a questionnaire was circulated to investigate the actual circumstances of the use of FEM analyses in the practical design of RC structures. General contractors, research institutes and universities were the objects of this investigation. Replies were received from both the fields of

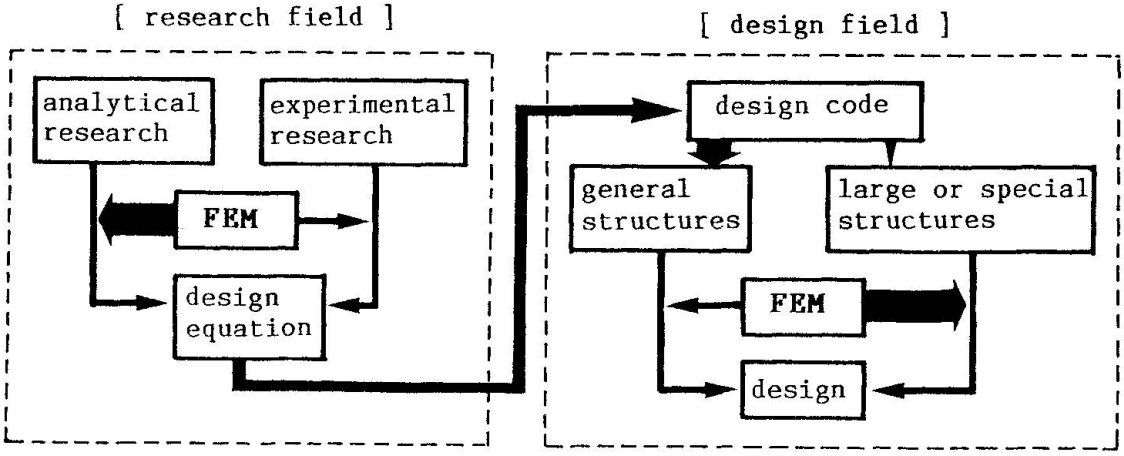

Fig.1 Present situation in the application of FEM to design

civil and architectural engineering. It is considered that the replies realistically represent the tendency of FEM analyses in the design of RC structures in our country.

This paper outlines the present situation and subjects to be solved in the application of FEM analyses to the design of RC structures according to the replies of the questionnaire.

2. PRESENT SITUATION IN THE APPLICATION OF FEM TO DESIGN

2.1 Summary of Replies of the Questionnaire

Practical design examples using FEM analyses were surveyed in the questionnaire. Questions covered the following:

(a) practical examples of the application of FEM analyses
(b) methods of finite element analysis applied to design
(c) evaluation of analytical results
(d) methods reflecting analytical results on practical design

Forty-four replies to the questionnaire were collected.

The replies concerning the practical examples of the application of FEM analyses were divided into five groups.

(1) the analysis of structures whose loading conditions are very complicated, such as floor slabs or base slabs
(2) the analysis of complicated or hollow structures that consist of many different plates and shells, such as underground tanks storing liquefied natural gas or nuclear reactor plants
(3) the analysis of specific parts of a structure where it is necessary to examine the internal stress distribution precisely, such as connections, openings or tendon anchorage zones
(4) the analysis concerning the thermal stress condition or heat conduction in a structure where thermal loads are predominant
(5) the analysis of thermal cracks in a massive concrete structure

Fig.2 shows an example of the application of an FEM analysis to the design. This is a finite element mesh for a reinforced concrete hollow "Kan-non (the goddess of mercy)" statue that consists of many different shells.

These examples can be summarized in three categories.

(1) cases that involve great difficulties in converting an original structure into an assemblage of simple structural members, such as beams, columns or frames.
(2) analyses concerning thermal problems
(3) cases that grasp the mechanical behavior of a structure accurately

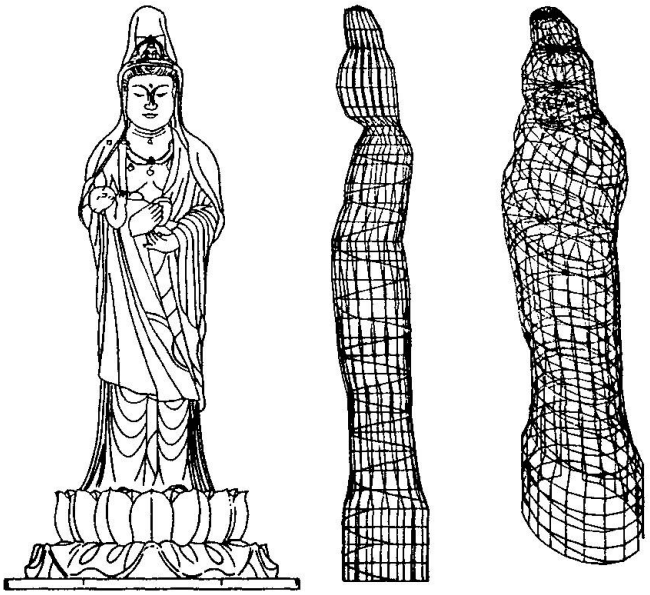

Fig.2 Finite element mesh for the goddess of mercy

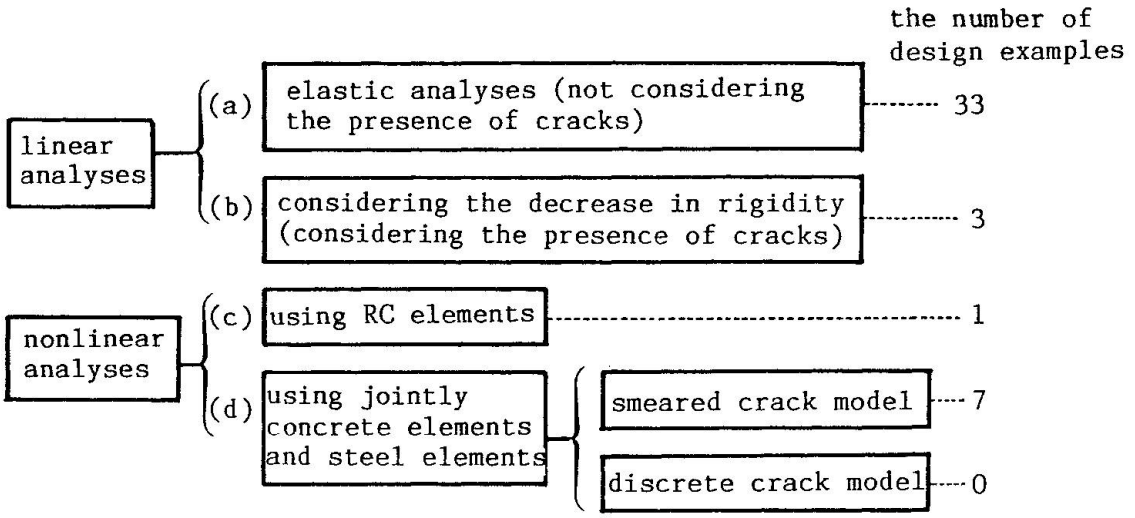

Fig.3 Classification of the methods of finite element analysis and the number of design examples

In general, methods of finite element analysis can be divided as represented in Fig.3. The figure on the right in Fig.3 indicates the number of practical design examples using FEM analyses in the replies.

At first glance it can be seen that most of the analyses applied in practical design are linear analyses. In addition nearly all are perfectly elastic, and don't consider the presence of cracks.

The methods of finite element analysis that consider the presence of cracks can be classified into three types, as represented in Fig.3.

Item (b) is a linear analysis. It assumes the decrease in rigidity according to the presence of cracks to be uniform throughout the whole of a structure. This method is called "an equivalent elastic analysis", and is generally used in cases where the design load levels are not excessively large and estimation of the overall nonlinearity of a structure is sufficient.

Item (c) is a nonlinear analysis. In this case, reinforced concrete elements are used and the behavior of cracks is not considered directly. Reinforced concrete elements can represent the total behavior of reinforced concrete, and the influence of crack propagation is already contained in the employed tension stiffening model. In this method, nonlinearity that is very near the actual behavior of reinforced concrete must be assumed.

Item (d) is also a nonlinear analysis. In this case, the nonlinearity due to the presence of cracks is considered directly. There are two models, that is "a smeared crack model" and "a discrete crack model" in this method. This method can predict the position, the propagation and the width of cracks.

The replies concerning the evaluation of analytical results and the reflection of them on practical design will be explained in Chapter 3.

2.2 Present Situation in the Application of a Linear Analysis

According to replies to the questionnaire, most of the FEM analyses applied to the practical design of RC structures are linear analyses. Nonlinear analyses

considering the presence of cracks and the material nonlinearity are not conducted except for special cases. In most practical design procedures, section forces are obtained by a linear analysis, and stresses of structural members are calculated by a conventional design method stipulated in a design code. A conventional design method ordinarily considers material nonlinearity with a simple form and permits a structure to be decomposed into simple structural members.

In the design of large-scale, complicated structures, such as nuclear reactor plants and underground tanks storing liquefied natural gas, however, the influence of cracks is usually considered. For these structures, the degree of the decrease in rigidity according to cracks is considerably large. To determine the section forces of these structures generated by thermal loads, for instance, the following methods are employed, taking account of the decrease in rigidity.

(1) the application of a pseudo elasto-plastic analysis
(2) the use of a uniform decreasing rate of rigidity
(3) the use of proposed formula predicting the decrease in rigidity

In a pseudo elasto-plastic analysis, a conventional structural analysis is first carried out to obtain section forces. In this structural analysis, the rigidity is determined by assuming that the total area of a section is effective. Secondly, an analysis calculating stresses from the obtained section forces is conducted. As a result of the stress analysis, if it is judged that an arbitrary element contains cracks, the corresponding element is replaced with an anisotropic one whose tensile strength perpendicular to the direction of cracks is zero. Finally the stress analysis is repeated with additional reinforcement arranged in the cracked elements. Though this method is very lucid, it is necessary to execute the analysis twice. Therefore, it demands a certain amount of extra cost for calculation and is troublesome.

In the method using a uniform decreasing rate of rigidity, the elastic rigidity is assumed to be uniform everywhere throughout the whole structure. Usually the uniform decreasing rate is evaluated as one half or one third of the original value. This is due to the presence of cracks and the influence of creep according to long-term thermal loads. Although this method is only tentative, it has been widely adopted in our country because of its ease of application.

In the method using the proposed formula, the decreasing rate of rigidity has to be determined adequately taking account of previous papers, experimental data measured in situ, or other design examples. The method to determine the decreasing rate for combinations of various types of loads is not necessarily proposed, therefore the judgment of the design engineer himself becomes significant. In a linear analysis which does not consider the presence of cracks, section forces and their distributions calculated from a conventional structural analysis are, in general, widely different from actual conditions. Considering the improvement of design, it is advisable to estimate the decrease in rigidity according to cracks. To improve design procedures, it is urgently required that guidelines or standards evaluating the decrease in rigidity be stipulated.

2.3 Present Situation in the Application of Nonlinear Analysis

Procedures for nonlinear analyses with high accuracy have been established in the field of analytical research. Accompanying the recent high-speed proces-

sing of computers, a nonlinear analysis that can predict the actual behavior of RC structures fairly well has become available for practical design. Nevertheless, at present most of the analyses applied to design are linear which consider the equivalent elastic rigidity instead of the actual nonlinearity, as represented in replies to the questionnaire. Even in cases where a nonlinear analysis is carried out, it was replied that the aim is only verification of the results of a linear analysis used in the practical design, or a preliminary analysis for a linear analysis.

Nonlinear analyses have been steadily improved to allow easy and rapid prediction of the actual behavior of RC structures, compared with former days. In spite of the circumstances, a nonlinear analysis still consumes more time and cost for calculation than a linear one. Therefore, in advance of the execution of an analysis for design, a design engineer has to take account of both the merits and demerits of a nonlinear analysis that can adequately predict the actual behavior but will require more time and cost. At that time, a design engineer has naturally accepted as true that the nonlinear behavior of RC structures can be predicted indirectly and almost accurately by a linear analysis corresponding to the level of design loads.

After accepting this situation, the following question was presented in the questionnaire. It represents a case requiring the carrying out of a nonlinear analysis. The replies obtained can be divided into four categories.

(1) the case where high reliability is necessary for practical design
(2) the case where rationalization for design and the saving of cost can be realized remarkably by a nonlinear analysis
(3) the case in which the nonlinearity of a structure is fairly large
(4) the case in which the results of a linear analysis may become dangerous

High reliability is necessary for the design of important structures, such as nuclear reactor plants. These structures have a great social influence. For these structures, the time and cost for calculation are given no consideration, as a reliable analysis accurately predicting actual behavior is essential. At present, this is the most important reason for the execution of a nonlinear analysis.

A remarkable rationalization of design and saving of cost will be realized, for instance in the case where a redistribution of bending moment can occur in statically indeterminate structures. According to the change from the elastic resistant mechanism of a structure to the inelastic one, section forces obtained by linear analyses will alter considerably. As the limit state design method or the ultimate strength design method becomes predominant, practical design examples corresponding to this case will increase.

The degree of nonlinearity of a structure is naturally influenced by the level of design loads. It is necessary to consider nonlinearity in a structure subject to seismic loads, since the displacement of a structure after yielding must be examined. Besides these structures, nonlinearity due to thermal cracks must be examined for massive concrete structures. In massive concrete, thermal cracks and the change of material properties in the process of concrete hardening have an important effect on analytical results. Under these circumstances, nonlinear analyses for massive concrete have been executed very frequently in our country.

When bending moment of a structural member may increase according to the redistribution or the displacement of a structure after yielding must be checked, it is possible that a linear analysis will provide the results on the dangerous

side.

A nonlinear analysis is indispensable for designs where high reliability and safety are required. However, if a nonlinear analysis is always applied to all types of design, design procedures may become irrational. It is important to adequately determine the adoption of a nonlinear analysis considering the intended structures and limit states, the level of design load and the deformation conditions.

3. METHOD REFLECTING ANALYTICAL RESULTS ON DESIGN

The method of reflecting the analytical results of an FEM analysis on practical design is an important matter to design engineers, researchers and developers of computer programs. An established method reflecting analytical results on practical design has not been obtained yet. Therefore, the means of dealing with analytical results differs case by case. However, there are a few almost unified methods according to intended structures or purposes of design.

In a plate bending analysis and a shell analysis, section forces are usually obtained as the output of a calculation. It is possible to use these results directly for a design. In such cases, section forces are rarely calculated by a nonlinear analysis. This is because a linear analysis generally provides conservative results for design. The margin can be incorporated into the degree of the safety for design. Furthermore, the rigorous accuracy of calculation is not necessarily required for a linear analysis.

To determine section forces in a plane stress analysis and a three-dimensional solid analysis, it is necessary to transform the obtained stresses into section forces. Since the obtained analytical results are influenced firmly by the fineness of divided elements, it is difficult to reflect them directly on design. However, in a plane stress analysis or a three-dimensional solid analysis, the shapes and boundary conditions can be assumed to be very similar to those of the actual structure. It is also possible to execute more rational and accurate analyses in comparison with a plate bending analysis or a shell analysis. Considering the convenience for design, it is desirable to apply obtained analytical results directly to practical design, for instance the determination of a section of a structural member or the arrangement of reinforcement. It is expected that the most suitable design method without transforming obtained stresses into section forces will be proposed.

Besides the reflection of analytical results obtained on practical design, some examples of their use as reference data only are reported in replies to the questionnaire. For the case of decomposing special structures into simple structural members, the results obtained are used as implements to examine whether the decomposition itself is adequate or not. Besides this kind of examination, results obtained are used to grasp the actual mechanical behavior of a structure. For these purposes, a nonlinear analysis is usually carried out to secure the safety of the conventional design method independent of a nonlinear analysis.

The following opinion was predominant in the replies. If section forces obtained by a nonlinear analysis are greater than the values estimated in the conventional design, the amount of reinforcement must be increased. On the other hand, if the section forces obtained are smaller than the estimated values, the amount of reinforcement should not be decreased.

In addition, nonlinear analyses have been executed in the following cases where

the degree of safety must be examined out of the application range of a design code or a standard, the validity of design methods stipulated in a design code must be verified, and the results of the design according to different design codes must be compared with each other.

4. SUBJECTS TO BE SOLVED IN FUTURE

Considering the present situation where the occurrence of large and complicated structures, special structures and new construction methods has been frequent, it is indubitable that the application of an FEM analysis to practical design of RC structures will increase rapidly. In these circumstances, some important subjects still remain to be solved.

(1) the certification for computer programs
(2) the preparation of guidelines on the application of FEM analyses for design

Many computer programs for FEM analyses are circulating at present. They can be divided into two types, one being programs developed individually and the other being purchased ones. They are being widely used. In the analysis of complicated structures, it is virtually impossible to verify all analytical results precisely. Design engineers cannot but believe the results to be right. Therefore, it is necessary to certify the validity of a computer program itself, especially for a nonlinear program.

Analytical results are often affected remarkably by the decomposition of an original structure into simple structural members, the division and proportion of finite elements, the assumption of input data and some other causes. Although an FEM analysis can compute stress conditions precisely within an arbitrary limited portion, on the other hand it is possible that an FEM analysis will provide an extremely large output of stresses in some elements. For the cases where the results are changed considerably according to the procedures employed, and extraordinary outputs are provided locally, it is not satisfactory for each design engineer to deal with these problems individually without any restrictions. This matter will bring about a decrease in the reliability of the design. It is urgently required that authorized guidelines for the application of FEM analyses be completed. The preparation of guidelines is intensively desired in the field of design.

5. CONCLUSIONS

Based on the replies to the questionnaire circulated by the JCI Committee, the present situation in the application of an FEM analysis to practical design and subjects to be solved in future were described in the outline. Within the limited replies, it can be adequately predicted that an FEM analysis has been used more often for practical design.

With regard to current tendencies, most of the FEM analyses applied to practical design are linear ones. However, practical examples using nonlinear analyses or linear analyses that indirectly consider nonlinearity are increasing steadily. It has been widely recognized that a nonlinear analysis must be executed in accordance with the intended structure or purpose of the design.

Considering these circumstances, the JCI Committee intends to examine the methods of reflecting analytical results, especially by using a nonlinear analysis, on practical design, and propose guidelines for the application of

FEM analyses to designs.

Acknowledgments

The authors express their deepest appreciation to Prof. H. Okamura who was the former chairman of the JCI Committee for his general advice and valuable suggestions, and also acknowledge the great efforts of the following members of the JCI Committee who replied to the questionnaire.

N.Inoue	Kajima Corporation	K.Maekawa	The University of Tokyo
M.Ueda	Takenaka Komuten Co.	A.Mikame	Fujita Corporation
T.Endo	Central Research Institute of Electric Power Industry	A.Murakami	Chubu Electric Power Co.
		J.Yamazaki	Tokyo Metropolitan University
H.Ono	Taisei Corporation		
I.Shiraishi	Kumagai Gumi Co.	H.Yoshikawa	Hazama-Gumi Co.
Y.Suzuki	Sumitomo Cement Co.	F.Watanabe	Kyoto University
K.Naganuma	Ohbayashi Corporation	Y.Watanabe	Shimizu Construction Co.

References

[1] H.AOYAMA and H.NOGUCHI, "Future Prospects for Finite Element Analysis of Reinforced Concrete Structures - A Compilation of Questionnaire Results from JCI-RCFEM Committee Members -", Finite Element Analysis of Reinforced Concrete Structures, pp.667-681, ASCE, 1986

[2] S.IKEDA and T.TSUBAKI, "Application of the Finite Element Method to the Design of Concrete Structures", Finite Element Analysis of Reinforced Concrete Structures, pp.621-644, ASCE, 1986

Leere Seite
Blank page
Page vide

Prediction of Response of Concrete Beams and Panels by Nonlinear Finite Element Analysis

Prédiction de la résistance de poutres et de panneaux en béton par l'analyse non-linéaire des éléments finis

Vorhersage des Verhaltens von Betonbalken und -Scheiben mittels nichtlineare Finite Element Berechnung

S. BALAKRISHNAN
Senior Engineer
Duthie, Newby, Weber Assoc.
Edmonton, AB, Canada

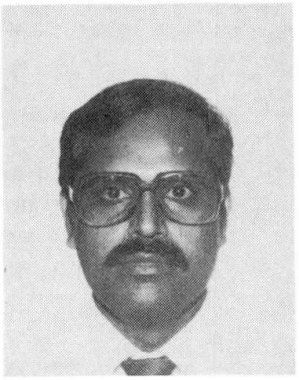

S. Balakrishnan received his Ph.D. degree in Civil Engineering from the Univ. of Alberta, Edmonton, Canada. He has had over 12 years of practical experience in the design of buildings and bridges. His research interests are in the areas of limit and finite element analysis of concrete structures.

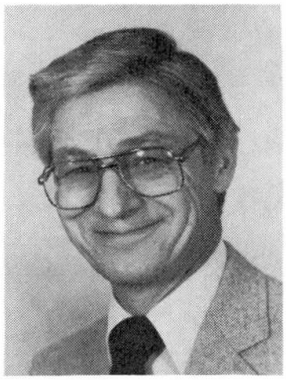

D.W. Murray is a civil engineer holding a B.Sc. from the Univ. of Alberta, Edmonton; a M.Sc. from Imperial College, London; and, a Ph.D. from the Univ. of California, Berkeley. He has been a member of the academic staff at the Univ. of Alberta since 1960.

D.W. MURRAY
Professor
Univ. of Alberta
Edmonton, AB, Canada

SUMMARY
In order for practising engineers to have confidence in the use of NLFEA (Nonlinear Finite Element Analysis) for concrete, there is a need for verification that the method gives results which consistently agree with test data on beams and panels exhibiting various failure modes. In this paper, finite element formulations are presented, and a simple constitutive relationship is described, which have been found to be effective in predicting behavior for a wide range of beams and panels.

RÉSUMÉ
Afin de permettre aux ingénieurs praticiens d'avoir confiance dans l'utilisation de l'analyse par méthode des éléments finis non-linéaires pour le béton, il faut vérifier que cette méthode donne des résultats qui sont en accord permanent avec des résultats d'essais sur des poutres et des panneaux ayant subi des dommages divers. La formulation par éléments finis est présentée; la relation constitutive simple décrite a permis de prévoir le comportement réel d'un grand nombre de poutres et de panneaux.

ZUSAMMENFASSUNG
Der Vergleich mit Versuchsresultaten soll dem Ingenieur in der Praxis Vertrauen in nichtlineare FE-Analysen (NLFEA) geben. Der Beitrag gibt FE-Formulierungen und einfache Werkstoffgesetze, die sich bei vielen Balken- und Scheibentragwerken bewährt haben.

1. INTRODUCTION

The vast majority of global structural analyses in engineering offices follow traditional patterns - linearized, simplified models in which the reinforced concrete system is assumed to be uncracked, homogeneous and isotropic. The internal forces and moments calculated from these models are then used to design the members based on ultimate strength using the code provisions which in turn have been based on simplified models and synthesis of experimental data. Special and complex structural problems are often solved using intuitive judgement and/or tests on small scale models. Even plasticity based methods involve assumptions regarding the material behavior and the use effectiveness factors to correlate with experimental data.

The finite element method (i.e., FEM), because of its ability to take into account the conditions of equilibrium, compatibility and nonlinear material behavior, is a valuable analytical tool which can be used to: (1) directly predict the structural response in the entire load range up to failure; (2) gain greater understanding of the behavior so that simpler but realistic models can be developed; and, (3) study the effects of important parameters on member behavior thus providing a firmer basis for code provisions.

However, in order for practicing engineers to have confidence in the FEM, there is a need for verification that the method gives results which consistently agree with experimental data for a wide range of geometric and material parameters. Often general purpose codes which purport to have the capability of nonlinear concrete analysis have proved to be a disappointment to practitioners. There is little point to a code which can properly predict flexural failure if it predicts such a failure when the true structural failure is a shear failure.

Also, in order for the practicing engineer to use the nonlinear FEM, the cost and time constraints must not be exceeded. The cost and time involved in the application of the nonlinear FEM must be competitive with other possible approaches, such as testing programs, or perhaps just using a larger factor of safety in design. Thus there is a need to determine the influence of various parameters used in the numerical analysis in predicting the behavior so that individual analyses can be tuned to the desired accuracy.

2. OBJECTIVES

The objectives of this paper are:

1. to describe a simple constitutive relationship for concrete which the authors have found to be effective in the solution of plane stress modeling of beams [1] and panels [2];

2. to demonstrate the applicability of the models by comparing the predicted behavior to the behavior observed in the laboratory for specimens exhibiting various types of failure modes;

3. to present the authors' experience with respect to the effects (on the analysis) of various material parameters and their importance relative to the various failure modes.

3. FINITE ELEMENT FORMULATIONS

A typical finite element model used by the authors for a beam structure is composed of quadratic serendipity concrete elements, embedded primary reinforcing steel, and distributed bond elements selectively placed along the reinforcement [1]. Where bond elements are included, nodal points along the

reinforcement layer, each with a single slip degree of freedom, must be added.

The formulation of isoparametric elements is available in the literature (see, for example [3], [4]). The formulations for the embedded reinforcement and bond elements are presented in [1] and summarized briefly in the following.

The the authors' knowledge, all embedded and distributed representations for reinforcement that are currently available in literature assume perfect bond between steel and concrete. An embedded reinforcement formulation including bond-slip is developed herein. Such a formulation obviates the need for locating the reinforcing element nodal points at the solid element boundaries.

The virtual work of a reinforcing element is given by

$$\sum_{m} \int \delta\varepsilon_s \sigma_s A_s dr$$

where A_s is the cross-sectional area of reinforcement; dr is the differential length; ε_s is the strain in reinforcement and σ_s is the stress in reinforcement. Considering the reinforcing element, as shown in Fig. 1, the steel displacement w_s at any point of the element in a direction tangential to the reinforcing bar is written as

$$w_s = w_c + w_b \qquad (3.1)$$

where w_c is the displacement of the concrete at that point as interpolated from nodal displacements and w_b is the bond slip (i.e. the relative displacement between the steel and the concrete).

From Fig. 1,

$$w_c = u \cos\theta + v \sin\theta \qquad (3.2)$$

Let $U_{b_1}, U_{b_2} \ldots U_{b_p}$ be p slip degrees of freedom of p nodes located on the reinforcement within the element.
Then,

$$w_b = \sum_{j=1}^{p} H_j U_{b_j} \qquad (3.3)$$

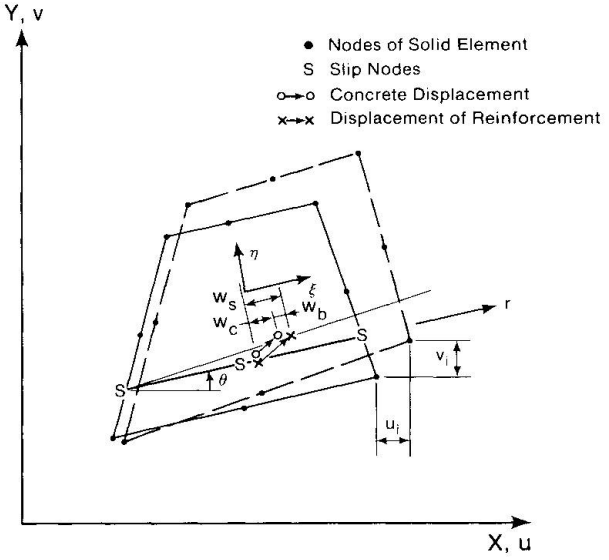

Fig. 1. Displacements for Embedded Bond Elements

where H_j are the shape functions used to interpolate the bond slip at any point. The strain in the reinforcing steel at any point is

$$\varepsilon_s = \frac{dw_s}{dr} \qquad (3.4)$$

From Eqs. 3.1, 3.2 and 3.4, and assuming that θ does not vary along the element,

$$\varepsilon_s = \frac{du}{dr}\cos\theta + \frac{dv}{dr}\sin\theta + \frac{dw_b}{dr} \qquad (3.5)$$

Considering for simplicity that the reinforcing element is placed parallel to a natural coordinate axis, say the ξ axis, the relationships

$$du = \frac{\partial u}{\partial \xi} d\xi + \frac{\partial u}{\partial \eta} d\eta \quad ; \quad dv = \frac{\partial v}{\partial \xi} d\xi + \frac{\partial v}{\partial \eta} d\eta \tag{3.6}$$

will reduce Eq. (3.5) to

$$\varepsilon_s = \frac{1}{J_s} \langle \cos\theta \quad \sin\theta \rangle \begin{bmatrix} \langle \frac{\partial N_i}{\partial \xi} \rangle & \langle 0 \rangle \\ \langle 0 \rangle & \langle \frac{\partial N_i}{\partial \xi} \rangle \end{bmatrix} \begin{Bmatrix} u_i \\ v_i \end{Bmatrix} + \frac{1}{J_s} \langle \frac{dH_j}{d\xi} \rangle \{U_{b_j}\} \tag{3.7}$$

wherein u_i, v_i are the nodal displacements, i = 1, 2, ... q; q = the total number of nodes for the solid element; N_i = the shape functions; j = 1, 2, ... p; and $J_s = \sqrt{\left(\frac{dx}{d\xi}\right)^2 + \left(\frac{dy}{d\xi}\right)^2}$.

The stiffness matrix for the reinforcing element is formed and assembled in the standard manner using Eq. 3.7 to describe the steel strain, and added to the stiffness matrix of the solid element.

The virtual work of the bond element is given by

$$V.W._{bond} = \delta \langle U_{b_j} \rangle \left[\sum_{m} \int_{-1}^{1} \{H_j\} D_b \langle H_j \rangle A_p J_s d\xi \right] \{U_{b_j}\} \tag{3.8}$$

where D_b is the bond stress producing unit slip, m is the number of bond elements in the solid element and A_p is the contact area per unit length of reinforcing steel. The factor in the brackets in the Eq. 3.8 is the stiffness matrix for the bond elements and is assembled with the solid and reinforcement element matrices in the standard manner.

4. CONSTITUTIVE MODEL

The approach taken herein is to attempt to find the simplest possible constitutive model that can capture those essential characteristics of reinforced concrete behavior which are necessary in order to reliably reproduce basic types of observed failure modes for a limited class of structures, namely, net reinforced concrete panels and reinforced concrete beams. Reliability of the model to achieve this result is the paramount consideration.

The model is intended for use in a 'smeared cracking' type of finite element analysis. A more detailed description of the constitutive model is given in [5]. It has a piecewise linear uniaxial stress-strain relationship, with tension softening and tension stiffening for tensile response, and strain

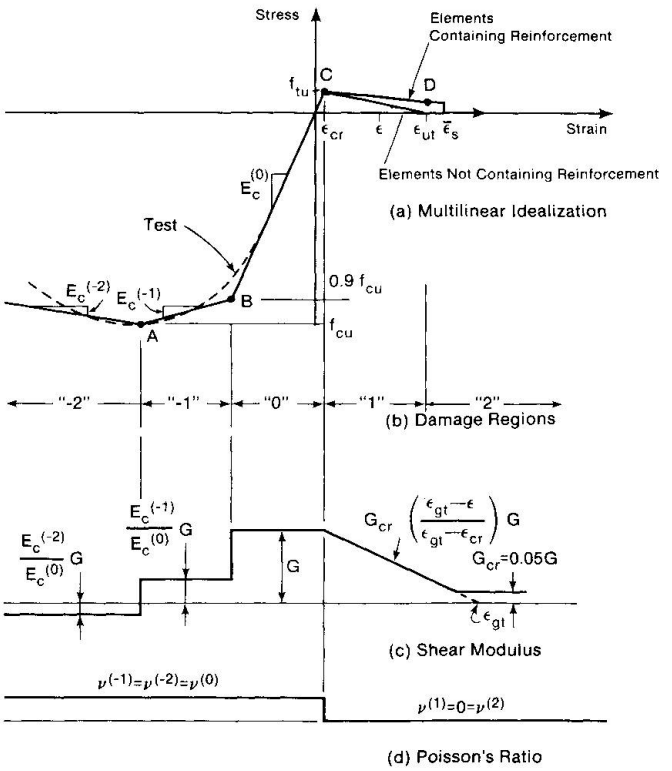

Note: superscripts in parentheses denote damage regions.

Fig. 2. Assumed Strain Dependence of Concrete Properties

hardening and strain softening for compressive response, as shown in Fig. 2. The points of slope discontinuity of the uniaxial curve divide the idealized stress-strain response curve into regions referred to as 'damage regions'. These also are shown in Fig. 2.

When used under biaxial stress conditions the model is considered orthotropic after cracking and the direction of cracking dictates the orientation of the orthtropic axes. The shear stiffness is considered to be piecewise linear and may be discontinuous between damage regions as indicated in Fig. 2. The peak values of the stress-strain curve under biaxial stress conditions are adjusted to those associated with the 'failure envelope' of Fig. 3, which is a modification of the Kupfer-Hilsdorf failure curve. The modification is in the tension-compression stress space and consists of the separate specification of the compressive and tensile failure curves. For load path OA in Fig. 3, the cracking occurs at A and the post-cracking compressive strength is given by the abcissa of B where AB is a horizontal line.

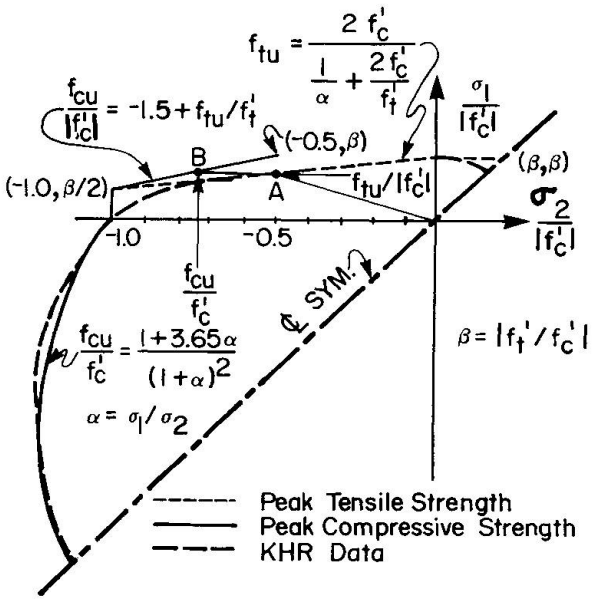

Fig. 3. Peak Strength Envelopes in Biaxial Stress Space

In the undamaged region, i.e., region "0" of Fig. 2, the constitutive relationship is considered isotropic and the incremental biaxial stress strain relationship is given by

$$\begin{Bmatrix} d\sigma_1 \\ d\sigma_2 \\ d\tau_{12} \end{Bmatrix} = \frac{E_c^{(0)}}{1 - \nu^2} \begin{bmatrix} 1 & \nu & 0 \\ \nu & 1 & 0 \\ 0 & 0 & \frac{1-\nu}{2} \end{bmatrix} \begin{Bmatrix} d\varepsilon_1 \\ d\varepsilon_2 \\ d\gamma_{12} \end{Bmatrix} \qquad (4.1)$$

with respect to any set of reference axes. Poisson's ratio is assumed constant as shown in Fig. 2.

Cracking is assumed to occur on the plane of maximum principal stress when this maximum principal stress reaches the dotted line of Fig. 3. The material is then assumed to be orthotropic with the axes of orthotropy parallel and orthogonal to the crack. Poisson's ratio is set to zero when cracking is initiated, and Eq. 4.1 becomes

$$\begin{Bmatrix} d\sigma_1 \\ d\sigma_2 \\ d\tau_{12} \end{Bmatrix} = \begin{bmatrix} E_c^{(1)} & 0 & 0 \\ 0 & E_c^{(k)} & 0 \\ 0 & 0 & G_{cr} \end{bmatrix} \begin{Bmatrix} d\varepsilon_1 \\ d\varepsilon_2 \\ d\gamma_{12} \end{Bmatrix} \qquad (4.2)$$

in which k indicates the damage region. The response in the two in-plane orthotropic directions is, therefore, uncoupled. Equations 4.1 and 4.2 have been used effectively with a 'fixed crack technique' for beams [1] and a 'rotating crack technique' for orthogonally reinforced elements [2].

In the rotating crack model, as adapted by the authors, the axes of orthotropy are assumed to coincide with the principal strain axes (total strains up to the previous iteration) even after cracking, whereas in the fixed crack model the axes of orthotropy are fixed parallel and perpendicular to the crack at the onset of cracking. The rotating crack model is used for orthogonally reinforced elements where it has been shown both theoretically [6,7] and experimentally [8] that crack direction may change, at least in an average sense. The fixed crack model is used for elements containing no reinforcement or reinforcement in one direction only, where appreciable crack rotation may not occur.

Two interrelated phenomena associated with cracking, namely 'tension softening' at the cracks, and the 'tension stiffening' effect of intact concrete segments between the macro cracks, should be taken into consideration in the determination of $E_c^{(1)}$, the post-cracking strain softening modulus. Tension softening is related to the fracture energy release rate (i.e. energy expended in the formation of a unit area of a crack, G_f for mode I cracking) by

$$\varepsilon_{ut} = \frac{2\,G_f}{f'_t\,S} \tag{4.3}$$

where ε_{ut} is the strain at which the normal stress at crack interface has reduced to zero (Fig. 2), S is the crack spacing and f'_t is the peak tensile stress as determined from a split cylinder test.

The tension stiffening is dependent on the crack spacing, reinforcement ratio and bond slip characteristics of the steel/concrete interface. Assuming a bilinear concrete stress variation and an incipient crack about to form midway between two macrocracks, tension softening and tension stiffening are combined [5] to produce the relationship

$$\sigma_t = \frac{f_{tu}}{2}\left\{1 + \frac{\varepsilon_{ut} - \varepsilon}{\varepsilon_{ut} - \varepsilon_{cr}}\right\} \quad \text{for} \quad \varepsilon_{cr} < \varepsilon < \varepsilon_{ut} \tag{4.4a}$$

and

$$\sigma_t = \frac{f_{tu}}{2} \quad \text{for} \quad \varepsilon > \varepsilon_{ut} \tag{4.4b}$$

The shear modulus of cracked concrete is dependent on the crack width and therefore, in a smeared crack approach, on the tensile strain. In order to account for dowel action and for numerical stability, G_{cr} is always taken to be greater than or equal to 5% of the uncracked concrete shear modulus. The value to be used for ε_{gt}, shown in Fig. 2, depends on the expected crack spacing and crack width. Based on numerical studies [1,2] it was found that for beams ε_{gt} of Fig. 2 can be taken to be equal to ε_{ut} whereas for net-reinforced panels (in which cracks are finer and more distributed) a value between 0.005 and 0.01 appears satisfactory.

It has been recognized that when strain localization occurs, standard tests no longer measure the fundamental material properties, but rather the structural system under test. (See, for example, [9].) Therefore, the strain softening modulus in compression should be related to the mesh size and the degree of confinement. At the present time, no reliable method appears to be available to relate the element size to a 'homogenized' compressive strain softening modulus. Again, based on numerical studies, a value of -0.05E is recommended for beams without web reinforcement. For beams with confining reinforcement, the expression in [10] was found to yield good results.

5. APPLICATION TO REINFORCED CONCRETE PANELS

The load-deformation behavior of orthotropically reinforced panels is characterized by significant changes in the orientation of the principal axes and reduction in stiffness after concrete cracks. The three major failure modes of the panels are: (1) ductile failure by both layers of steel yielding, designated as the 'D' mode of failure herein; (2) brittle failure by crushing of concrete in compression, designated as the 'B' mode herein; and (3) crushing of concrete after one layer of steel yields, denoted as the 'DB' mode herein.

The rotating crack model was used, in conjunction with the constitutive relationships and the post-cracking compressive strength criterion described in Section 4, to predict the behavior of some of the panels tested by Vecchio and Collins [8]. The results are summarized in Table 1. Comparison to the experimental results is shown in Fig. 4. The prediction using the empirical relationships of Vecchio and Collins [8] is also shown in Fig. 4. Panels PV4 and PV11 failed in the 'D' mode; Panels PV10, PV19, PV21 and PV29 failed in the 'DB' mode; Panels PV23, PV25 and PV27 failed in the 'B' mode. Panels PV19, PV27, PV25 and PV29 were the subject of an international competition [11].

It is seen that the failure load and the global stress-strain predictions using the FEM are reasonably accurate. The failure mode has been correctly predicted in all cases. Failure loads for panels failing in the D or DB modes have been accurately predicted using the FEM and are close to those obtained using plasticity based methods [12]. Failure loads of panels failing in the B mode have been somewhat underestimated, mainly due to the underestimation of the tension stiffening contribution. Panels PV27 and PV23 contain the same reinforcement ratio and were made of concrete of the same cylinder compressive strength but PV27 was loaded in pure shear whereas PV23 was loaded in biaxial compression in addition to shear. The FEM predicts an increased shear strength for Panel PV23 due to the action of compressive stresses.

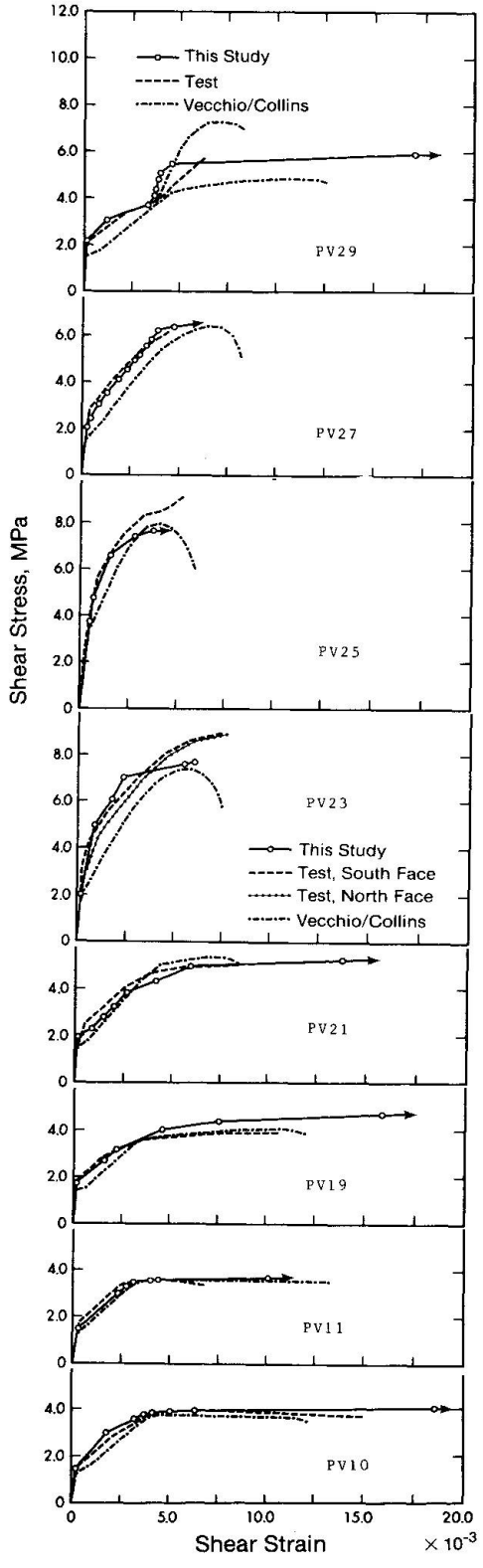

Fig. 4. Comparison with Tests for Vecchio/Collins Panels

Panel	Loading Condition $\tau:f_x:f_y$	Steel Reinforcement X Direction ρ_x	f_{sx} MPa	Y Direction ρ_y	f_{sy} MPa	Concrete f'_c MPa	Experimental† Failure Mode	Failure Load MPa	FE Prediction Failure Mode	Failure Load MPa	Experimental / Finite Element
PV4	1:0:0	.01056	242	.01056	242	26.6	D	2.89	D	2.60	1.11
PV10	1:0:0	.01785	266	.00999	276	14.5	DB	3.97	DB	4.00	0.99
PV11	1:0:0	.01785	235	.01306	235	15.6	D	3.56	D	3.60	0.99
PV19	1:0:0	.01785	458	.00713	299	19.0	DB	3.95	DB	4.45	0.89
PV21	1:0:0	.01785	458	.01296	302	19.5	DB	5.03	DB	5.20	0.97
PV23	1:-0.39:-.39	.01785	518	.01785	518	20.5	B	8.87	B	7.60	1.17
PV25	1:-.69:-.69	.01785	466	.01785	466	19.2	B	9.12	B	7.70	1.18
PV27	1:0:0	.01785	442	.01785	442	20.5	B	6.35	B	6.25	1.02
PV29	1:0:0 1:-1:-1	.01785	441	.00885	325	21.7	DB	5.87	DB	5.90	1.0

† Ref. [8]
D - Both x and y direction reinforcement yielded at failure.
DB - Y direction reinforcement yielded; X direction reinforcement not yielded, concrete crushing failure.
B - Neither reinforcement layer yielded at failure; concrete crushing failure.

Table 1. Finite Element Prediction of Panel Failure

Panel PV29 was loaded in pure shear until one layer of reinforcement yielded. Subsequent shear loading was accompanied by the application of biaxial compressive stresses of equal magnitude. The fact that the behavior of this panel has been predicted with reasonable accuracy shows that the FEM and the post cracking compressive strength criterion as developed herein may be used for nonproportional loading.

6. APPLICATION TO REINFORCED CONCRETE BEAMS

The principal modes of failure in R/C beams are: (1) ductile flexural failure by yielding of primary reinforcement, (2) diagonal shear failure of beams without web reinforcement, (3) shear-compression failure of beams with web reinforcement, (4) compressive failure of concrete in over-reinforced beams, (5) brittle failure of 'compression struts' in deep beams, and (6) 'local' failure such as bearing failure and anchorage bond failure.

The 'fixed crack model', in conjunction with the constitutive relationship described in Section 3, was used to predict the behavior of a number of beams exhibiting the different failure modes described above. Table 2 lists some of the beams analyzed and Figs. 5, 6 and 7 show their load-deflection behavior. Fig. 5 illustrates a flexural failure, Fig. 6 illustrates shear failures and Fig. 7 illustrates bearing and compressive strut failures.

In most nonlinear finite element analyses the failure load is assumed to have been reached when there is failure of convergence of force and/or displacement vector norms, or if the tangent stiffness matrix contains a zero or negative element on the diagonal. The corresponding load is referred to as the collapse load although it might be the numerical procedure that has failed and not the structure. Thus, it is important to confirm that failure of the structure has in fact occurred and to determine the mode and causes of failure.

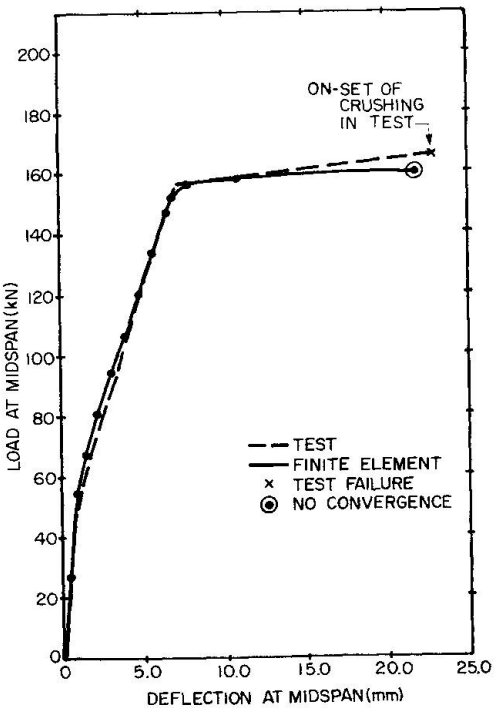

Fig. 5. Comparison with Tests for Beam Flexural Failure

Beam[7]	Reference	Failure[8] Mode	a/d	Web Reinforcement?	Span m	Depth mm	Reinforcement %	Load in Test kN	Load by NLFEA kN	Test Load / NLFEA Load
BUS J-4	[13]	SY	4.33	No	3.96	457	1.09	167	160	1.044
BRS 0A1	[14]	DT	3.97	No	3.66	461	1.81	334	343	0.974
BRS 0A2	[14]	DT	4.90	No	4.57	466	2.27	356	356[1] 400[2]	1.000
BRS 0A3	[14]	DT	6.94	No	6.40	461	2.74	37.8	400	0.945
BRS A1	[14]	SC	3.92	Yes	3.66	466	1.80	467	427	1.094
BRS A2	[14]	SC	4.93	Yes	4.57	464	2.28	489	445	1.099
BRS A3	[14]	FC	6.91	Yes	6.40	466	2.73	467	511	0.914
ROM 1/1.0	[15]	CS	1.0	No	2.0	950	0.95	1204[3] 1398[4]	1180[5] 1200[6]	1.093
LEW WT3	[16]	BF	0.5	Yes	1.44	1385	0.29	1290	1216	1.061

Mean = 1.025

(1) Based on relative vertical displacement
(2) Based on failure of convergence
(3) Compressive failure on North end
(4) Compressive failure on South end
(5) Quadratic elements
(6) Bilinear elements
(7) BUS = Burns-Siess
BRS = Bresler-Scordelis
ROM = Rogowski-MacGregor
LEW = Leonhardt-Walther

(8) Failure Mode Notation
SY = Flexural failure by steel yielding
DT = Diagonal tension failure
SC = Shear compression failure
FC = Flexural compression failure
CS = Compressive strut failure
BF = Bearing failure

Table 2. Finite Element Prediction of R/C Beam Behavior

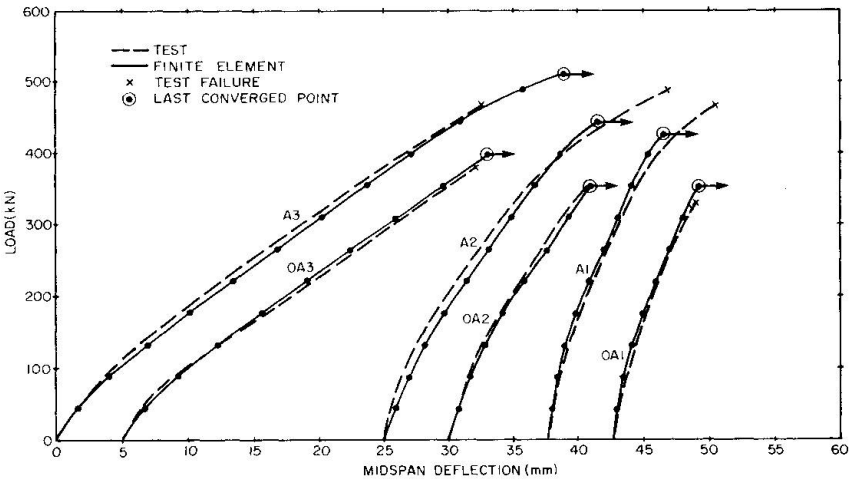

Fig. 6. Comparison with Tests for Beam Shear Failures

A number of failure 'indicators' may be used for this purpose. Details of these indicators are described elsewhere [1,17]. However, a short description of the most important is as follows.

The failure mode of beams failing by primary steel yielding can be simply verified by steel and concrete stresses and strains at the final load step. For shear critical beams without web reinforcement, the indicators are: (1) the relative vertical displacement (sometimes referred to as 'thickening' [14]) between the top and bottom faces of the beam shows marked increase before failure, Fig. 8; (2) the shear strains tend to be of the same order of magnitude as normal strains, Fig. 9; (3) steel and concrete flexural stresses are well below their maximum values; and, (4) the crack pattern shows cracking near the neutral axis in an almost horizontal direction and extending into the compression region, Fig. 10. For beams failing in diagonal compression (i.e failure of a compressive strut), the compressive stress plot as shown in Fig. 11 gives an indication of the failure mode.

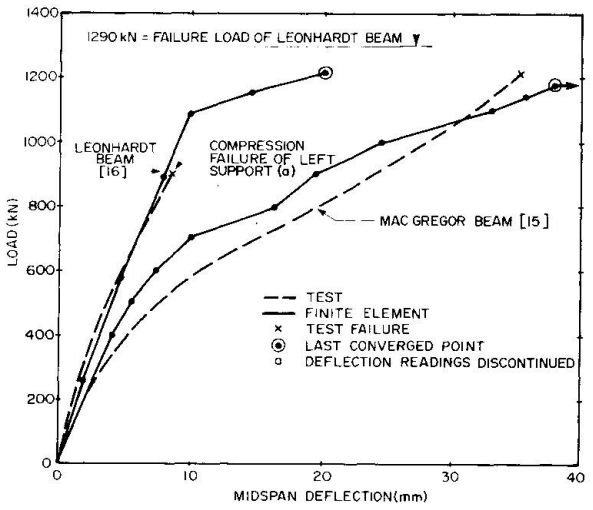

Fig. 7. Comparison with Tests for Bearing and Strut Failures

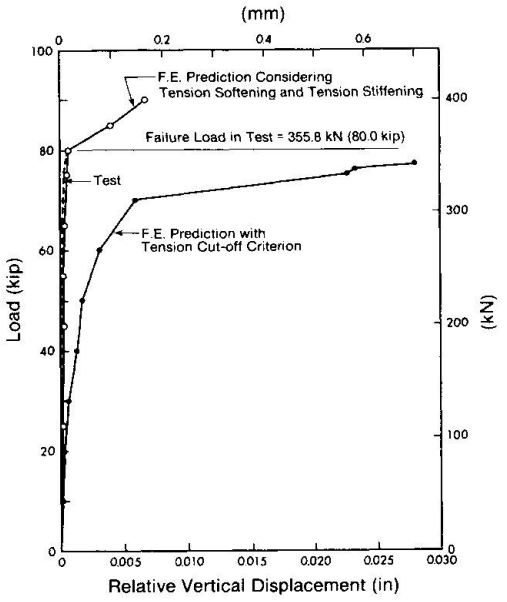

Fig. 8. Detection of Beam Shear Failure by Thickening

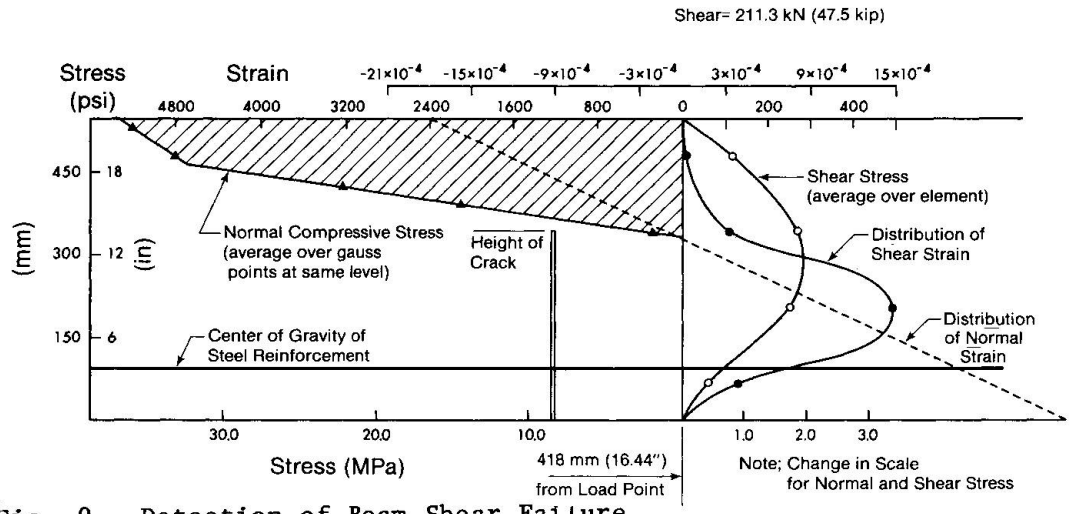

Fig. 9. Detection of Beam Shear Failure by Shear Strain

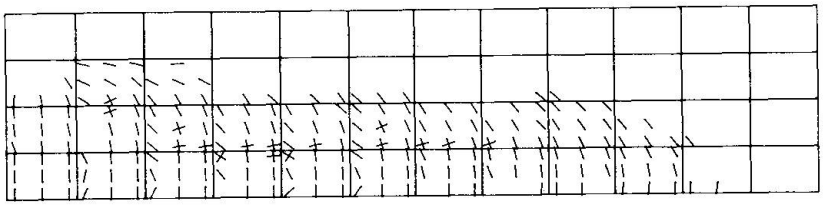

Fig. 10. Detection of Beam Shear Failure by Cracking

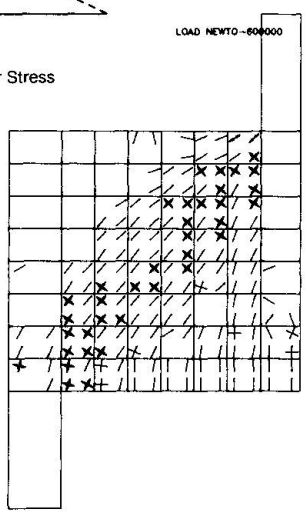

Fig. 11. Diagonal Strut Compression Failure

7. INFLUENCE OF MATERIAL PARAMETERS ON THE FAILURE PREDICTION

In the authors' experience, the predicted response is often insensitive to the precise values of the parameters required to describe the curves of Fig. 2 and 3. However each feature of these curves is important in predicting some aspect of behavior as various failure modes appear. For example, a tension cut-off criterion failed to predict satisfactorily the failure load and failure mode of shear critical beams. For this class of beams, it is also important to adequately represent the dependency of shear stiffness of cracked concrete on crack width (i.e., on crack strain in smeared crack analysis). The use of a constant shear retention factor leads to failure predictions which are highly dependent on the actual factor adopted. For beams failing in shear-compression, such as those containing high web reinforcement ratios, and for panels failing before steel yielding, the compressive strain hardening and softening moduli significantly influence the failure mode and failure load. The post-cracking compressive strength of concrete has a major influence on the failure load of deep beams and panels with high reinforcement ratios.

8. CONCLUSIONS

1. The major conclusion of the study reported in this paper is that the finite element method can be used to closely predict the behavior of reinforced concrete members subjected to in-plane forces if proper care is taken in modeling the material characteristics. The load deflection behavior, crack pattern, failure load and failure mode can be predicted with an accuracy that is acceptable for engineering purposes.

2. In order to obtain reliable predictions, it appears to be necessary to properly include consideration of major sources of nonlinearity in reinforced concrete, namely: tension softening and tension stiffening; compressive strain hardening and strain softening; variation of shear modulus with crack width; and, bond slip between steel and concrete. For proper 'homogenization' of these material properties, structural details and response characteristics must be included in their determination. This requires that the analyst be knowledgeable about how the behavior of the structure will affect these properties. Techniques of estimating these properties are given in [1], but are not included herein because of space limitations. More detailed descriptions of the analyses will appear subsequently in the literature [2,5,17].

9. REFERENCES

1. BALAKRISHNAN, S. and MURRAY, D.W., Finite Element Prediction of Reinforced Concrete Behavior, Structural Engineering Report No. 138, Department of Civil Engineering, University of Alberta, July 1986.

2. BALAKRISHNAN, S. and MURRAY, D.W., Prediction of RC Panel Behavior by NLFEA, Submitted for publication to the Journal of Structural Engineering, ASCE, New York, 1987.

3. BATHE, K.J., Finite Element Procedures in Engineering Analysis, Prentice-Hall, Englewood Cliffs, New Jersey, 1982.

4. ZIENKIEWICZ, O.C., The Finite Element Method, McGraw-Hill Book Company (UK) Ltd., London, 1977.

5. BALAKRISHNAN, S. and MURRAY, D.W., Concrete Constitutive Model for NLFE Analysis of Structures, Submitted for publication in the Journal of Structural Engineering, ASCE, New York, N.Y., 1987.

6. GUPTA, A.K. and HABIBOLLA, A., Changing Crack Direction in Reinforced Concrete Analysis, Report, Dept. of Civil Engineering, North Carolina State University, Raleigh, 1982.

7. COPE, R.J. and RAO, P.V., Non-linear Finite Element Strategies for Bridge Decks, IABSE Colloquium on Advanced Mechanics of Reinforced Concrete, Delft, 1981.

8. VECCHIO, F.J. and COLLIS, M.P., Response of Reinforced Concrete to In-Plane Shear and Normal Stresses, Publication No. 82-03, Department of Civil Engineering, University of Toronto, March 1982, 332 p.

9. DE BORST, R., Nonlinear Analysis of Frictional Materials, Doctoral Thesis, Delft University of Technology, Delft, The Netherlands, 1986.

10. VALLENAS, J., BERTERO, V.V. and POPOV, E.P., Concrete Confined by Rectangular Hoops and Subjected to Axial Loads, Report No. UCB/EERC-77/12, University of California, Berkeley, 1977.

11. COLLINS, M.P., VECCHIO, F.J. and MELHORN, G. An International Competition to Predict the Response of Reinforced Concrete Panels, Canadian Journal of Civil Engineering, Vol. 12, No. 3, 1985, pp. 624-644.

12. NIELSEN, M.P., Limit Analysis and Concrete Plasticity, Prentice-Hall Inc., New Jersey, 1984.

13. BURNS, N.H. and SIESS, C.P., Repeated and Reversed Loading in Reinforced Concrete, ASCE Journal of the Structural Division, Vol. 92, ST5, 1966, pp. 65-78.

14. BRESLER, B. and SCORDELIS, A.C., Shear Strength of Reinforced Concrete Beams, ACI Journal, Vol. 60, NO. 1, 1963, pp. 51-73.

15. ROGOWSKY, D.M., MACGREGOR, J.G., and ONG, S.Y, Tests of Reinforced Concrete Deep Beams, ACI Journal, Proceedings, Vol. 83, No. 4, 1986, pp. 614-623.

16. LEONHARDT, F. and WALTHER, R., Wandertige Trager, Report, Deutscher Ausschuβ für Stahlbeton, Heft 178, Berlin, 1966.

17. BALAKRISHNAN, S., ELWI, A.E. and MURRAY, D.W., Application of FEM to Predict Concrete Beam Behavior, to be submitted to the Journal of Structural Engineering, ASCE, New York, 1987.

Examples of Non-Linear Numerical Analysis with DIANA

Exemples d'analyse numérique non-linéaire avec DIANA

Beispiele nichtlinearer, numerischer Berechnungen mit DIANA

Theo MONNIER
Institute TNO-IBBC
Delft, The Netherlands

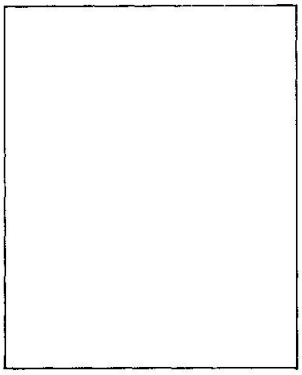

The author, born in 1935, got his civil engineering degree at the Delft University of Technology. He was for 17 years Head of the Department for Concrete Structures of TNO-IBBC and is now deputy-director of the Institute.

SUMMARY
A number of examples of non-linear numerical analysis with DIANA are made to illustrate the actual possibilities and the progress made with advanced concrete mechanics. The numerical model appears to be a new and powerful instrument especially for specific practical studies and research purposes more generally.

RÉSUMÉ
Certains exemples d'analyses non-linéaires numériques avec DIANA permettent d' illustrer les possibilités actuelles et le progrès dans la mécanique des structures en béton armé. Il est évident que le modèle numérique est un instrument nouveau et puissant pour des études pratiques, ainsi que pour la recherche en général.

ZUSAMMENFASSUNG
Eine Anzahl von Beispiele nichtlinearer numerischer Berechnungen mit DIANA wurde ausgeführt um zu illustrieren welche Möglichkeiten entstanden sind und welche Fortschritte mit rechnischer Mechanik von Konstruktionen aus Stahlbeton gemacht wurden. Es stellte sich heraus dass das numerische Modell ein neues und starkes Hilfsmittel für praktische Studien und für Forschung im allgemeinen ist.

1. INTRODUCTION

1.1 General

The Dutch "Concrete mechanics project" is an on-going co-operative research program. The objective of this project is to analyse the structural behaviour of reinforced concrete members by simulation through an advanced numerical model. In this numerical scheme - which accounts for the geometry of the structure under consideration - advanced material-models are applied and additionally basic-models for effects from cracking of concrete, bond-slip behaviour between reinforcement and concrete and aggregate interlock for stress transfer in cracks. The investigations are carried out by material-scientists and specialists in numerical modelling and applied mechanics.
The Dutch Technical Universities of Delft and Eindhoven, the Rijkswaterstaat - a division of the Ministry of Transport and Public Works - and the Institute for Applied Scientific Research on Building Materials and Structures (TNO-IBBC) are the participants in this co-operative program. The activities are financially supported by CUR - centre for civil engineering research, codes and specifications - and MaTS - marine technological research.

1.2 Examples of analysis

Although three numerical models have been developed, the study now concentrates for several years specifically on DIANA, a general purpose finite element code for the analysis of three dimensional structures.
This report concerns a number of examples of non-linear numerical analysis of reinforced concrete structures made with DIANA. The examples are completely explained in Heron 1987 nr. 3: "Examples of non-linear analysis of reinforced concrete structures with DIANA", by dr.ir. J.G.M. van Mier, ir. C.R. Braam, ir. H. Groeneveld, ir. J. F. Marcelis, prof. Chr. Meyer and ir. J.G. Rots.
The examples include the simulation of three structural details (a tooth support of a beam, a corbel and a beam to columm connection), three global structures (deep beams in two variants, a tunnel section and a LNG-storage tank subjected to fire) and two dynamic analysis (a beam falling on a shock absorbing element and an explosion in a tunnel). All simulations are two dimensional except for the storage tank, which is treated as an axi-symmetric problem.

1.3 Application

In principle the non-linear numerical analysis concerned, fit into a design-procedure like experimental model studies do. This means that the practical application of these analysis will be limited to specific cases in which design has been carried out e.g. by linear analysis or on the basis of equilibrium conditions and non-linear compatibility must be checked properly by specific studies. Of course, this will concern complex combinations of action effects in most cases. Other situations in which additional analysis may be required concern for instance: expected non-linear stress-distributions as in deep beams or redistribution of action-effects specifically at lower load levels or combined with shear. For unlimited use of non-linear analysis in this practical scheme, the simulation of the real behaviour of the structure under consideration must be reliable. In the future this status may be expected in a wide range of application.
Nowadays, the numerical simulation technique appears to be applicable in certain practical cases already. However, it should be mentioned that the analyses must be carried out by experienced model-engineers, who are familiar with the programs, the underlying material-models and structural behaviour of reinforced concrete structures as well.
Having regard to the state of the art of this moment, the numerical models provide for a new and powerful instrument, especially for research purposes. The use of this numerical analysis may take place in these cases under the required circumstances with guidance and support of specialists or even in combination with experiments. This will result in a better understanding of the behaviour of

reinforced concrete structures under conditions where problems still exist e.g. in certain cases where shear governs the behaviour.
The examples to discuss have been chosen in order to demonstrate the current possibilities of a non-linear numerical analysis of reinforced concrete structures with DIANA.

1.4 DIANA

For most of the information about DIANA and for a description of the material-models available in DIANA reference is made to the Heron 1987, nr. 3 mentioned before.
An exception is made for the models related to crack-formation and bond, because these phenomena will be met later in this survey.
In DIANA a smeared crack concept is used. When a non-linear analysis of an unreinforced concrete structure is carried out, the energy release rate, the G_f concept, is used. The stress-crackstrain diagram is transformed into the bilinear diagram of figure 1.

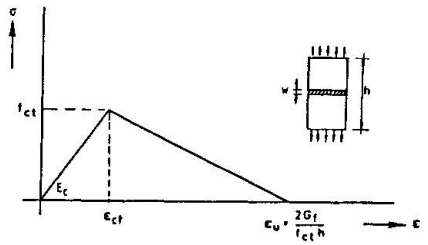

Fig. 1. Linear softening model.

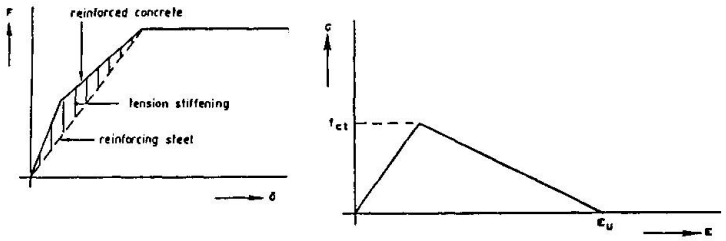

Fig. 2. Tension stiffening concept

When a reinforced concrete structure is analysed, the tension-stiffening concept is used. The principle is explained in figure 2. The tension-stiffening concept is applicable for the analysis of a reinforced concrete structure with uniform distributed reinforcing bars and when cracks are expected to develop perpendicular to the direction of the bars. This is a rather severe restriction:in general cracks do not intersect the reinforcement perpendicularly, but more likely under a certain angel. The assumption of uniformly distributed reinforcing bars generally does nog apply also for structures. Note that average stresses are calculated and not the maximum steel stresses that occur in cracks. This is a consequence of the smeared crack approach.
When full bond between steel and concrete is assumed, the reinforcement is modelled by bar elements which are embedded in the concrete. However, when relative displacements between reinforcement and concrete are allowed, special slip-elements (two-dimensional springs) can be applied. The consequence of this approach is that the element-mesh must be adjusted to the reinforcement grid. When numerous reinforcement bars are present, this may lead to an enormous number of elements. Thus, it is very important to decide in an early stage if the application of bond-slip elements is necessary.
The behaviour of bond-slip elements is described by means of two constitutive equations. The first concerns the bond shear stress with the slip along the bar. This relationship is taken as a bi-linear diagram. The second equation describes the relation between the radial component of the bond stress and the radial displacement. The latter becomes important when radial confinement is present.

2. THE EXAMPLE-CALCULATIONS

2.1 A METRO-beam

This beam is a prefabricated prestressed concrete beam with a total span of 33 m

and forms part of the substructure of the METRO system in Rotterdam. In order to limit the total height of the structure, the beams are provided with tooth-shaped ends for supports. The beam is shown in figure 3.

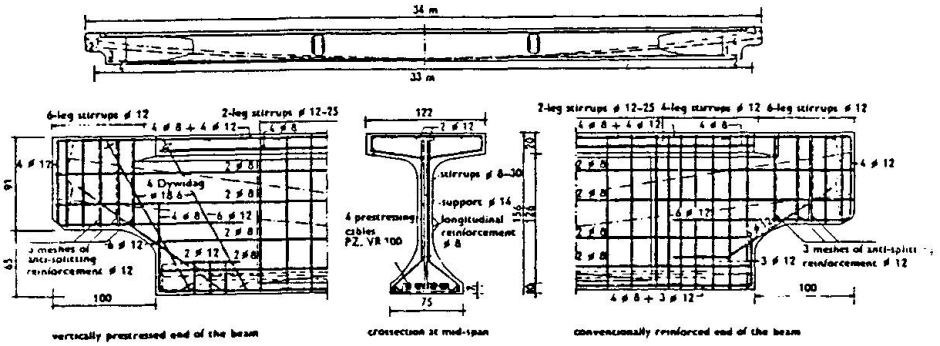

Fig. 3. Elevation of the beam.

The concerning beam has been subject of full scale and small scale experiments in 1965. That is why the one tooth structure of the beam was conventionally reinforced and the other has been prestressed additionally in vertical direction. Although the beam has been loaded in flexure also, to consider the global behaviour, the main problem of course was the tooth structure. The tooth structure was mainly designed on the basis of equilibrium conditions and global compatibility. A check of the real behaviour was necessary. Further consideration of this design was furthermore worthwhile because of the large number of beams to produce.
The analysis covers the simulation of the behaviour of the beam loaded in flexure and the behaviour of the conventionally reinforced tooth structure which was - as in the experiments - relative heavely loaded near the support.
The numerical simulation of the flexural behaviour of the beam fits rather well with experiments. Load-deflection curves and cracking are calculated accurately, see figure 4.

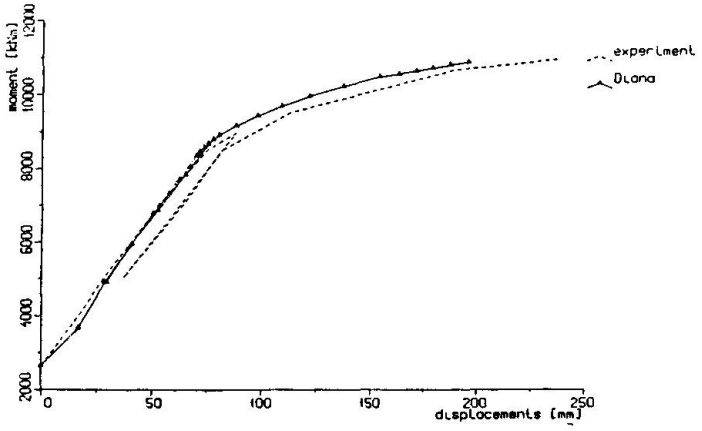

Fig. 4. Moment-deflection at midspan.

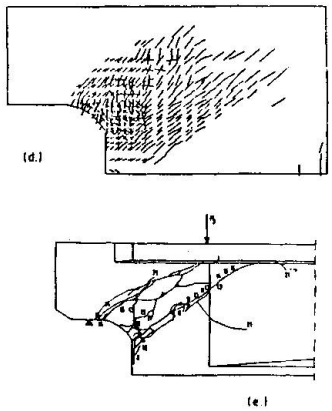

Fig. 5. Calculated and experimental crack patterns in the tooth.

In the analysis of the conventionally reinforced tooth structure, crack initiation as well as the direction of crack propagation are simulated quite well, see figure 5. However, the development of the second diagonal crack was not observed quite right in the analysis.
The localized character of the diagonal cracks that were observed in the experiment cannot be simulated objectively with the current model for tension-

stiffening that has been used. The value of ε_{us} needed for crack propagation clearly determines the rate at which the diagonal crack in the throat propagates. The dependency of the total structural behaviour on this parameter is such that predictions of the structural response is not very well possible. This parameter has been varied to study the influence of the variation and finally fitted to about the right number.
This means that for the right prediction of the behaviour of details like this the bond-slip model is necessary. However, the use of that model causes practical difficulties with regard to the number of required elements.
In spite of the fact that a precize prediction of the structural response of the tooth structure is not very well possible, more insight in the qualitative structural behaviour can be obtained from a numerical simulation by investigation of the influence of some of the model parameters.

2.2 A corbel

This example concerns a single corbel on one side of a columm, see figure 6. Corbels like this one are rather widely used, while the analysis and design sometimes may be rather difficult. The concerning corbel was subject of experimental study in 1961.
The analysis of this example was carried out in two variants. At first an analysis was made with perfect bond between reinforcement and concrete. In a second analysis the effect of using bond-slip elements between the main reinforcing bars and the concrete has been considered.
The bearing capacity and the global behaviour of the corbel at failure has been predicted satisfactory with the two dimensional perfect bond model.
The results give a good impression of the way how action effects are distributed within the corbel and the column, see figure 7 and 8.

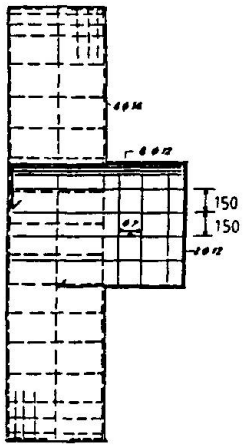

Fig. 6. reinforcement of the corbel

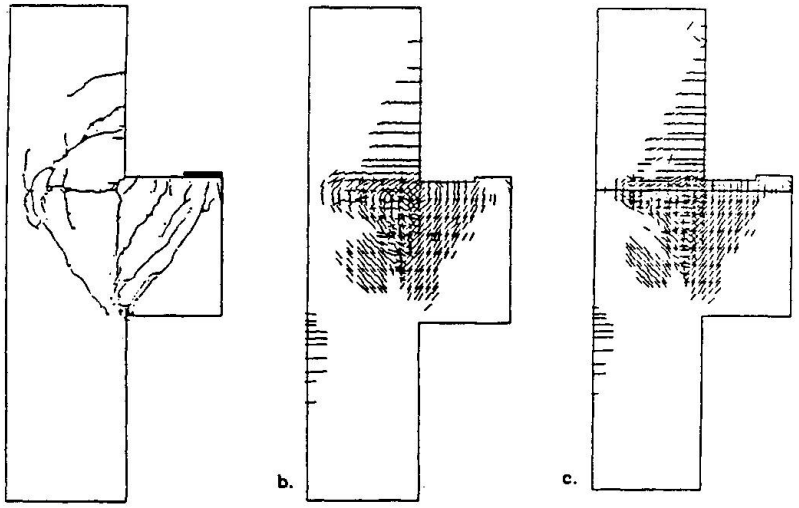

Fig. 7. a. crack pattern at failure
b. computed perfect bond
c. computed bond-slip

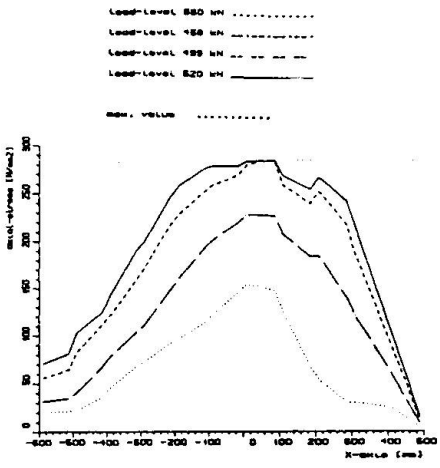

Fig. 8. axial stresses in the bond-slip bar

The current models - the perfect bond and bond-slip elements around the main reinforcement only - the simulation of the localized cracking is not very accurate. Refining of the element mesh and bond-slip elements for all reinforcement may give better results in this respect. However, this creates

difficulties regarding the amount of elements required in this case.

2.3 A beam-column connection

In this example a single-bay portal frame is modelled, see figure 9.

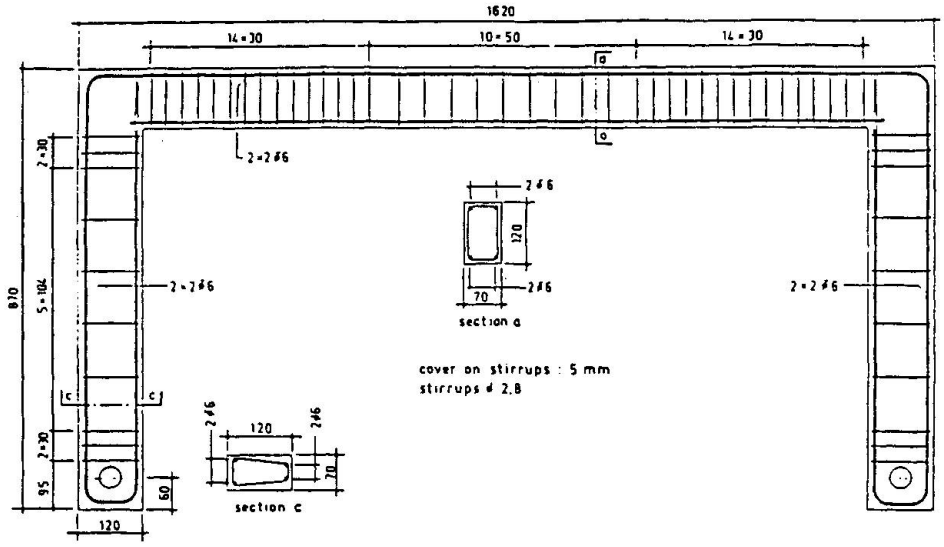

Fig. 9. Portal frame

Special attention has been paid to the structural detailling of the beam to column connection. The behaviour of this joint is interesting because one might easily assume that the joints are as strong as the connected members. However, in certain cases the strength of the joint may be lower.
In this case the beam-column connection is subjected to a negative moment and the behaviour of the joint and the frame has been simulated. Some of the results are compared with findings from experiments.
This numerical simulation gave a good impression about the global behaviour of the frame (see figure 10) and the structural mechanism in the corner-joint.

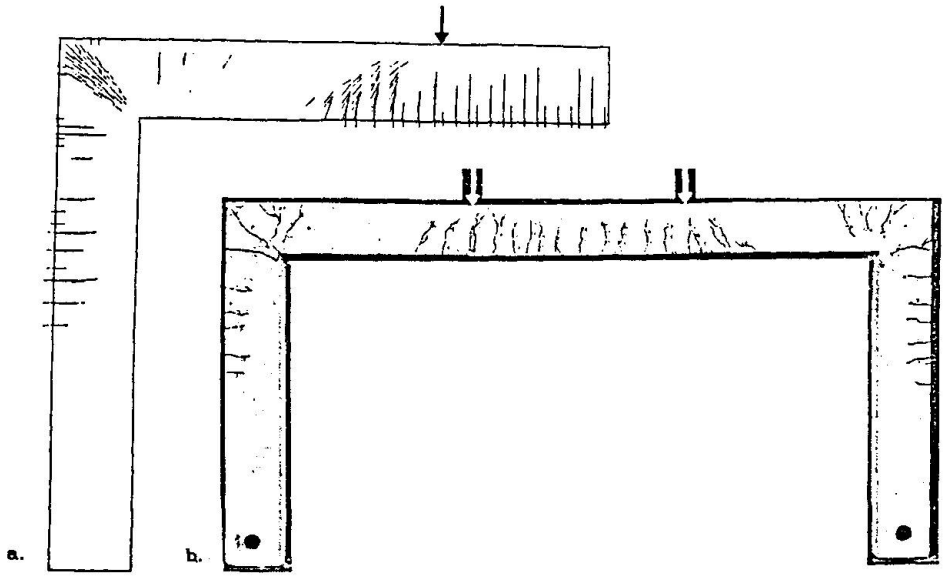

Fig. 10. a. Cracks at failure
b. Experimental crackpattern at failure

After cracking occurred at the corner of the frame, large compressive stresses developed in the diagonal between beam and column. This phenomenon corresponds well with a simple system of equilibrium of internal forces in that region, where the said compression-diagonal transfers the components of the tensile

reinforcement to the compression zones of beam and column at this corner. In the experiments the compression-diagonal caused the splitting tensile stresses at the bend of the tensile reinforcement perpendicular to the plan of the curved bar. This, of course, could not occur in the two-dimensional analysis. For the same reason a localized diagonal corner crack suddenly appeared in the analysis, which developed much more gradual in the experiment.
More detailed research of the behaviour of concerned corner detailling therefore would require a full three-dimensional analysis.

2.4 Analysis of a tunnel-section

The analysis concerns a part of a cross-section through an existing tunnel, see figure 11.

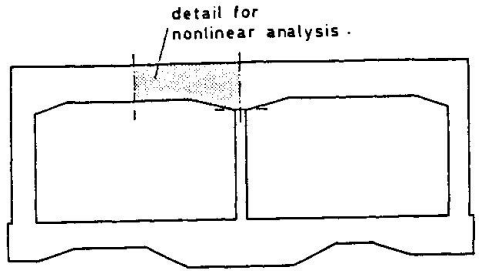

Fig. 11. Cross section of tunnel-struction

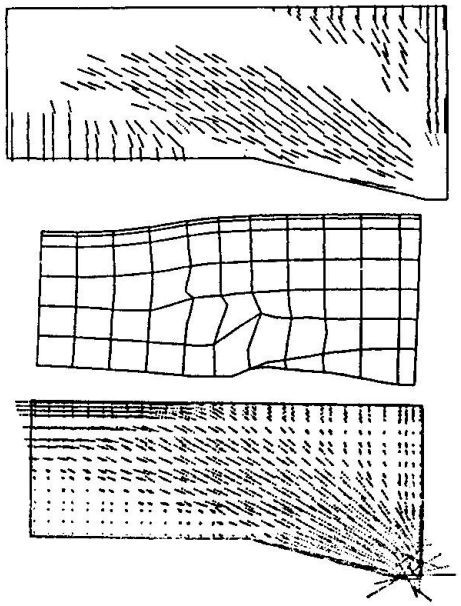

Fig. 12. Crack patter, incremental deformations and principal stress trajections at failure

In this case no experimental information is available. The analysis serves a design-check. The main problem is to check the bearing capacity near the middle support. In this part a considerable redistribution of moments is necessary to reach the required bearing capacity. In the part of the section of concern all main reinforcement will yield before the ultimate capacity will be reached. The question was whether this region would have sufficient strength to withstand the belonging shear force while the main reinforcement yields.
The non-linear simulation of a part of the tunnel-section gave very good results. The development of the crack formation, due to flexure and shear, is predicted qualitatively well.
The redistribution of internal stresses, due to crack formation, appears significantly in the analysis. At ultimate an arch-effect develops, which is in equilibrium with the tensile reinforcement in the span, see figure 12. The bond-slip elements appeared to be a feasible model also at the splices. The analysis made use as much as possible of the possibility to limit the section to consider by applying realistic edge-conditions.

2.5 Deep beams

Deep beams are usually analysed and designed on the basis of linear calculation. The behaviour after crack-formation is difficult to estimate. This holds especially when deep beams extend over several supports. Therefore, a non-linear analysis of deep beams forms part of the series of examples considered.
The first example comprises the analysis of a deep beam on two supports, figure 13. In the second example a deep beam extending over three supports is simulated numerically, figure 14.

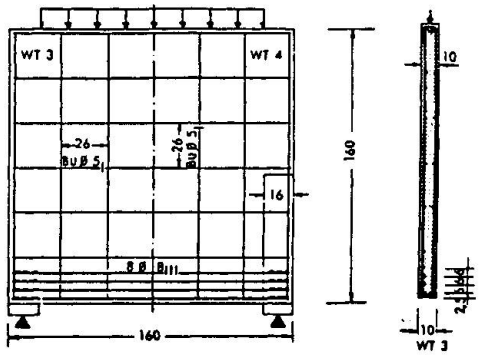

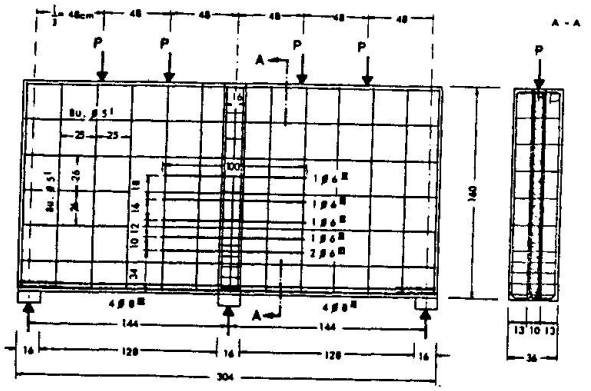

Fig. 13. Deep-beam on two supports. Fig. 14 Deep-beam on three supports

In both cases results of experiments by Leonhardt and Walter are available for comparison.
A realistic simulation of the structural behaviour of reinforced concrete deep beams is possible. The load-deflection curve observed in the experiments and the crack pattern are quite well simulated, figure 15.

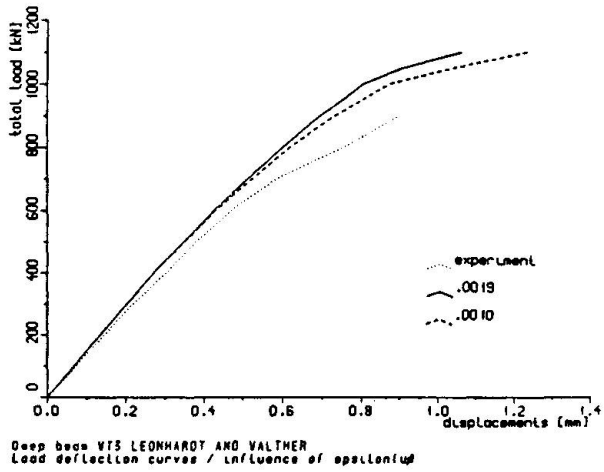

Fig. 15. Comparison between calculated and experimental load-deflection.

However, a specific fit of the tension-stiffening parameter ε_{us}, was necessary to find satisfactory results. This means a more direct modelling of the bond phenomena would be better, also in these cases.
The behaviour of the deep beam on two supports is, after cracking of the central region, completely determined by the compressive response of a 'column' above the support. The results indicate, that as soon as the central region is separated from the 'column', failure is inevitable. This separation seems to occur through the development of a dominant crack in the beam, just next to the support. This dominant crack was not observed in the experiment.

The behaviour of the deep beam on three supports was determined by steep shear cracks; as soon as this crack develops and the reinforcement in the crack yields, failure is inevitable, figure 16.

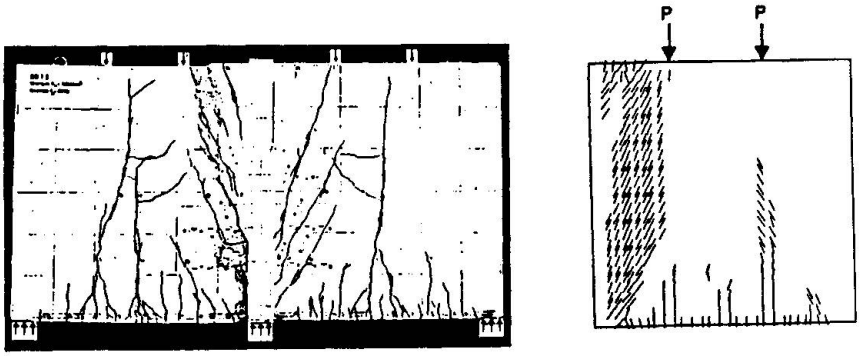

Fig. 16. cracking failure in the experiment and calculated strains.

The compressive response of the 'column' above the supports is not important for failure in this case, but seems to influence the stiffness.

2.6 A LNG storage tank

The storage tank which is investigated, is analysed and designed by Muller (1965). The tank is shown in figure 17.

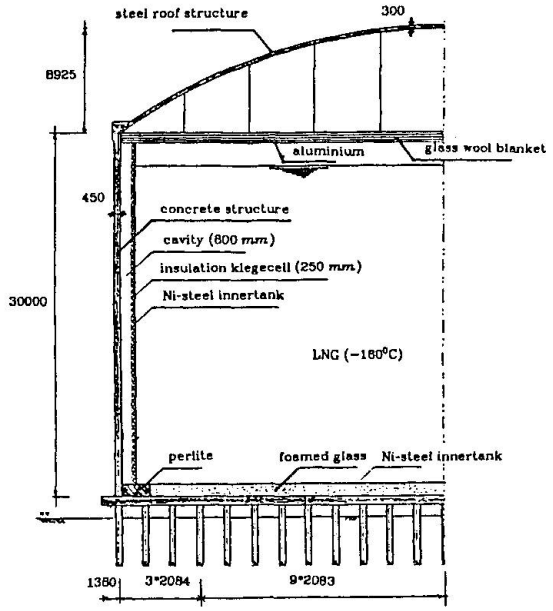

Fig. 17. Cross-section of the LNG tank

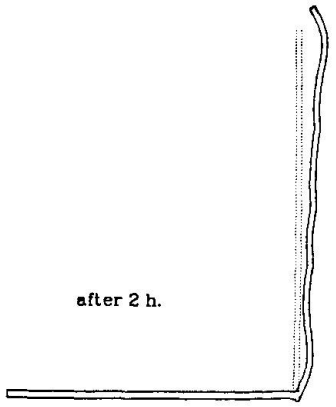

Fig. 18. Deformation of the tank

The roof and the base are monolithically connected to the wall.In this example two analysis were carried out.
The tank subjected to the water test; the behaviour of the tank subjected to static loading was checked.
The tank subjected to fire-load. It is assumed that the heat is caused by a burning adjacent storage tank producing a thermal radiation of 30 kW/m^2 constant over the height of the tank and constant in time during 40 hours.
The effect of high temperatures on the properties of the concerning materials have been taken into account.
In both cases the analysis is treated as an axi-symmetric problem.
The water test analysis demonstrated good agreement between 'elementary calculations' at one hand and 'numerical simulation' on the other hand. No cracking was observed when the tank was subjected to the water test, which indicates that the tank was designed well.
The result of the fire-load analysis are shown by means of numerically calculated crack patterns and deformations and are in agreement with theoretical considerations, figure 18.
However, one should realise that some simplifications were made in the numerical analysis. The most important ones are that combined plasticity and temperature dependency and 'transient strain'-effects are not taken into account.

2.7 Beam falling on a shock absorbing element

This analysis has been performed to show the possibility to make dynamic non-linear calculations with DIANA. The beam considered is 8.15 m long, supported at one end by a hinge, around which the beam can freely rotate in a vertical plane. The other end of the beam is lifted vertically to the desired drop-height. The beam falls on a shock absorbing element and undergoes severe bending within fractions of a second after striking the shock absorber. Figure 19 shows the arrangement as described.

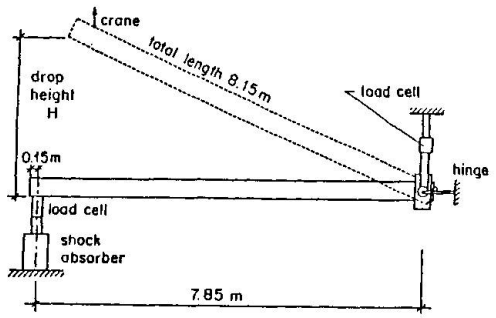

Fig. 19. Test set-up

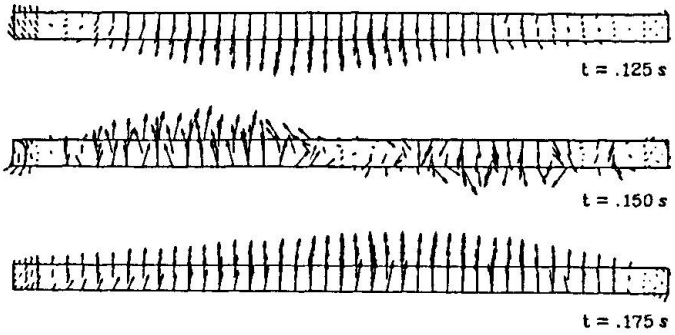

Fig. 20 Velocity field as calculated

Is has been shown that a non-linear dynamic finite element analysis is possible. Good results can be obtained, figure 20.
In the analysis the stiffness of the beam was a little overrated, resulting in somewhat smaller deflections and a higher frequency than observed in the experiment. The influence of dynamic loading on the material properties has been overestimated. Further research in this field seems necessary. But in general the numerical results can stand a comparision with the experimental results.
Development of a spring element with hysteresis could improve the results of this analysis, because a better model for the shock absorber could be implemented then.
Such an improvement can be expected too from a concrete model with even better unloading behaviour than the model that was applied in this analysis.

2.8 Dynamic analysis of under water tunnel for gas explosion

Tunnels passing under water ways are normally designed to resist loads associated with dead weight, soil, water and traffic. In the event of an internal gas explosion, the tunnel experiences a load reversal. The question may be whether an accidental gas explosion can cause failure of the tunnel.
Figure 21 shows a typical cross-section which was the subject of non-linear analysis. The main objective of the analysis was to predict the response of the tunnel to the load, associated with a hypothetical internal gas explosion, figure 22.

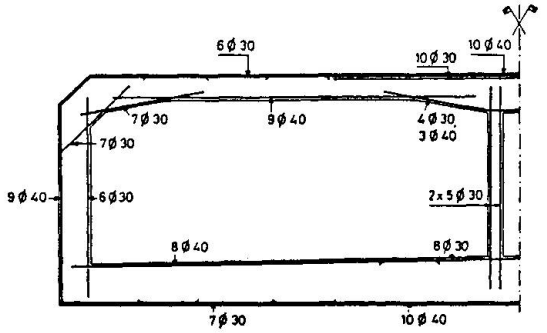

Fig. 21. Tunnel reinforcement for a 1.5 m wide section

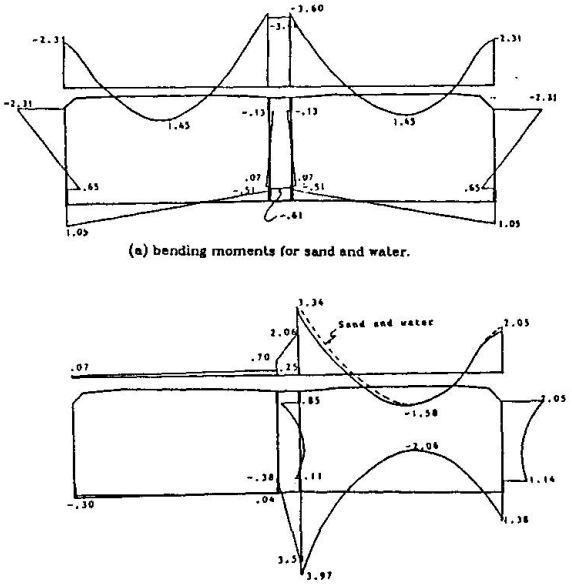

Fig. 22. Bending moments obtained with frame element model

It appears from the analysis, that a conventionally reinforced under water tunnel is unlikey to survive an internal gas explosion.
DIANA appears here a powerful tool to provide rational solutions for complex non-linear dynamic analysis problems.
However, such an analysis is a very difficult task, which may take an experienced analyst at least one full month or more and consumes considerable computer resources. These man-hours and computer expenses are needed primarily for the step-by-step development of the finite element model and its verification.

3. CONCLUSION

The application of the non-linear numerical model DIANA as discussed may largely increase the structural insight. It may serve as a simulation tool, a research tool or as a means to improve codes as well. Yet in general an analysis is a difficult task and must be carried out by an experienced model-engineer who is familiar with the adopted material-models and with structural behaviour.
The practical application for design activities of this tool is close to further studies by experiments. That should be beared in mind with regard to the knowledge required and the time and costs involved. However, the use of a finite element package in a simple form may already give considerable insight in structural behaviour.
The performance of the program still seemed rather problem dependent in some cases. This of course puts some restrictions on its predictive power. However, it appears that this weakness mainly follows from the use of simplified models like tension-stiffening where bond-slip elements would have been more appropriate. The use of bond-slip elements has been avoided as much as possible in order to reduce the amount of elements and computation time. In some cases this appears to be too rough for good results.
Nevertheless in some examples the computation time was very much. However, this will decrease with further developments of computer-technology. One should bear in mind, that relative much of this time is spent nearby the ultimate state. For an analysis up to 70% of the bearing capacity roughly only 30% of the total computer time is needed. For the practical application of non-linear analysis, this may be an important fact.
The further development of this powerful non-linear numerical model is worthwhile.

REFERENCES

Ammann, W., M. Mühlmatter and H. Bachmann (1982), "Versuchen an Stahlbeton- und Spannbetonbalken unter stossartiger Beanspruchung. Teil 3: Versuchsresultate der Balken P1, P2 und B1 bis B8", Bericht Nr. 7709-3, Institut für Baustatik und Konstruktion ETH Zürich.

CUR (1969), "Loading tests on a full-size suspended beam and a model of this beam for a Metro Viaduct at Rotterdam", Report no. 40, Netherlands Committee for Concrete Research (CUR).

Leonardt, F. und Walther, R. (1966), "Wandartige Träger", Deutscher Ausschuss für Stahlbeton, Heft 178, Berlin.

Muller, T.K. (1985), "Concrete tanks, subjected to fire load", Graduate thesis, Part II, Delft University of Technology, Delft, The Netherlands (in Dutch).

Niedenhoff, H. (1963), "Untersuchungen über das Tragverhalten von Konsolen und kurzen Kragarmen" dissertation, Technische Hochschule Karlsruhe.

Strobrand, J. and Kolpa, J.J. (1983), "The Behaviour of Reinforced Concrete Column-to-Beam Joints - Part 1: Corner Joints Subjected to Negative Moments", Research Report 5-83-9, Delft University of Technology, Department of Civil Engineering.

Leere Seite
Blank page
Page vide

Redistribution of Inner Forces in Hyperstatic Reinforced Concrete Structures

Redistribution des forces internes dans des structures hyperstatiques en béton armé

Umlagerungen von inneren Kräften in statisch unbestimmten Stahlbetontragwerken

M. MEHL
Dr.Ing.
Consulting Engineer
Vienna, Austria

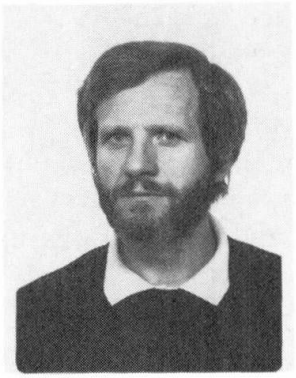

Manfred Mehl, born 1943, research assistant at TU-Vienna from 1971 to 1981 at the Institute of 'Stahlbeton und Massivbau', has specialized in reinforced concrete research. Since then he works in the field of design and construction of underground railways, partly doing some research in the FE-analysis of RC-structures.

E. HAUGENEDER
Dr.Ing.
Technodat
Vienna, Austria

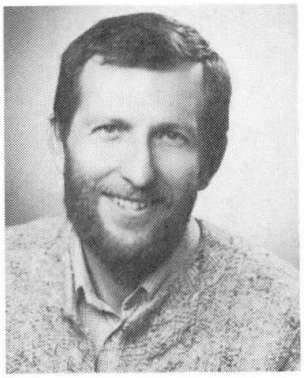

Ernst Haugeneder is working for TECHNODAT, Technische Datenverarbeitung G.m.b.H. in the field of Finite Element Application and Development. He is also responsible for the Viennese office of the company. Ernst Haugeneder is 41 years old, married and father of two nice boys.

SUMMARY

The redistribution behaviour of an inner tunnel wall subjected to injection pressure is studied. From the calculation using the FEM several conclusions concerning the carrying behaviour and redistribution can be drawn. The FEM provides a model which explains the arising damage very well. Furthermore, the results agree with those of comparable experiments. As a comparison an estimate is carried out on the basis of beam theory supposing plastic hinges.

RÉSUMÉ

L'étude traite du comportement et de la redistribution des efforts sur la surface intérieure d'un tunnel par suite de pressions d'injection. Sur la base de calculs à l'aide de la méthode des éléments finis, plusieures conclusions sont tirées sur la résistance et la redistribution des efforts. La méthode des éléments finis fournit un modèle qui permet également d'expliquer les dommages naissants. Les résultats concordent avec ceux d'expériences comparables. Une estimation est faite sur la base de la théorie de la poutre supposant des rotules plastiques.

ZUSAMMENFASSUNG

Am Beispiel einer durch Injektionsarbeiten überbeanspruchten Tunnelinnenschale werden die Umlagerungsvorgänge studiert. Aus der Nachrechnung mit Hilfe der FEM können einige Schlüsse auf das Tragverhalten und den Verlauf der Umlagerungsvorgänge gezogen werden. Die Nachrechnung liefert ein gutes Modell zur Erklärung der aufgetretenen Schäden, ebenso zeigt sich eine gute Übereinstimmung mit Ergebnissen aus vergleichbaren Versuchen. Zum Vergleich wird eine Abschätzung auf der Basis der Stabtheorie unter Annahme von plastischen Gelenken durchgeführt.

1. DESCRIPTION OF THE SITUATION

Water seepage was observed to occur over large regions of a tunnel between slurry trench walls, shown in figure 1. In order to rectify this the leaking regions were impregnated with waterproofing agent by the PU-method. During the injection work the appearance of horizontal cracks in the region about the middle of the wall was observed upon which the injection work was stopped. The assesment of the damage showed that cracks of up to 1.6mm in width had occured over a length of 30m and that the wall had bowed out to up to 17mm. The largest crack widths correlated approximately with the largest deflexion. The uncompressed wall had an average accuracy of $\pm$3mm. The damage can be assumed to be caused by exeeding the permissable injection pressure combined with the growing of a gap between the inner wall and the slurry trench wall.

2. THE PROBLEM

What was aimed for was:

.) a more exact explanation of the damaging process and cracking as well as a value for the highest injection pressure.
.) an estimation of the damage sustained by concrete and reinforcement on the outer side of the wall which is obscured from view.
From the calculations one could expect to be able to draw conclusions concerning the redistribution process.

The chosen example seemed especially advantegeous due to the following:
.) The calculation procedure for an existing situation with unambiguous loading history limits the width of the spectrum of possible interpretations.
.) The different reinforcement strengths and effective heights do not correspond to the stress resultants occuring under elastic conditions and consequently can be expected to cause large redistributions of the inner forces.

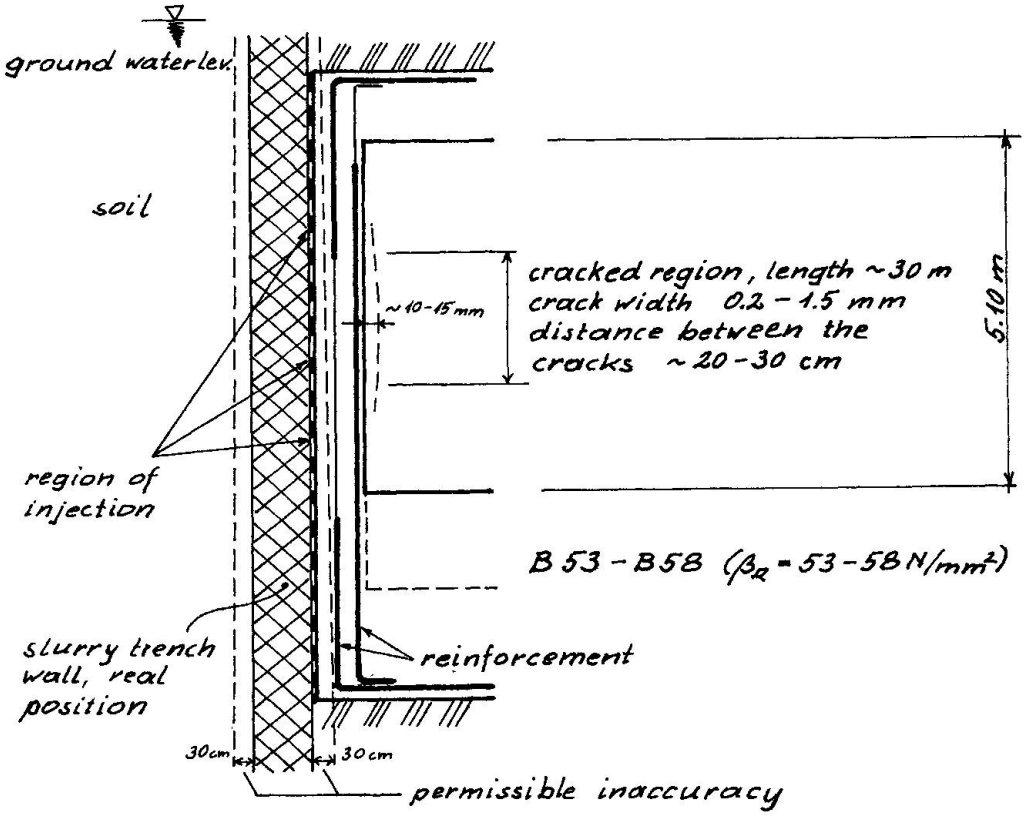

Fig. 1 Cross section of tunnel with cracked region

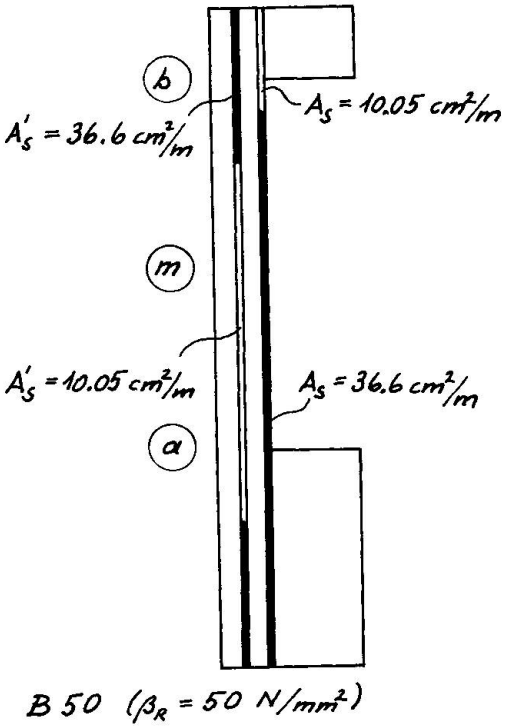

Fig. 2 Cross section with reinforcement

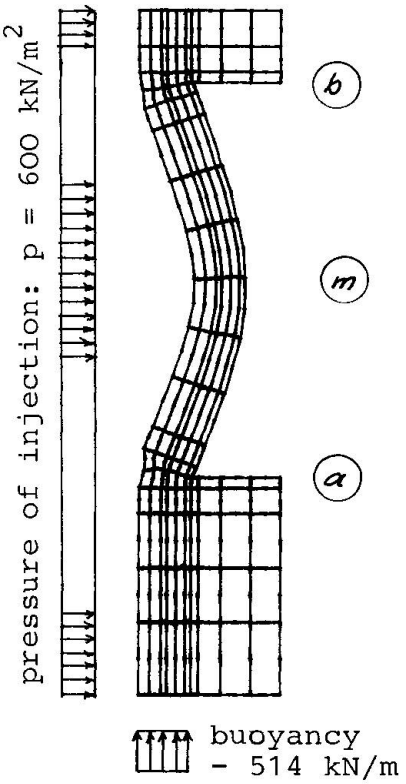

Fig. 3 Ultimate load: FE-mesh and deformation

3. FINITE ELEMENTE ANALYSIS

3.1 Fundamentals

There are a great number of numerical models used for reinforced concrete (see e.g. /1,2/).
The material model for reinforced concrete used in the present work is based on the following assumptions:

a) Restrictions of crack width and crack spacing require a minimum reinforcement distributed over the whole structure. This reinforcement is imagined to be smeared. Consequently reinforced concrete is treated as a compound material.

b) In compression the material is mathematically described by a 3-D plastic-isotropic hardening model based on a formulation of Shareef and Buyukozturk /3/ (fig. 4a)

c) The hardening function follows closely the parabola of the Austrian Standards - ÖNORM. (fig. 4b). For uni-axial compression ideal plasticity is assumed after 2‰ total strain.

d) Below tensile strength the model behaves linear elastically. If one or both principal stresses reaches the tensile strength cracking is assumed. From then on no additional load can be applied until the reinforcement is able to carry the load (fig. 4c).
Above 2.4‰ total tensile strain, again ideal plasticity assumed.

e) Concentrated reinforcement, e.g. as may occur in beams or panels, is modelled by additional bar elements or plane elements and a bi-linear stress-strain relationship for steel.

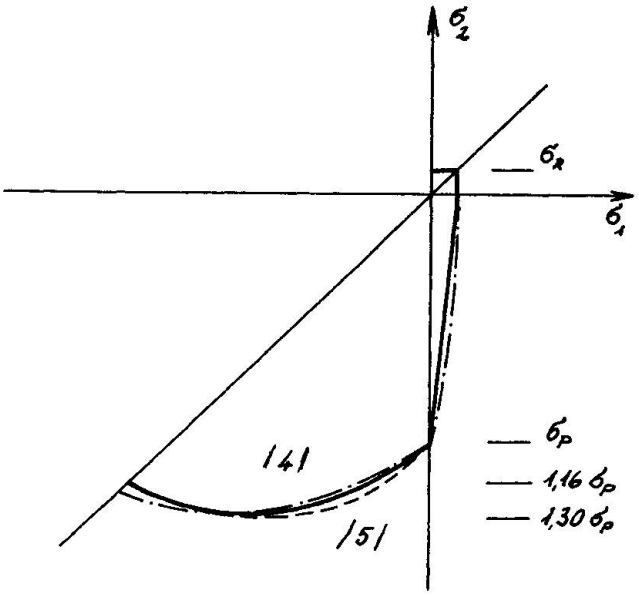

Fig. 4a Fracture envelope in the $\sigma_1 - \sigma_2$ plane

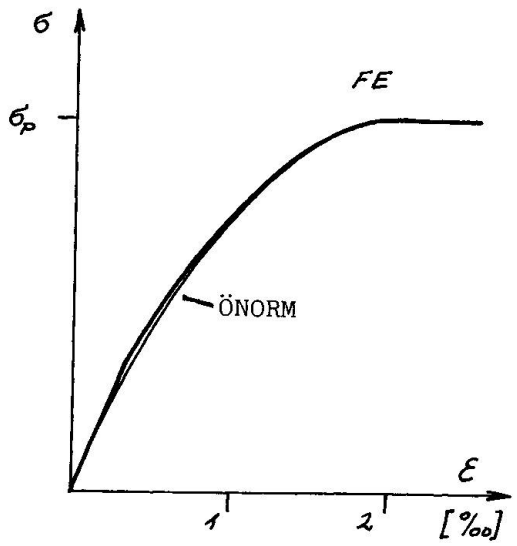

Fig. 4b Stress-strain diagramm of the FE-model and of ÖNORM under uni-axial compression

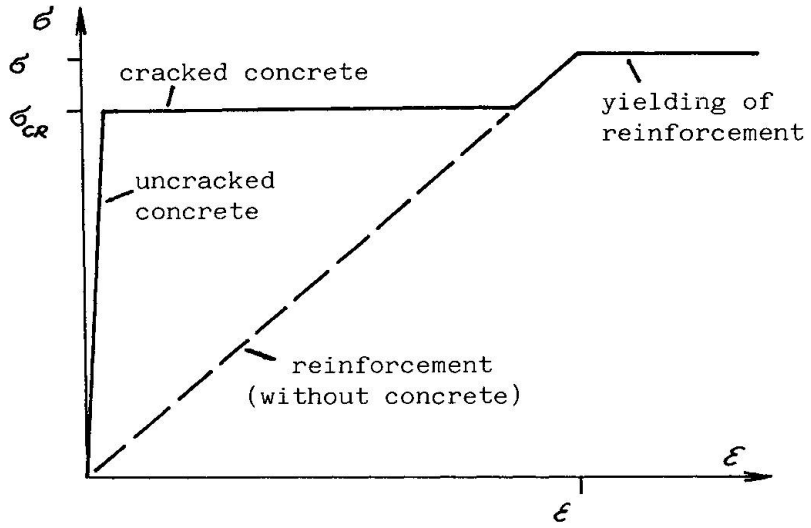

Fig. 4c Stress-strain diagram of reinforced concrete under uni-axial tension

The model parameters are: the comprehensive and tensile strengths of concrete and the directions, cross-section areas and yield stresses of the reinforcement. The model has been tested on a series of simple examples with comparison to some well known experiments /4,6/. Also, a number of RC-beams have been analyzed. The collapse load as well as the type of failure agreed excellent with experience and analytical calculations according to the Austrian Standards. Details are described in /7/.

3.2 Results of the calculations

The finite Element calculations were carried out using the experiences from /7/. Summarizing, there are no extra restraints for the mesh layout necessary due to the nonlinear material behaviour. The chosen mesh is shown in fig. 3. The material parameters are for concrete: σ_p=37,5 N/mm², σ_{cr}=3,75 N/mm²; for steel σ_f=510 N/mm².

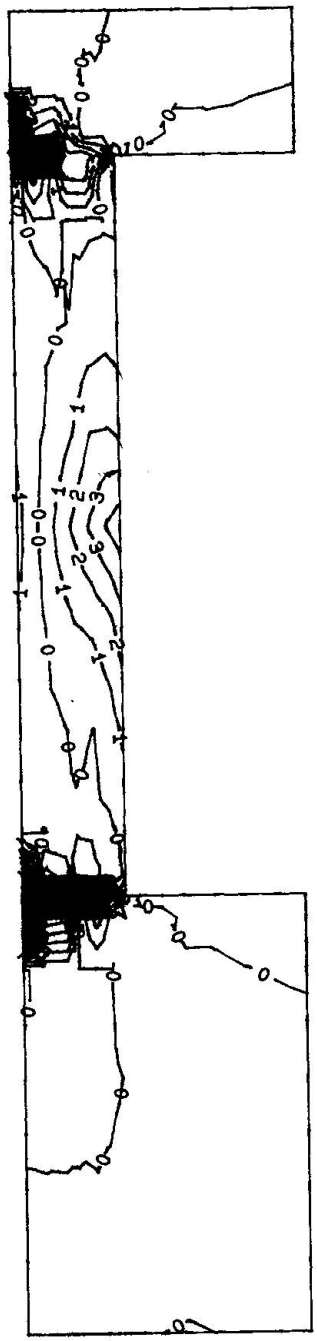

b) Strains ε_{by}

a) cracked regions

Fig. 5 Status of overloading deformation at "m": 14.9 mm

According to the FEM calculation the injection pressure at collapse is slightly greater than 600 kN/m^2.

At this load the largest strain on the inside of the wall is 2.1‰, which would have caused crack widths of about 0.4 to 0.6 mm with the observed distances of 20 to 30 cm between the cracks. Conversely, from the observation of the largest crack widths of 1.0 to 1.5 mm one can conclude that the largest strains at these points are about 5‰. Therefore, during the injection process the pressure must briefly have been sustancially higher. Due to the movement of the wall the volume of the gap increased and the pressure was relieved. However, this caused the reinforcement to yield and so the cracks in the highly strained tensile regions of the concrete opened wide.

In order to asses the damage caused by overloading calculations using the FEM were continued up to a load of 650 kn|m^2, i.e. just beyond the ultimate load. With a deflexion of 14.9 mm a strain of 4.4‰ occured in the middle of the innerside of the wall. Figure 5 shows the occuring strains and the cracked zones. The reinforcing steel is so heavily strained in the crossestions "a", "m" and "b" that a further increase in stress is no longer possible. However, the largest strain of 13.6‰ in "a" is much lower than strains that have been measured in comparable experiments. In the crossection "b" the concrete is strained about 2‰. This is the highest level ever reached, which is also within permissable limits.

The redistribution process: In figs. 6 and 7 the process of deflexion, the concrete stresses and the steel stresses are plotted versus the applied load.

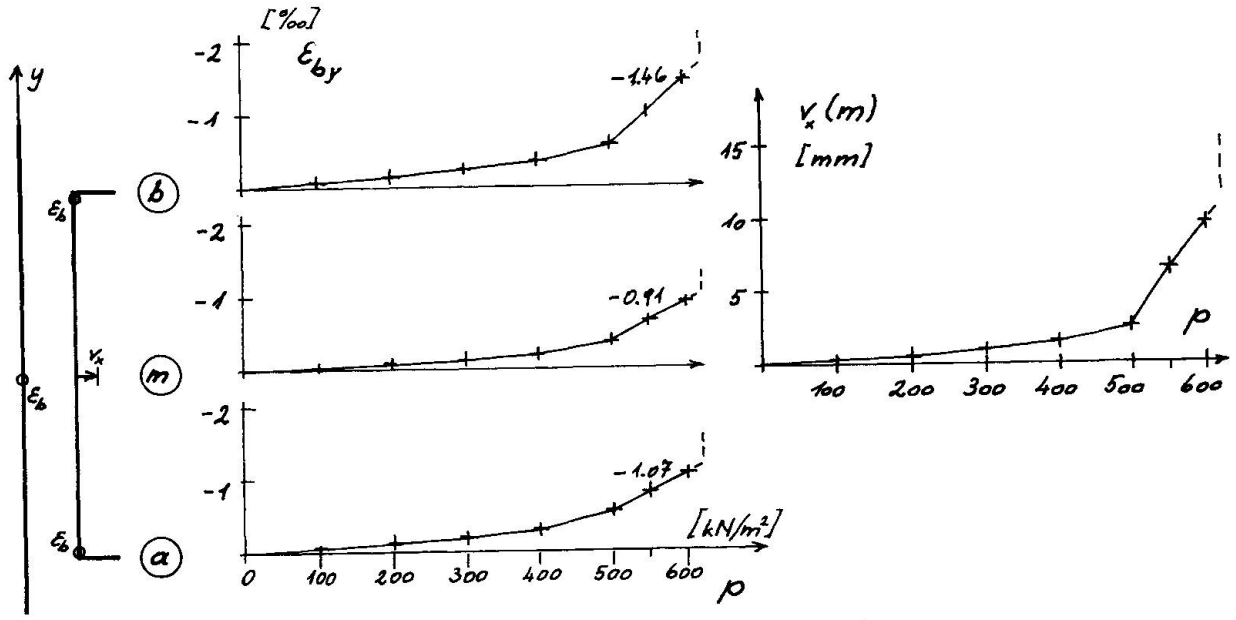

Fig. 6 a) Characteristic results on the regions of compression b) Deflexion of "m"

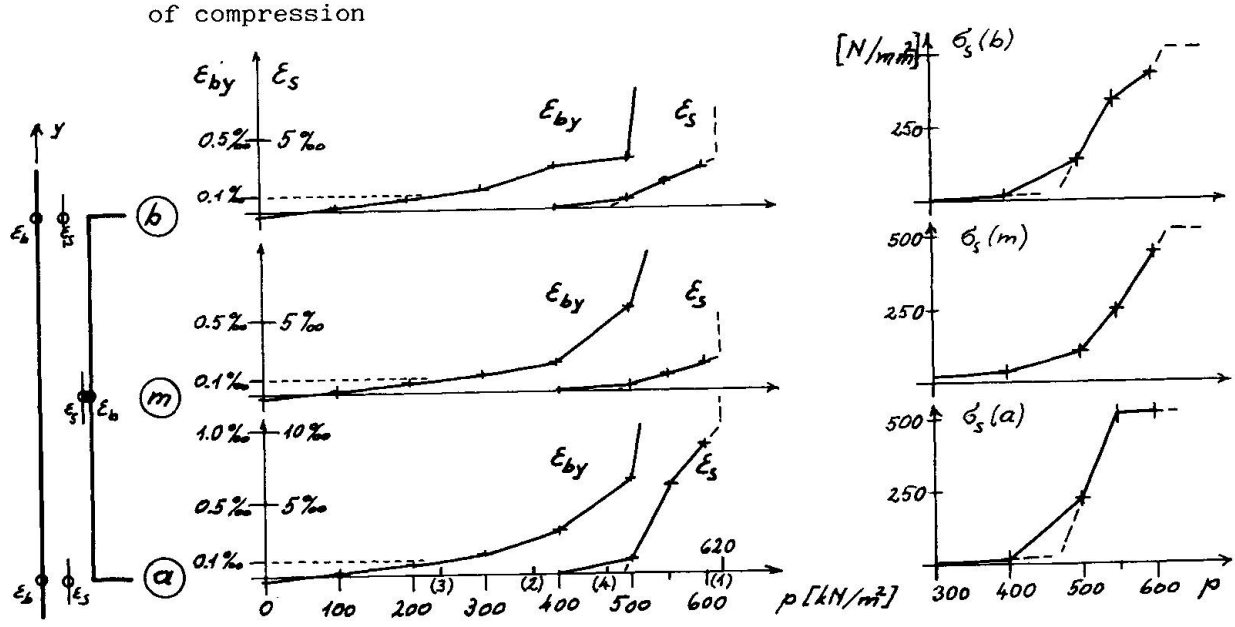

Fig. 7 Characteristic results in the tensile regions

(1) calculated ultimate load $p_u \sim 620$ kN/m² ($600 < p_u < 650$)
(2) calculated service load $p_s = 620/1.7 = 365$ kN/m²
(3) cracking ($\varepsilon_b \geq 0.1$‰) above $p_c = 230$ kN/m² ≙ 620.3|8
(4) forces in reinforcement increase above $p_r = 460$ kN/m² ≙ 620.3|4

The numerical results show that from a load of 300 kN|m² onwards (just under half the ultimate) the first signs of a non-linear behaviour are evident. At the three most stressed points, "a", "m" and "b", the edge strains are greater than 0.1‰, at these points the concrete starts to crack.
At a loed of 400 kN/m² (this approximately represents the permissable service load) the formation of cracks is so advanced that the reinforcement in "m" starts to sustain considerable tension. This situation diverges heavily from a linear elastic analysis where the bending moments in the edges of a clamped beam are twice as high as in the middle of the beam.

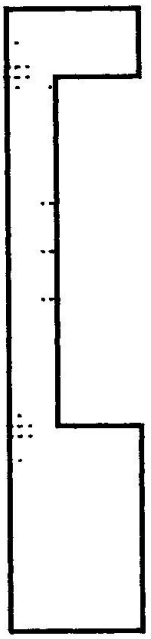

Fig. 8 cracked regions under service load

Figure 8 shows the distribution of cracked zones at service load.
At the ultimate load the inner forces are redistributed such that they represent approximately the actual carrying capacities of the individual crossections.

Comparison with experiments: The results of the calculations correspond with the experimental results of other published sources /8,9,10/. Redistribution starts immediately with the onset of cracking of the concrete and proceeds in continuity up to the ultimate load. Even with a further increase in deformation after reaching the ultimate load the strains that occur stay well under the permissable values.
Plastic hinges in the sense of beam theory with actual rotations do not occur.

4. COMPARATIVE CALCULATION

As a control a comparative calculation was carried out based on beam theory. This was done using the assumption of plastic hinges and following /11/. The system and the individual load steps up to the occurence of a failure under kinetic conditions are shown in figure 9.

Taking the effective span as reference length we obtain a value of 590 kN for the maximum possible pressure of injection. This represents a value bearly under the load obtained via the FEM.
An important element in this method is the reaching of a value for the permissible rotation and a comparison of this with the rotation occuring in practice. In the given problem with prescribed deformation this is only possible via an estimate of the deflexion. In the given case the permissible rotation is not reached; not even if one takes into account the violation of Bernoully's Hypothesis. However, this can only be seen as a rough estimate based on the geometrics of the situation.

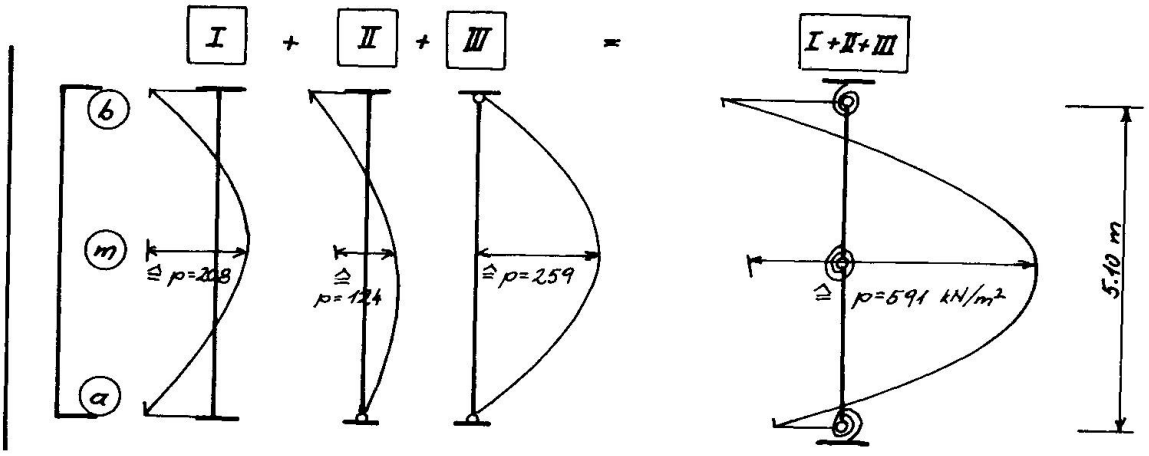

Fig. 9 Comparative calculation based on plastic hinges: system will bending moments and load steps

5. SUMMARY

With this example of a single instance of damage due to forced deformation the FE analysis proved to be a powerful tool in understanding the mechanism of the load redistribution. The remaining insecurities are substantially less important than those associated with an estimate based on the occurence of plastic hinges.

This example also shows, that load redistribution is, above all, a consequence of cracking of the concrete in the tensile regions already beginning with low load levels. An obvious rotation as would be expected cannot be observed; the strains stay below permissible values.

Literatur

/1/ CHEN, W.F.: Plasticity in reinforced concrete. McGraw Hill 1982.

/2/ MANG, H.A., J.E. EBERHARDSTEINER: Collapse Analysis of RC Shells Based on an New Fracture Criterion. Proc. of FE Analysis of RC Structures. Tokyo, Japan, 1985.

/3/ SHAREEF S.S., O. BUYUKOTURK: Constitutive Modelling of Concrete in Finite Element Analysis. MIT Report No. R 83-16, 1983.

/4/ KUPFER, H.: Das Verhalten des Betons unter mehrachsiger Kurzzeitbelastung unter besonderer Berücksichtigung der zweiachsigen Beanspruchung. DASt-Heft 229, 1973.

/5/ LIN, T.C.Y., A.H. NILSON, O.F. SLATE: Biaxial Stress- Strain Relations for Concrete. ASCE Vol 98, ST 5. (1025-1034) 1972.

/6/ FALKNER, H.: Zur Frage der Rißbildung durch Eigen- und Zwängsspannungen infolge Temperatur in Stahlbetonteilen. DASt-Heft 208, 1969.

/7/ HAUGENEDER, E., M. MEHL: Nichtlineare Berechnung von Stahlbeton mit Finiten Elementen. Forschungsbericht des BMfBT, Österreich. In Vorbereitung.

/8/ WOIDELKO E.-O., SCHÄFER K., SCHLAUCH J.: Nach Traglastverfahren bemessene Stahlbeton-Plattenbalken. Beton- und Stahlbetonbau 1986, S.197-201, 214-248.

/9/ SCHLAICH J.,STEIDLE P.:Tragfähigkeit und Verformbarkeit von Stützen bei großen Verschiebungen der Decken durch Zwang. Beton- und Stahlbetonbau 1986, S. 230-235.

/10/BIEGER K.-W., MO Y.-L.: Zur Momentenumlagerung in Stahlbeton-Rahmentragwerken. Beton- und Stahlbetonbau 1985, S. 94-99, 137-140.

/11/DILGER W.: Veränderlichkeit der Biege- und Schubsteifigkeit bei Stahlbetontragwerken und ihr Einfluß auf Schnittkraftverteilung und Traglast bei statisch unbestimmter Lagerung. Deutscher Ausschuß für Stahlbeton, Heft 179, Berlin: W. Ernst & Sohn, 1966.

Ultimate Load Capacity of an Iceberg-Loaded Gravity Base Structure

Résistance ultime d'une structure gravitaire soumise aux effets d'icebergs

Grenztragfähigkeit einer Schwergewichtsplattform unter Eisberglast

Charles J. VOS
Prof. in Constr. Techn.
Delft Univ. of Techn.
Delft, The Netherlands

Charles J. Vos was trained in civil engineering at the Universities of Delft (The Netherlands) and Leeds (U.K.). Since 1963 he has been active in the design of heavy civil engineering structures like bridges, quaywalls and concrete offshore structures. Since 1982 he also teaches construction technology of concrete structures at Delft University.

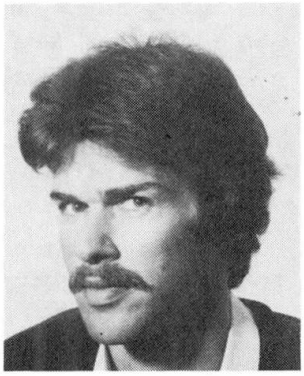

Dick den Hertog, born 1958 obtained his civil engineering degree at the University of Technology, Delft. For one year he participated in the design of steel jackets for the North Sea. Since 1985 he has been in the consulting subsidiary of the HBG and involved in complex and offshore structures.

Dick den HERTOG
Civil Engineer
Delta Marine Consult.
Gouda, The Netherlands

SUMMARY

The peripheral energy-absorbing wall of a concrete fixed oil production platform in an iceberg environment has been analysed. The iceberg energy absorption is achieved by means of triangular projections, which are supported by internal walls. The reinforcement of these projections has been determined by plane frame analysis and a plastic lattice model technique. A non-linear analysis has been executed to determine the ultimate load capacity of a projection. This has been performed with the finite element program package DIANA.

RÉSUMÉ

Le mur périphérique absorbeur d'énergie d'une plateforme fixe en béton pour la production pétrolière, devant résister aux icebergs, a été analysé. L'absorbtion de l'énergie des icebergs est réalisée à l'aide de renforts extérieurs triangulaires, qui sont supportés par des cloisons internes. Le dimensionnement de ces renforts extérieurs a été déterminé à l'aide d'une analyse élastique bidimensionnelle, puis à l'aide d'un modèle de treillis en élasto-plasticité. Une analyse non-linéaire a permis de déterminer la résistance à la rupture d'un renfort extérieur. A cet effet le programme aux éléments finis DIANA a été utilisé.

ZUSAMMENFASSUNG

Die energieverzehrende äussere Wand einer festen Betonplattform für Ölproduktion im Eisberggebiet wurde untersucht. Die Absorption der kinetischen Energie des Eisbergs wird erreicht durch dreieckförmige Vorsprünge auf einer inneren Stützwandkonstruktion. Für die Bemessung wurden die Vorsprünge als ebene Rahmen und als Fachwerk mit plastischem Materialverhalten idealisiert. Eine nichtlineare Berechnung zur Bestimmung der Grenztragfähigkeit der Vorsprünge wurde verwendet. Die Berechnung wurde mit dem FE-Programmpaket DIANA durchgeführt.

1. INTRODUCTION

In 1985 an alternative concrete structure study for a fixed oil production platform in the Hibernia field located on the Grand Banks, 200 miles off Newfoundland, was executed by Grand Banks Constructors on behalf of Petro-Canada Inc. of Calgary. Grand Banks Constructors is a Joint Venture comprising Northern Construction Company Ltd., a subsidiary of Morrison-Knudsen Company Inc., McNamara Construction Ltd., a subsidiary of George Wimpey Canada Ltd., and Delta Marine Consultants a subsidiary of Hollandsche Beton Groep (HBG) from The Netherlands.

In this study, six concepts of a gravity base structure, capable of operating during heavy storms and in an iceberg region, have been designed to a preliminary level. The benefits resulting from the six concepts were evaluated and the most advantageous chosen for conceptual design. The selected concept was further investigated in order to optimize the main parameters e.g. height, diameter etc. The concept development, further lay-out studies and optimizing program resulted in a cylindrical caisson (Fig. 1). The key data of the selected concept are presented in Table 1.

Supported by computer analyses, the most effective shape of the caisson peripheral wall in order to resist iceberg impact forces and to withstand stresses due to hot oil in the storage compartments has been developed. This work resulted in a platform with triangular projections, supported by internal walls, in order to absorb the iceberg energy by crushing of the ice (Fig. 2).

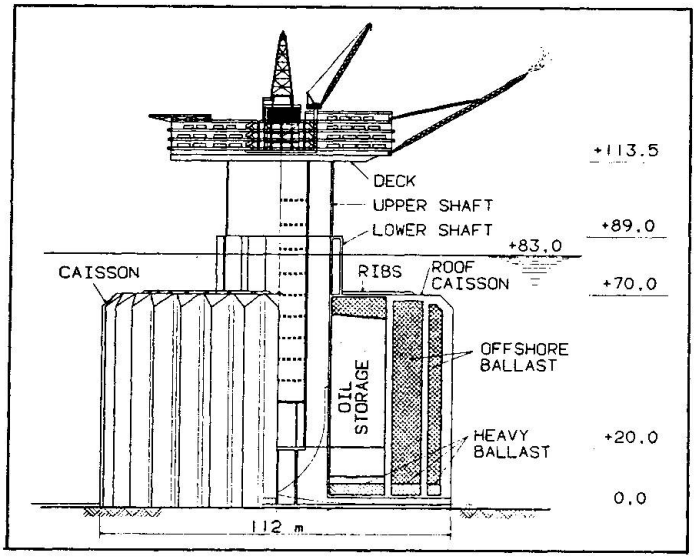

Fig. 1 Selected concept; view and vert. cross section

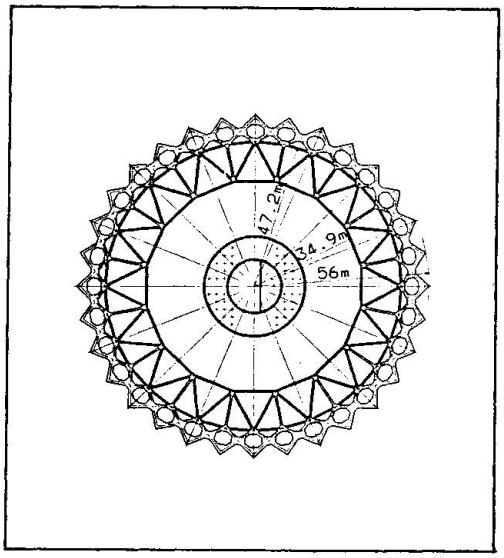

Fig. 2 Horizontal cross section caisson

Table 1 Key data of the selected concept

TOPSIDE FACILITIES		
DRY WEIGHT [TONS]	OPER. WEIGHT [TONS]	DECK WEIGHT [TONS]
29500	34500	7900

ENVIRONMENTAL FORCES			
ICEBERG		WIND, WAVE & CURRENT	
SHEAR FORCE [MN]	OVERT. MOMENT [MNm]	SHEAR FORCE [MN]	OVERT. MOMENT [MNm]
1075	62350	1500	59200

OIL STO-RAGE
[BBLS]
900000

FLOATING STABILITY		
GM IN TOW [m]	DISPLA-MENT IN TOW [m³]	MIN. GM DURING DECK-MATING [m]
9.1	59400	1.8

BALLAST QUANTITIES	
DRY WT. HEAVY BALLAST [TONS]	DRY WT. OFF-SHORE BALLAST [TONS]
154000	371000

MATERIAL QUANTITIES		
CON-CRETE [m³]	MILD STEEL [TONS]	PRE-STRESS. STEEL [TONS]
165000	4000	1350

A separate analysis for the design of the triangular projections has been performed for two main reasons:
- the peripheral wall represents a type of structural concrete member which is poorly covered in theory, codes and practice. It is in fact, in horizontal cross section, a "statically indeterminate, heavily loaded, deep beam".
- the projections represent more than 35 percent of the structural concrete quantity in the platform and a construction period of 16 months on the critical path.

The purpose of this analysis was to reduce the reinforcement in the projections which are exposed to the design ice load and to arrive at recommendations for the most effective shape and size. In order to achieve this, five steps of analysis have been performed successively, representing conventional methods as well as most advanced computer techniques. The five steps of analysis have been summarized in chapter 2.

The paper presented describes the steps of analysis as executed by Delta Marine Consultants, the engineering subsidiary of the HBG in order to determine the reinforcement of the triangular projection and its ultimate load capacity.

2. SUMMARY OF THE STEPS OF ANALYSIS

2.1 Preliminary projection sizing

Due to the shape of the projections, shear deformations cannot be neglected and thus the slender beam theory cannot be used. For this reason, a deep beam theory has to be used.

By application of the lower bound approach in order to determine the load capacity of a deep beam, the so-called "plastic lattice model analysis" has been developed. This technique is used to describe a mechanism of load transfer. The theory about the collapse mechanisms in deep beams has been described in detail [1].

The boundary conditions for a plastic lattice model analysis are:
- a selected static allowable distribution of stresses has to be in equilibrium with the static and kinematic boundary conditions.
- elastic deformations are negligible compared to plastic deformations.
- only compressive stresses are present in the concrete.
- all tensile forces are carried by the steel.
- the steel has an ideal plastic behaviour.
- the ultimate load capacity of the plastic lattice model is achieved when the stresses in one or more of the basic elements equal the allowable compressive stress or the yield stress.
- changes in geometry, which occur prior to collapse of the structure, are neglected. The equilibrium equations can be drawn up for the original dimensions of the structure.

The basic elements in the plastic lattice model are: (Fig. 3)
- compressive struts in the concrete
- tensile elements for (prestressed) steel
- so-called "hydrostatic joints" with bi-axial stress state

By application of the plastic lattice model analysis, the preliminary sizes of the triangular projection have been determined.

2.2 Determination of sizes of the projection supporting walls

In order to determine the load transfer by the triangular projection and the projection supporting walls, a three-dimensional finite element model with 640 elements has been made of half the platform. The center of impact of the ice load is situated 40.7 m above mudline, which results in the highest vertical and horizontal bending stresses (Fig. 4). The magnitude of the load equals F=538 MN (incl. $\gamma_f = 1.3$) on half the structure.

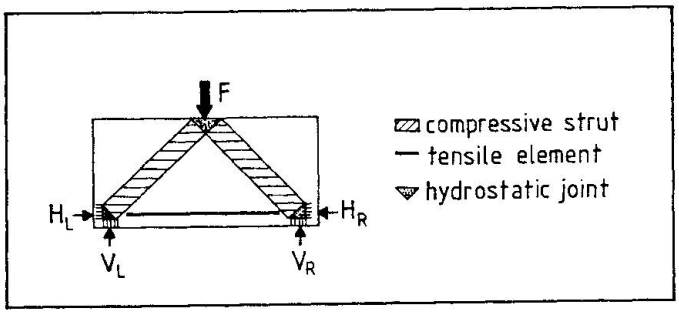

Fig.3 Basic elements plastic lattice model

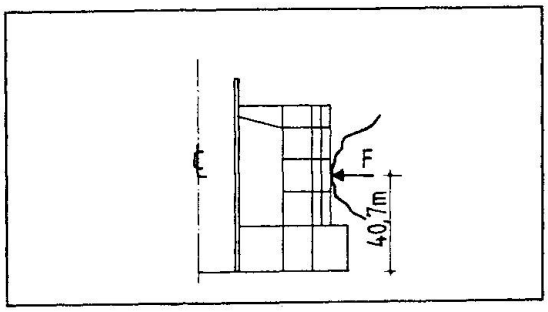

Fig.4 Iceberg load on platform

From the results of the elastic analysis, the sizes of the projection supporting walls have been derived.

2.3 Preliminary design of the projection reinforcement

A two-dimensional model of one triangular projection has been analysed by using plane frame beam elements in order to find the elastic load transfer. With the results of the linear elastic analysis, a final plastic lattice model has been constructed to establish the projection reinforcement under design ice loading of 5.2 MPa.

2.4 Final determination of the projection reinforcement

To check the sizing of the projection, as executed in section 2.3, a finite element analysis with 302 linear elastic elements has been made by using the program package DIANA. This analysis has led to some minor corrections of the reinforcement. For elements with high tensile stresses under design loading, the modulus of elasticity for the concrete has been reduced in accordance with the element reinforcement.

2.5 Determination of ultimate load capacity of the projection

After the analysis with linear elastic elements, the element mesh in the vicinity of the ice load has been refined. This part contains non-linear elastic elements with reinforcement. The ultimate load capacity of the projection has been determined by using the finite element package DIANA-NONLIN. Within this computer program material models with associated parameters have been used as presented in Table 2. For more information regarding this subject, reference is made to [2] and [3].

UNREINFORCED CONCRETE IN TENSION	FRACTURE ENERGY G_f TENSILE STRENGTH f_{ct} CRACKBAND WIDTH h SHEAR RETENTION FACTOR β
REINFORCED CONCRETE IN IN TENSION	TENSION-STIFFENING SHEAR RETENTION FACTOR β
CONCRETE IN COMPRESSION	INTERNAL FRICTION ANGLE φ COHESION c TENSION CUT-OFF CRITERION UNIAXIAL COMPR. STRENGTH f_{cc} YOUNG'S MODULUS E_c
REINFORCING STEEL	YIELD STRESS f_{sy} YOUNG'S MODULUS E_s

Table 2 Parameters for modelling

3. DETERMINATION OF PROJECTION REINFORCEMENT

3.1 Plane frame analysis and plastic lattice model analysis

The triangular projection has been analysed by using the computer program STRESS with plane frame beam elements. The influence of one adjacent projection has been taken into account by defining springs with axial and rotational stiffness at the support points. The ice loading of 4 MPa, present on one side, has been multiplied by a load coefficient $\gamma_f = 1.3$ to obtain the design loading of 5.2 MPa [4].

Since ice load on both sides of the projection gives lower bending moments, this load condition has not been analysed in detail. The computer model of the projection, as used for the plane frame analysis, is presented in Fig. 5. The members of the computer model coincide with the centre lines of the triangular projection.

The results of the plane frame analysis with linear elastic load distribution are presented in Fig. 6. By using these results, a plastic lattice model for the main part of the projection has been drawn (Fig. 7).

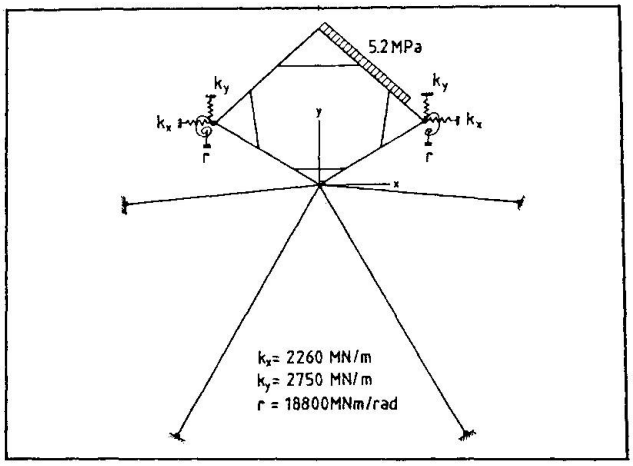

Fig. 5 Plane frame model of projection

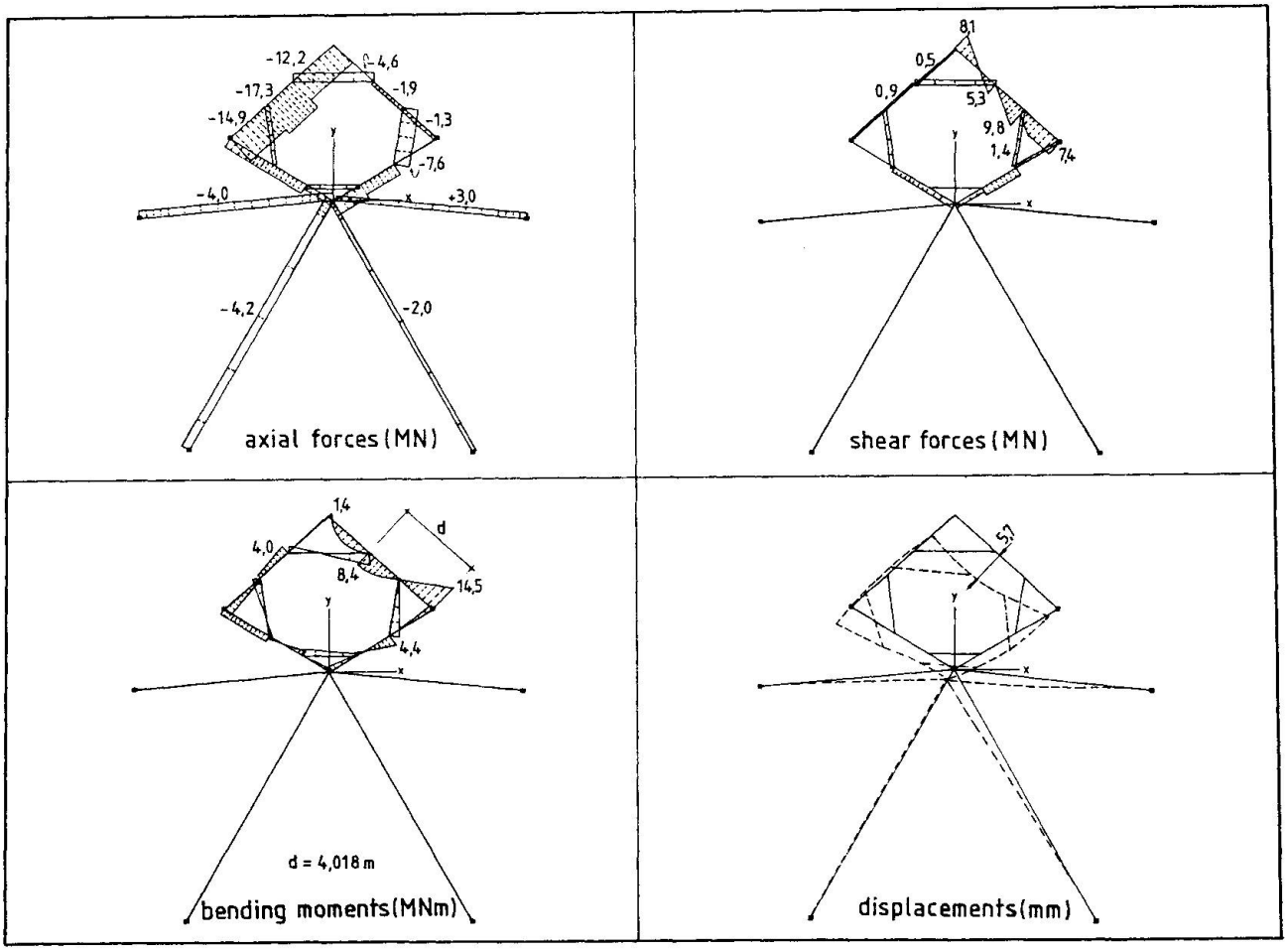

Fig. 6 Results of plane frame analysis

In the struts the allowable compressive strength of concrete f_c has been derived from [4] as follows:

- characteristic cylinder strength f_{ck} = 48 N/mm²
- material coefficient γ_m = 1.4
- maximum resistance against bending moment $f_c = 0.85 * f_{cr}$
  where: $f_{cr} = f_{ck} / \gamma_m$ = 34.3 N/mm²
- maximum resistance against axial force (uniaxial compressive strength)
  $f_c = 0.85 * 0.85 * f_{cr}$ = 24.8 N/mm²

The uniaxial compressive strength of the concrete determines the width of the compressive struts and the tensile elements according the formula:

$w = F/f_c$

where : w = width of strut
F = compression or tension force
f_c = allowable compressive strength of concrete

The force in the tensile element F_t = 6.82 MN represents the tension force in the reinforcement. The required quantity of reinforcement has been derived from:

$A_s = \gamma_m * F_t/f_y$

where : γ_m = material coefficient of steel = 1.15
F_t = force in tensile element
f_y = yield stress of steel = 415 N/mm²

This resulted in reinforcement of 25 mm diameter bars at 100 mm centres (Ø 25-100) and 35 mm diameter bars at 75 mm centres (Ø 35-75) at the inner side of the projection walls.

The reinforcement at the connection point with the adjacent projection has been determined by using the axial force of 5.6 MN (tension) and the bending moment of 16.7 MNm. The required quantity of reinforcement resulted in 35 mm and 40 mm diameter bars at 75 mm centres (Ø 35-75 and Ø 40-75 resp.) at the outer side. Since the compressive struts fit in the concrete structure, shear reinforcement (stirrups) are not compulsory for load transfer. However, to achieve more ductility, a minimum quantity of stirrups has been applied over a 2.4 m length in the walls of the projection. [1]

3.2 Finite element linear elastic analysis

A finite element analysis has been executed by using the program package DIANA. For this analysis three triangular projections with supporting walls have been modelled with 302 linear elastic elements. Eight-noded plane strain elements have been used, with nine integration points. The model has fixed supports in the internal ring whereas the supports in the external ring only have a spring with axial stiffness. In order to simulate the adjacent projection, the support of the projection itself has two springs with axial stiffness and one spring with rotational stiffness (Fig. 8).

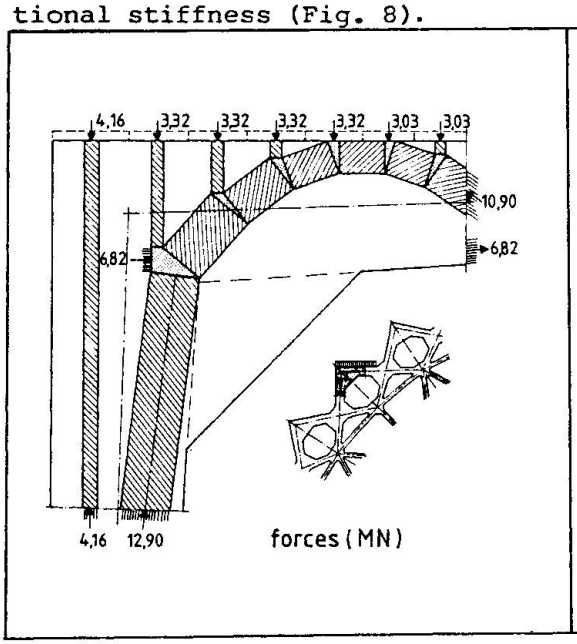

Fig. 7 Plastic lattice model part of triangular projection (load = 5.2 MPa; γ_m = 1.3)

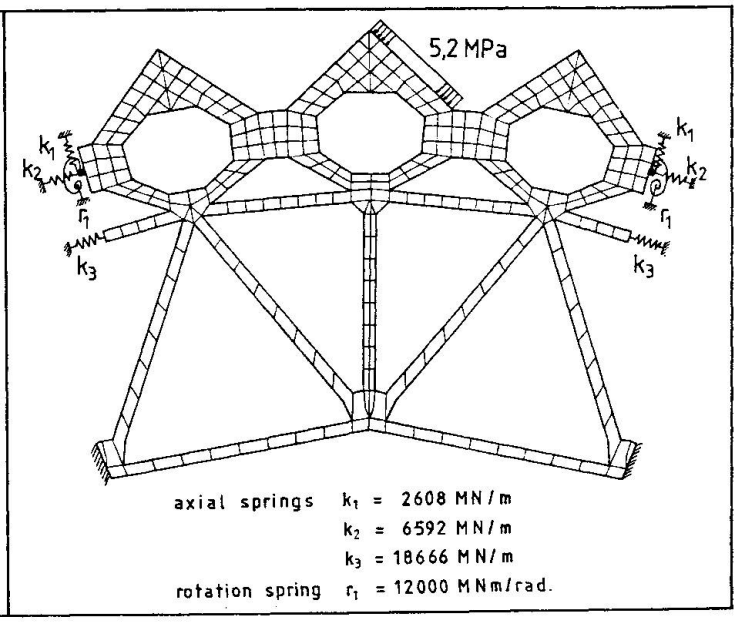

Fig. 8 Finite element model with boundary conditions and design ice loading

Comparison of the results of the linear elastic analysis with those of the plastic lattice model resulted in the following conclusions:

- by taking into account the rotational stiffness of three adjacent triangular projections instead of one, the reinforcement in the connection between the projections is reduced to approx. 70%, whereas the displacement halfway along the loaded projection wall is increased with a factor 2.5
- the tension force in the ice loaded projection wall is approx. 75% of the tension force determined in the plastic lattice model analysis. This proves the statement that the design method, by using a plastic lattice model, is conservative for the determination of the ultimate load capacity of the triangular projection.

By using the results of the plastic lattice model and the finite element analysis, the reinforcement in the projection has been determined (Fig. 9), by taking into account the following considerations:

- in the outer skin of the projection adjacent to the loaded projection wall, a tension force is present which cannot be neglected.
- the reinforcement in the projection is symmetrical.
- for practical reasons 3 different bar diameters and 4 different centre to centre distances have been selected.
- the minimum reinforcement in the projection is Ø 25-100 horizontal and Ø 30-200 vertical.

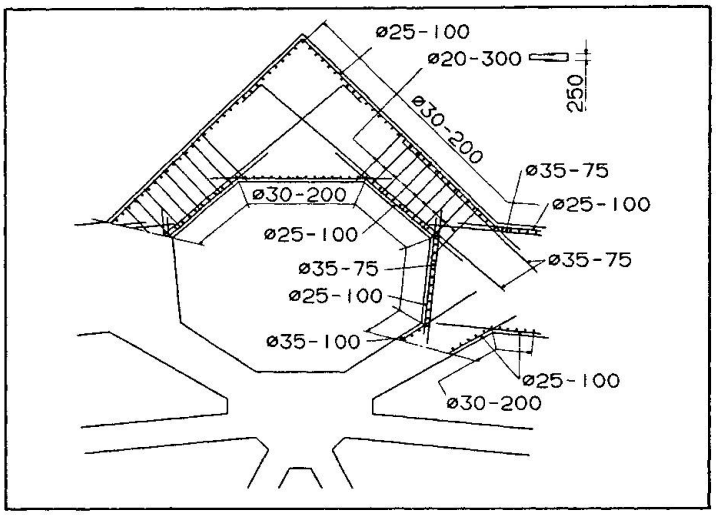

Fig. 9 Reinforcement in projection

4. NON-LINEAR ANALYSIS OF TRIANGULAR PROJECTION

In order to determine the ultimate load capacity of the projection, a fine element mesh of the model in the vicinity of the ice loading has been generated (Fig. 10). The 152 elements of the fine mesh have non-linear elastic behaviour and they contain reinforcing steel, which has been modelled as replacing steel plates with orthogonal properties (Fig. 11).

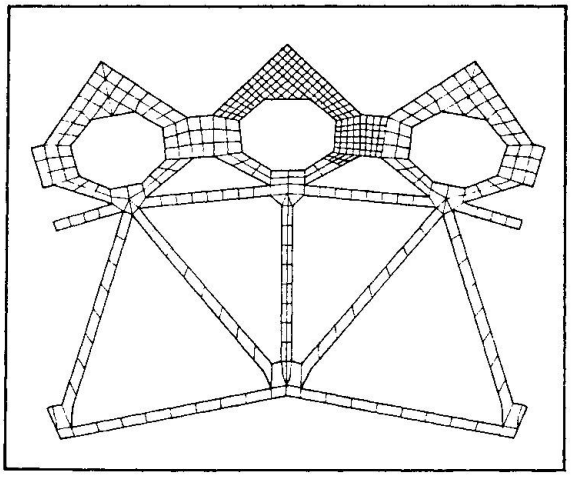

Fig. 10 Computer model for non-linear analysis

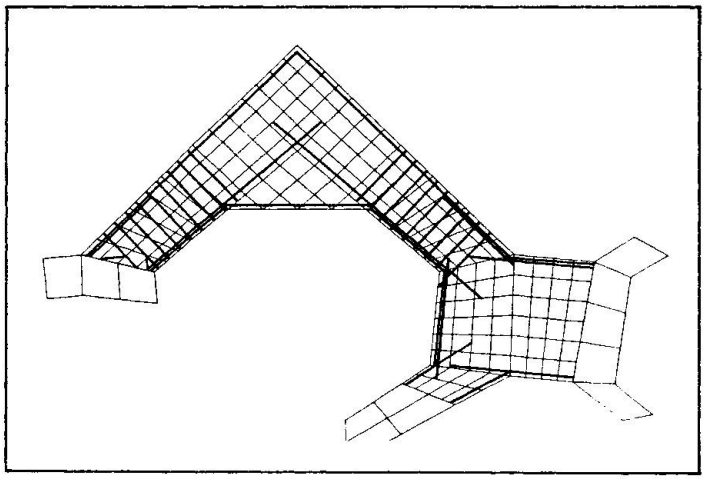

Fig. 11 Element mesh with non-linear elastic elements and reinforcing steel

The anchorage length of the bars has not been modelled. Perfect bond was assumed to exist between steel and concrete. The other concrete elements have elastic material behaviour. The Young's modulus of the concrete for a part of the external ring has been reduced to E_c = 2730 N/mm² according to [4] because the results of the plane frame analysis as well as the results of the linear elastic analysis presented in this part element stresses, which exceed the concrete tensile strength.

The material parameters used in the analysis for the non-linear elastic elements, both for the concrete and the reinforcing steel have been summarized in Table 3.

The non-linear analysis, taking into account aggregate interlock and using the smeared crack approach, has been executed with the finite element program package DIANA-NON-LIN.The non-linear analysis has been performed by incremental, iterative procedures, using load steps of appropriate magnitude. The failure of the triangular projection has been defined to occur if no convergence is achieved after addition of a load increment. The loading on the projection has been increased from 0 MPa to 9.1 MPa by load steps of decreasing magnitude. After a total load of 9.1 MPa no convergence has been achieved for another load step due to start of yielding of the reinforcement at the inner side of the loaded projection wall. This means that the ultimate load capacity of the triangular projection equals 9.1 MPa. The results of the non-linear analysis of the projection are presented for the minimum design ice loading of 5.2 MPa (Fig. 12) and for the ultimate ice loading of 9.1 MPa (Fig. 13).

CONCRETE	E_c = 35000 N/mm² ν = 0.2 f_{cc} = 48 N/mm² f_{ct} = 4.8 N/mm² TENSION CUT-OFF CRITERION I ε_{us} = 0.00198 β = 0.20 φ = 30° c = 13.86 N/mm²
REINFORCING STEEL	E_s = 210000 N/mm² f_{sy} = 415 N/mm²

Table 3 Material parameters non-linear elastic elements.

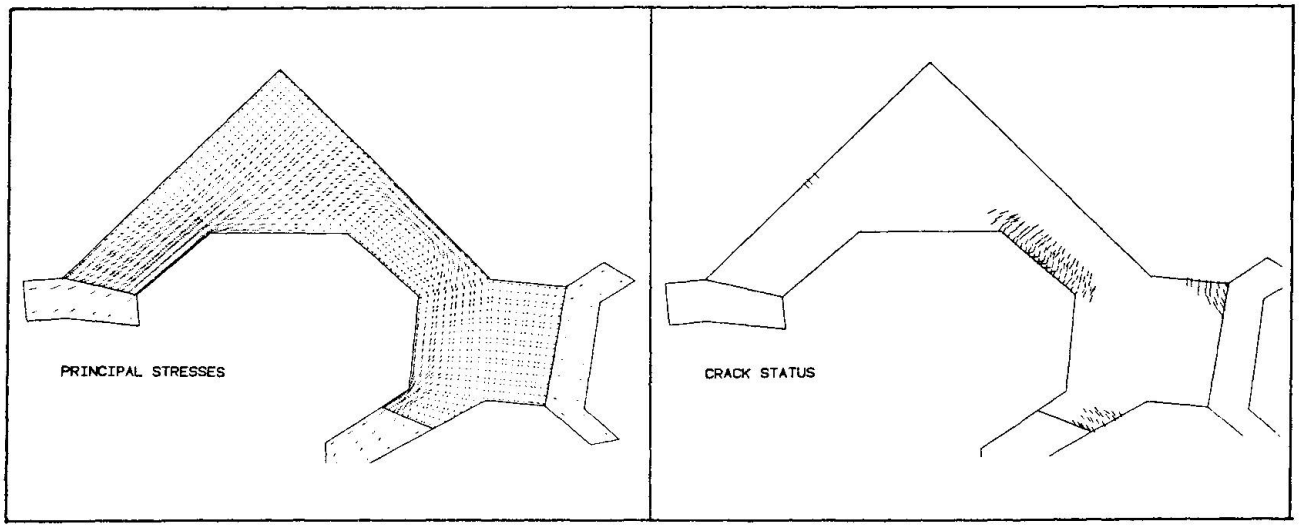

Fig. 12 Results after minimum design ice loading (5.2 MPa)

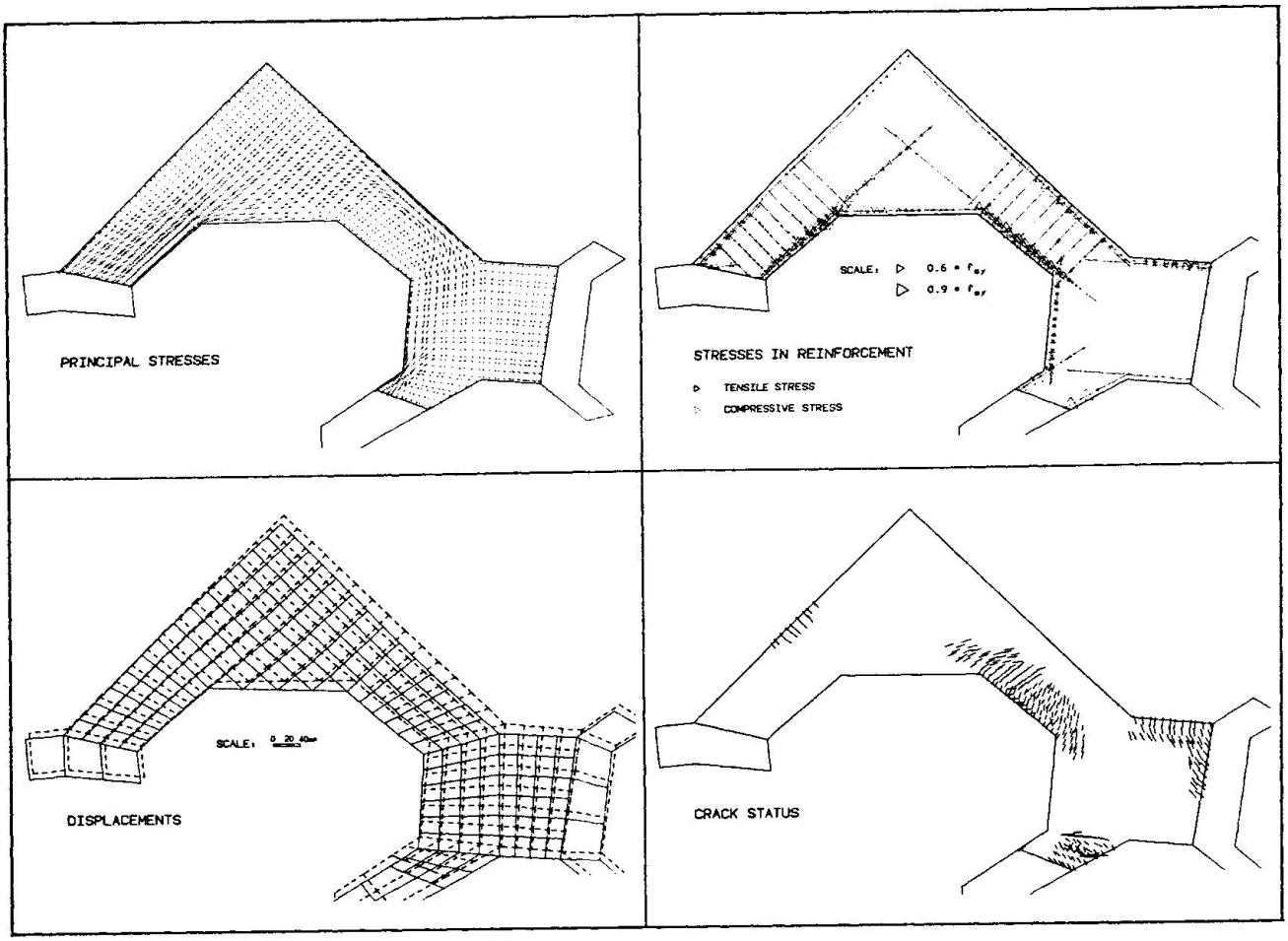

Fig. 13 Results after ultimate ice loading (9.1 MPa)

5. DISCUSSION OF RESULTS

The ultimate ice loading, equal to 9.1 MPa as computed in the non-linear elastic analysis, represents a load coefficient γ_f = 2.28 on the ice crushing strength of 4 MPa. This exceeds the minimum required load coefficient γ_f = 1.3 with a factor m = 1.75. Although the plastic lattice model analysis is a lower bound approach for the ultimate load capacity of a structure, it is preferred to predict the ultimate load capacity of a structure as accurately as possible. However, other studies on behaviour of deep beams have demonstrated that the ratio between predicted load capacity by using the plastic lattice model analysis and load at failure as found in laboratory model tests varies considerably [5].

In order to explain the above mentioned factor m two items have been further investigated:
- the magnitude of the material coefficient of concrete
- the influence of the plane frame model on the tensile force in the inner side of the wall and the lay-out of the compressive struts.

5.1 Material coefficient of concrete

In order to determine the required projection reinforcement by using the plastic lattice model analysis, the ice crushing strength of 4 MPa has been multiplied by a load coefficient γ_f = 1.3. The allowable compressive strength in the concrete struts f_c = 24.8 N/mm² has been calculated by taking into account a material coefficient γ_m = 1.4. This resulted into a force in the tensile element of 6.82 MN, which resulted in reinforcement of Ø 35-75 and Ø 25-100.

In the non-linear analysis of the triangular projection, the uniaxial compressive strength of the concrete f_{cc} has been taken equal to the characteristic cylinder strength, without taking into account a material coefficient. To check the influence of the material coefficient on the required reinforcement in the projection, as determined by application of the plastic lattice model analysis, a model has been drawn for γ_f = 1.3 and γ_m = 1.0 (Fig. 14). This means that in the concrete struts the allowable compressive strength equals f_c = 34.7 N/mm². From the plastic lattice model it can be derived that the tensile force in the reinforcing steel has been reduced with approx. 10% to 6.10 MN. This means that, by using the same material coefficient γ_m for concrete in the plastic lattice analysis model and in the non-linear analysis, the factor m will be reduced to approx. 1.58.

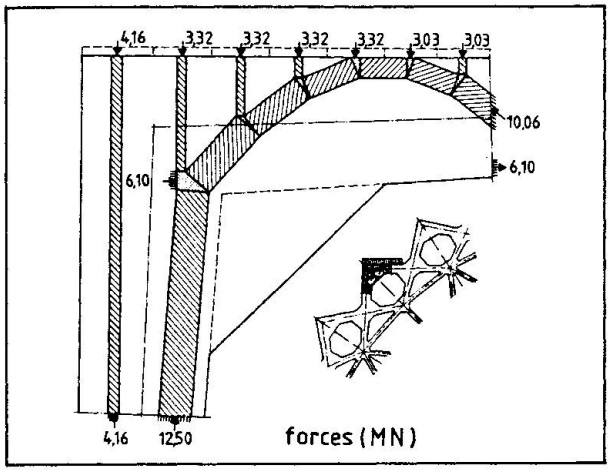

Fig. 14 Plastic lattice model part of triangular projection (load = 5.2 MPa, γ_m = 1)

5.2 Plane frame model of projection

Comparison of the compressive struts in the plastic lattice model as presented in Fig. 7 with the principal stresses as presented in Fig. 12, shows that the maximum bending moment in the loaded projection wall is achieved in different locations. This is probably an explanation for the high load capacity of the triangular projection as found in the non-linear analysis. In order to get the direction of the compressive struts in the plastic lattice model similar to the direction of the principal stresses, two other plane frame models of the projection have been made. For these computer models, the distance d of the maximum bending moment to the connection joint and the tension force F_t in the tensile element of the loaded projection wall have been determined (Fig. 15).

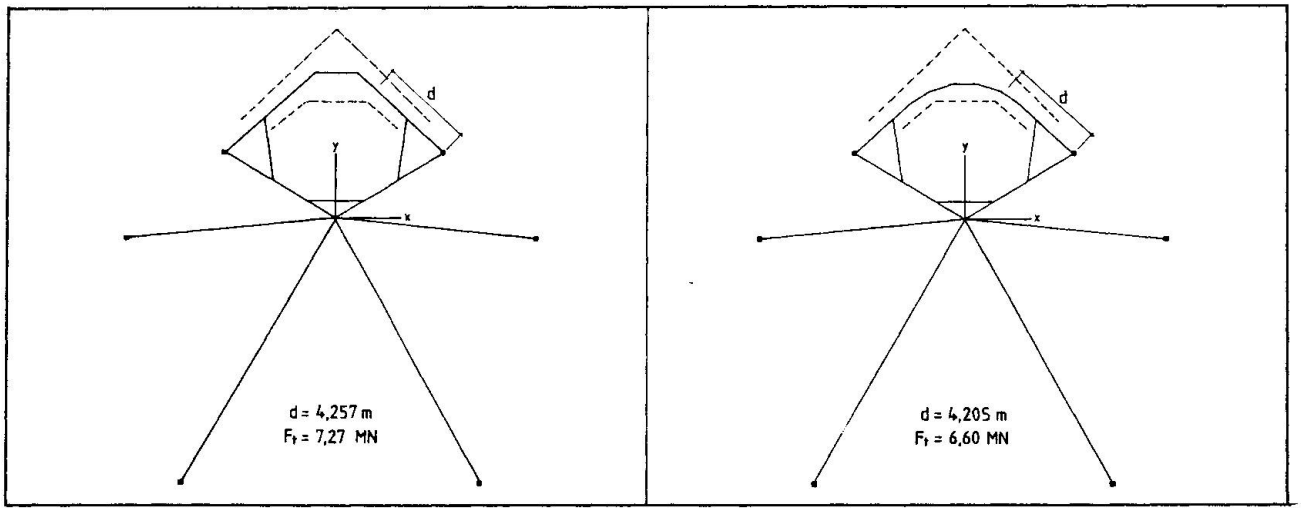

Fig. 15 Alternatives plane frame model of triangular projection

By comparing the results as presented in Fig. 15 with the plane frame analysis as described in section 3.1, it is demonstrated that the direction of the compressive struts in the loaded projection wall is hardly dependant on the plane frame model of the projection, and it is still different from the direction of the principal stresses as found in the non-linear analysis. The differences of the force F_t in the tensile element for both alternatives are well within 10% of the value F_t = 6.82 MN, as found in section 3.1.

5.3 Internal shape of the projection

From the direction of the principal stresses as presented in figures 12 and 13, it is clear that the internal corners of the triangular projection cause stress concentrations, which are critical for failure if compressive stresses are not present in all directions. In order to avoid spots with stress concentrations, it is recommended to re-shape the internal of the projection (Fig. 16).

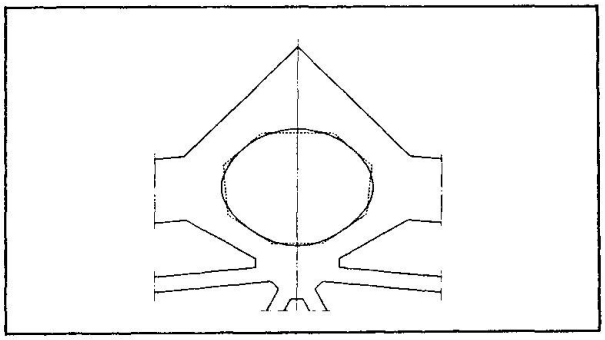

Fig. 16 Recommended shape of projection internal

6. CONCLUSIONS

With regard to the determination of the required reinforcement in the triangular projection of the peripheral wall of an iceberg resistant offshore structure and with regard to the determination of its ultimate load capacity, as presented in this paper, the following conclusions have been drawn:

- The modelling of the triangular projection for the plane frame analysis has little influence on the direction of the compressive struts and the required quantity of reinforcement as determined in the plastic lattice model analysis.
- The sizing of the projection by using the plastic lattice model technique is conservative for the determination of the ultimate load capacity of the projection, which exceeds the design load with a factor 1.58.
- As the concrete compressive struts fit in the projection walls, as presented in the plastic lattice model analysis, shear reinforcement (stirrups) is not necessary. This has been proved in the non-linear analysis. However, to achieve ductility of the structure it is recommended to apply the minimum quantity of stirrups in the projection walls.
- The failure of the triangular projection is induced by yielding of the reinforcing steel at the inner side of the loaded projection wall.

REFERENCES

1. CEB-FIP Model Code for concrete structures. Bulletin d'information Nos. 146 and 150/1982.
2. MIER J.G.M. van et al., Examples of Non-Linear Analysis of Reinforced Concrete Structures with DIANA-NONLIN, September 1986.
3. ROTS J.G., NAUTA P., KUSTERS G.M.A and BLAAUWENDRAAD J., Smeared crack approach and fracture localization in concrete. HERON Vol. 30, 1985.
4. DnV Rules for the design, construction and inspection of offshore structures. Reprint, 1981.
5. ROGOWSKI D.M., MACGREGOR J.G., Shear strength of deep reinforced concrete continuous beams. Structural Engineering Report no. 110. Department of Civil Engineering University of Alberta, Edmonton, Canada.

Leere Seite
Blank page
Page vide

Nonlinear Analysis of Reinforced Concrete Roof Using Shell Elements

Analyse non-linéaire de toitures en béton armé, à l'aide d'éléments de coques

Nichtlinearer Berechnung eines Betondachtragwerks mit Hilfe von Schalenelementen

Ole STRØM
Doctor Engineer
Veritas Research
Høvik, Norway

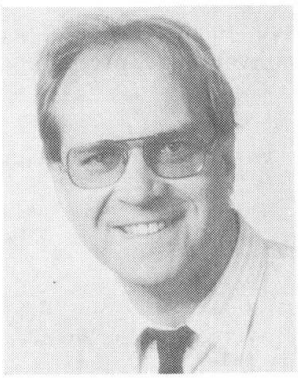

Ole Strøm, born 1958, got his civil and doctor's engineering degree at the Norwegian Institute of Technology, Trondheim, Norway. For the last four years he has worked with the nonlinear finite element program FENRIS, and then mainly with reinforced concrete.

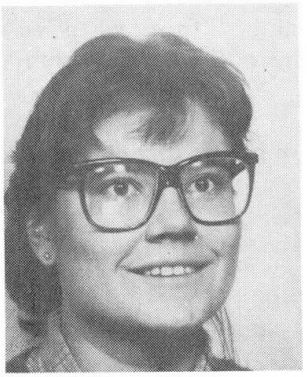

Anne Vasbotten, born 1962, got her civil-engineering degree at the Norwegian Institute of Technology, Trondheim, Norway. Her diploma work was about reinforced concrete roofs using shell elements.

Anne VASBOTTEN
Civil Engineer
Norwegian Inst. of Techn.
Trondheim, Norway

SUMMARY

This paper deals with nonlinear finite element analyses of reinforced concrete shell roofs. Four noded shell elements, based on the theory of free formulation, are used together with a nonlinear concrete- and reinforcement-model. The general elastic-plastic flow theory is combined with the load surface theory of Chen and Chen. This theory allows for different properties in tension and compression. Hardening, cracking and crushing are handled. Smeared cracking with two independent crack directions may be introduced when cracking.

RÉSUMÉ

L'article a pour objet l'analyse de coques en béton armé par la méthode des éléments finis non-linéaires. Des éléments de coques à quatre noeuds basés sur la théorie de la formulation libre sont utilisés en même temps qu'un modèle non-linéaire de béton et de renforcement. La théorie générale d'écoulement élastique-plastique est combinée avec la théorie des charges superficielles de Chen et Chen. Cette dernière théorie permet de considérer des propriétés différentes en tension et en compression. Le durcissement, la fissuration et l'écrasement sont étudiés. Des fissurations homogénéisées avec deux directions indépendantes peuvent être introduites.

ZUSAMMENFASSUNG

In diesem Beitrag werden nicht-lineare Finite-Elemente-Analysen für Schalendecken aus Stahlbeton durchgeführt. Dabei werden vier Knotenelemente unter Zugrundelegung der Theorie der freien Formulierung zusammen mit einem nicht-linearen Modell für Beton und Stahl angewandt. Die allgemeine elasto-plastische Fliesstheorie wird mit der Grenzflächentheorie von Chen u. Chen kombiniert. Die Theorie erlaubt die Anwendung verschiedener Eigenschaften für Zug- und Druckbelastung. Erhärtung, Rissbildung und Druckversagen werden behandelt. Die Bildung von ausgeglichenen Rissen mit zwei unabhängigen Rissrichtungen kann auch eingeführt werden.

1. THE QUADRILATERAL SHELL ELEMENT

The four noded shell element is based on the free formulation [1,2]. This element is initially planar and has three translational and three rotational freedoms per corner node. The convergence of the elements, which is well documented in [1,2], are assured through satisfaction of the so-called "individual element test".

The incremental equilibrium is expressed through the relation

$$\Delta \mathbf{S}_{int} = \mathbf{k}_T \Delta \mathbf{v} = (\mathbf{k}_{mat} + \mathbf{k}_{geom})\Delta \mathbf{v} \tag{1}$$

The tangential or incremental stiffness $\mathbf{k}_T$ is comprised of material and geometric stiffness contributions. The material stiffness is obtained from the convential expression

$$\mathbf{k}_{mat} = \int_V \mathbf{B}^T \mathbf{C}_T \mathbf{B} dV \tag{2}$$

where $\mathbf{C}_T$ is the tangential or incremental material law. The strain-producing matrix, $\mathbf{B}$, is given by

$$\mathbf{B} = \frac{1}{V}\mathbf{L}^T + \tilde{\mathbf{B}}_{qh}\mathbf{H}_h \tag{3}$$

Where V is the volum of the element, and $\mathbf{L}$ is the so-called "lumping matrix". $\tilde{\mathbf{B}}_{qh}$ is "energy orthogonal" with respect to the rc-modes. $\mathbf{H}_h$ is the inverted, generalized h-modes [1,2].

The geometric stiffness matrix $\mathbf{k}_{geom}$ for a flat shell element may be derived from the incremental form of the virtual work principle. The geometric stiffness for in-plane (membrane) action is uncoupled with the out-of-plane (bending) action [1,2].

In the co-rotated reference system the internal, element nodal reaction forces $\mathbf{S}_{int.}$ is found from the usual expression

$$\mathbf{S}_{int} = \int_V \mathbf{B}^T \sigma dV \tag{4}$$

Where σ is the Cauchy stress.

The forces and stiffness matrices are found by using two by two Gausian integration over the area of the quadrilaterial. Over the thickness eight Lobatto points are used.

2. THE COROTATED "GHOST" REFERENCE DESCRIPTION

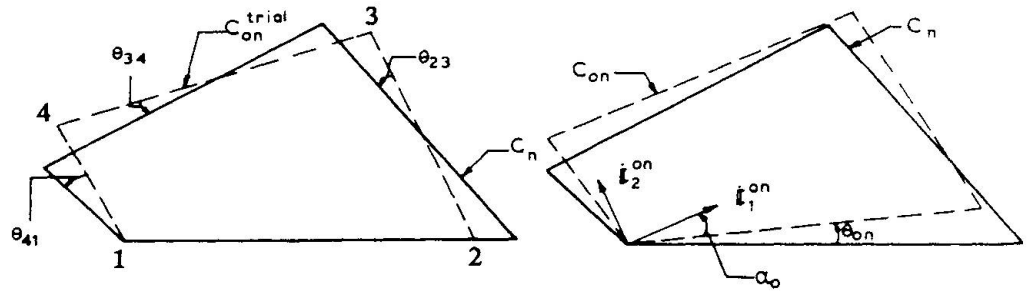

Fig. 1 Quadrilateral shell element in deformed and corotated configuration

A Langrian description of the displacements is used. The deformation of each element is referred to the initial configuration of each element. This reference configuration, C_{on}, is closely displaced and rotated along with the deformed configuration in order to minimize the rigid-body part of the rotational motion.

The direction of the local x-axis goes through nodes 1 and 2 of the "ghost" reference C_{on}. The normal to the plane of the "ghost" reference is taken as the vector formed by the cross-product of the vectors formed by the two diagonals of the deformed element. The corners 2, 3 and 4 of the warped quadrilateral are projected onto the reference plane. The "ghost" reference C_{on} is then rotated in its plane such that the sum of the squared deviatoric angles Θ_{ij} from the projected element C_n is minimized [1,2], see Fig. 1. The "ghost" reference will then be objective with respect to the rotations.

3. THE FLOW THEORY BY CHEN AND CHEN

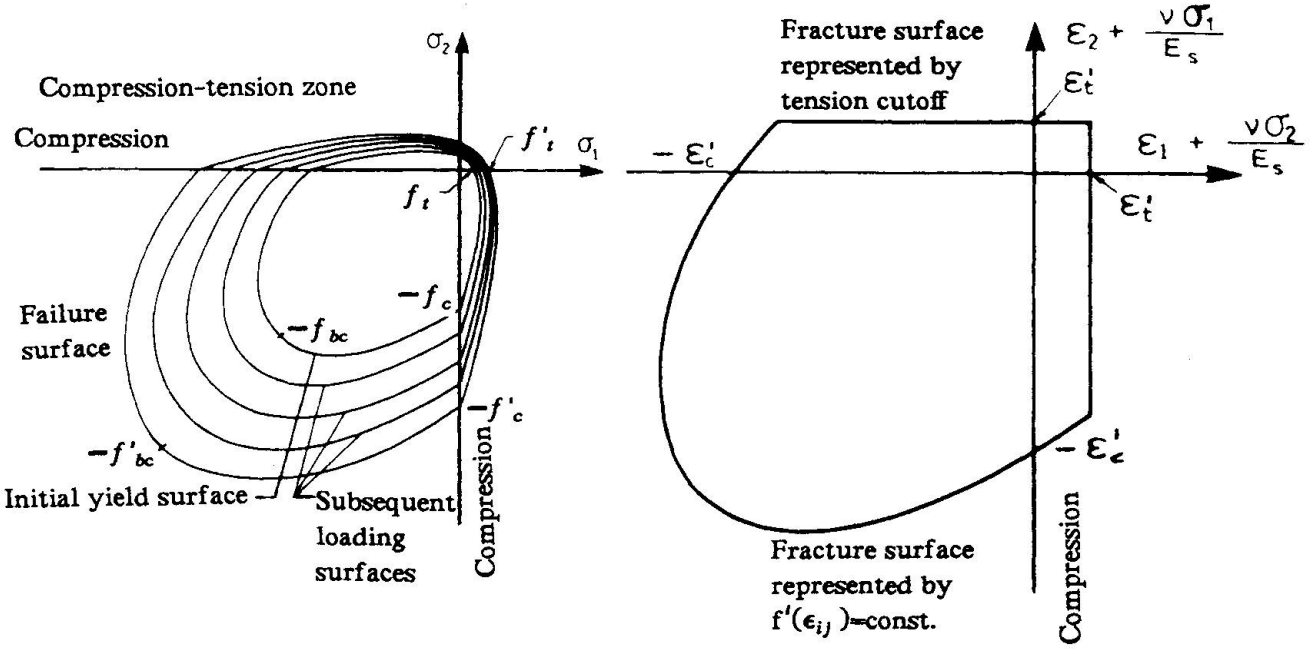

Fig. 2 a) Loading surfaces of concrete in the biaxial stress plane. b) Fracture surface defined by strain components in the biaxial strain plane.

Chen and Chen postulated an initial, non-smooth yield surface with subsequent loading surfaces, and a failure surface for concrete. These surfaces in two-dimensional principal stress space are traced in Fig. 2a. The concrete is treated as an elastic-plastic strain hardening material with fracturing behaviour in tension.

Three mathematical equations are used to define Chen and Chen's loading surfaces [3,4,5] :

1) An initial discontinuous loading surface

$$f_o = \sqrt{J_2^\sigma - \frac{1}{12}(I_1^\sigma)^2 \pm \frac{1}{12}(I_1^\sigma)^2 + \frac{A_o}{3}I_1^\sigma} - \tau_o \tag{5}$$

2) Subsequent loading surfaces

$$f = \frac{\sqrt{J_2^\sigma - \frac{1}{12}(I_1^\sigma)^2 \pm \frac{1}{12}(I_1^\sigma)^2 + \frac{\beta}{3}I_1^\sigma}}{\sqrt{1 - \frac{\alpha}{3}I_1^\sigma}} - \tau \tag{6}$$

3) An ultimate failure loading surface

$$f_u = \sqrt{J_2^\sigma - \frac{1}{12}(I_1^\sigma)^2 \pm \frac{1}{12}(I_1^\sigma)^2 + \frac{A_u}{3}I_1^\sigma} - \tau_u \tag{7}$$

The material constants, A_o, τ_o, A_u and τ_u are functions of the material parameters f_c, f'_c, f_t, f'_t, f_{bc} and f'_{bc}, see Fig. 2a. Here, f'_c, f'_t and f'_{bc} denote the ultimate strength of concrete under uniaxial compressive loading, uniaxial tensile loading, and equal biaxial compressive loading, respectively, while f_c, f_t and f_{bc} denote the initial yield strength of concrete under uniaxial compressive loading, uniaxial tensile loading and equal biaxial compressive loading. The positive-negative sign in the third term in Eqs. (5) to (7) represents the loading function in the "compression-compression zone" and the "tension-compression and tension-tension zone", respectively. The loading surfaces, which are functions of the history of loading, are derived from an isotropic expansion of the initial yield surface, until coincidence with the failure surface f_u is reached. The failure surface f_u is the outmost extreme loading surface. The constants α and β are found by the claim that the loading surface shall coincide with the initial yield surface and the failure surface as extreme cases.

For the case of plane stress ($\sigma_{zz} = \sigma_{xz} = \sigma_{yz} = 0$) the incremental stress strain relation will be [3] :

$$\begin{Bmatrix} d\sigma_{xx} \\ d\sigma_{yy} \\ d\sigma_{xy} \end{Bmatrix} = \frac{E_o}{(1-\nu^2)} \begin{bmatrix} 1-\omega\Phi_{11} & \nu-\omega\Phi_{12} & -\omega\Phi_{13} \\ & 1-\omega\Phi_{22} & -\omega\Phi_{23} \\ & & \frac{(1-\nu)}{2}-\Phi_{33} \end{bmatrix} \begin{Bmatrix} d\varepsilon_{xx} \\ d\varepsilon_{yy} \\ 2d\varepsilon_{xy} \end{Bmatrix} \tag{8}$$

in which

$$\frac{1}{\omega} = 2(1-\nu)J_2^\sigma - (1-2\nu)\sigma'^2_{zz} - 2(1+\nu)\rho\sigma'_{zz} + 2(1+\nu)\rho^2 + (1-\frac{\alpha I_1^\sigma}{3})\frac{H(1-\nu^2)}{E_o}\sqrt{2J_2^\sigma + 2\rho^2} \tag{9}$$

where E_o is the initial modulus of elasticity, and ν is Poisson's ratio. Further we have that σ'_{xx}, σ'_{yy}, σ'_{zz} are the deviatoric stress components, I_1^σ is the first invariant of the total stresses and J_2^σ is the second invariant of the deviatoric stresses. ρ is given by :

$$\rho = \frac{(\pm 3 - \kappa^2)}{18} I_1^\sigma + \frac{(\beta + \alpha\tau^2)}{3} \tag{10}$$

Φ_{11}, Φ_{12}, Φ_{13}, Φ_{22}, Φ_{23} and Φ_{33} [3,4,5] are functions of Poisson's ratio, the deviatoric stress components and ρ.

The strain-rate function, H, depends upon the current state of stress, strain and straining history. H may be written as :

$$H = (\frac{2}{3})^{1.5} |\bar{\sigma}_{xx}| \frac{E_o E_t}{(E_o - E_t)} \tag{11}$$

where $\bar{\sigma}_{xx}$ is the one-dimensional compressive stress corresponding to the total equivalent plastic strain, which is given by :

$$\bar{\varepsilon}_p = \int d\bar{\varepsilon}^p = \int \sqrt{\frac{2}{3} d\varepsilon_{ij}^p d\varepsilon_{ij}^p} \tag{12}$$

Since $\bar{\varepsilon}^p$ and $\bar{\sigma}_{xx}$ always are related to the compression part of the one-dimensional stress-strain curve, the tangent stiffness, E_t, will also always be from the compression branch of the one-dimensional stress-strain curve.

4. TENSION CRACKING AND CRUSHING OF CONCRETE

If the stress point is outside the failure surface in the tension-compression zone or in the tension-tension zone in Fig. 2a a crack is formed in the plane of the shell element and normal to the greatest principal stress. The direction of this crack will be stored and unaltered through the further calculations. And this crack will influence the local stiffness matrix as long as the strain normal to the crack is greater than zero. If later the second principal stress becomes greater than f_t' an additional crack is formed. The direction of the second crack is not necessary normal to the first crack. Also the second crack direction will be stored and unaltered through the further calculations. The second crack will only influence the local stiffness matrix as long as the strain normal to the crack is greater than zero. Alternatively cracks can also be formed if the strain criterion (14) is exceeded.

When cracking the constitutive matrix is taken to be modified from the initial linear elastic matrix. The total- and incremental-stress normal to the crack drops to zero. If two cracks are formed both normal stresses drop to zero and the stiffness matrix will be a zero matrix except for the diagonal value for eventually retained shear.

The strain criterion of Chen and Chen [3,4,5], which is illustrated in Fig. 2b, is mathematically expressed as :

$$f'(\varepsilon_{ij}) = J_2^{\varepsilon} + \frac{A_u}{3}\frac{\varepsilon_c'}{f_c'} I_1^{\varepsilon} = \tau_u^2 \left(\frac{\varepsilon_c'}{f_c'}\right)^2 \tag{13}$$

or

$$\varepsilon_1 = \varepsilon_t' - \frac{\nu\sigma_2}{E_s} \quad , \varepsilon_2 = \varepsilon_t' - \frac{\nu\sigma_1}{E_s} \tag{14}$$

where I_1^{ε} is the first invariant of the total strains, and J_2^{ε} is the second invariant of the deviatoric strains. ε_1 and ε_2 are the two principle strains, while σ_1 and σ_2 are the stresses in the direction of the principle strains. E_s is the one-dimensional secant stiffness for the stresses σ_1 and σ_2.

If the stresses lies outside the compression-compression failure surface, then the concrete is crushed at this integration point. All stresses then remain at the ultimate level, while the stiffness matrix for the same integration point drops to a zero matrix.

5. THE REINFORCEMENT

The reinforcement is modelled with shell elements placed eccentric to the midpoint of the concrete. The total expressions for the internal forces and the global stiffness matrix are found by summation of the contributions from the elements representing the concrete and the elements representing the reinforcement.

Fig. 3 shows the modelling of the reinforcement bars. θ_1 and θ_2 are the angles between the x-axis and the reinforcement types 1 and 2, respectively. The reinforcement types 1 and 2 have only material stiffness in the directions θ_1 and θ_2, respectively, and a transformation to the x-y system has to be carried out [7].

The reinforcement bars are "smeared out" as a continuous plate, see Fig. 4. The thickness of the equivalent reinforcement layer i is [7]

$$t_i = \frac{n\ A_{si}}{d} \tag{15}$$

in which A_{si} is the cross-sectional area of one bar in the reinforcement layer i, d is the width between the bars and n is the number of reinforcement layers with exactly same material

properties and direction. The concrete is, over the height, "cutted" into a specified number of layers with equal thickness. The numerical integration over the concrete thickness will be by a summation of the influence from each layer.

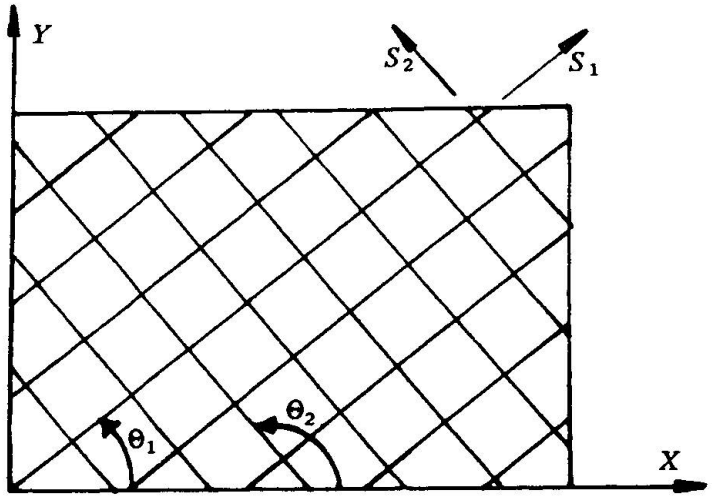

Fig. 3 Reinforcement bars implemented in a membrane element.

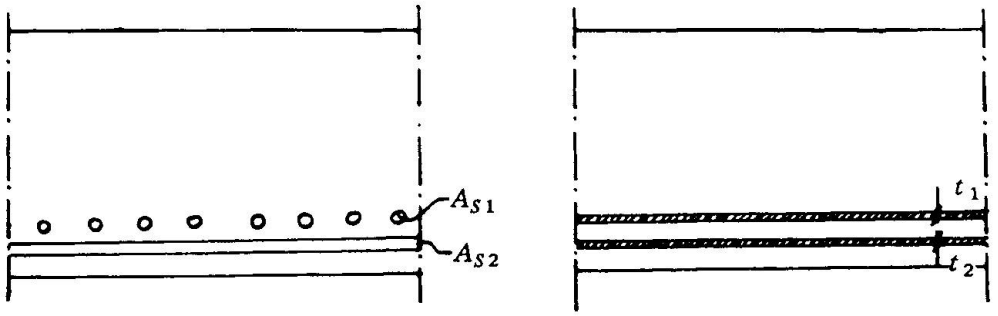

Fig. 4 Idealization of the reinforcement bars.

6. NUMERICAL EXAMPLE

The cylindrical shell roof supported on end diaphragms suggested by Scordelis and Lo [8], has become a classical problem for testing shell elements. The geometry of the shell is given in Fig. 5. For the analysis presented here [9] a 8x8 mesh is used for the nearest quarter of the roof. The accuracy of the 8x8 mesh, and the verification of the shell elements with linear material is well documented in the refs. [1,2], and it is not discussed here.

Fig. 6a shows the material properties for the concrete of quality C45. The compression strains/stresses is according to the norwegian code [10]. The tension strains/stresses are one tenth of the compression strains/stresses. Poisson's ratio is set equal to 0.18. The quality K40TS of the reinforcement is idealized as three straight lines, which is shown in Fig. 6b.

The load-deflection curve of the midpoint of the roof is shown in Fig. 7. The reinforcement was modelled both in $0^o/90^o$ and $45^o/135^o$ to the x-axis. As shown in Fig. 7 the two analysis had the same behaviour up to $P=12.0 \cdot 10^5$N. For higher loads the $0^o/90^o$ analysis was a little bit stiffer. The investigations show further the fault by modelling reinforced concrete structures as a structure with linear behaviour. The first non-linear stadium is a consequence of the non-linearities in the compression part of the equivalent stress/strain curve of Fig. 6a. For concrete

with high f_c/f'_c-ratio the linear behaviour in Fig. 7 would have been higher too.

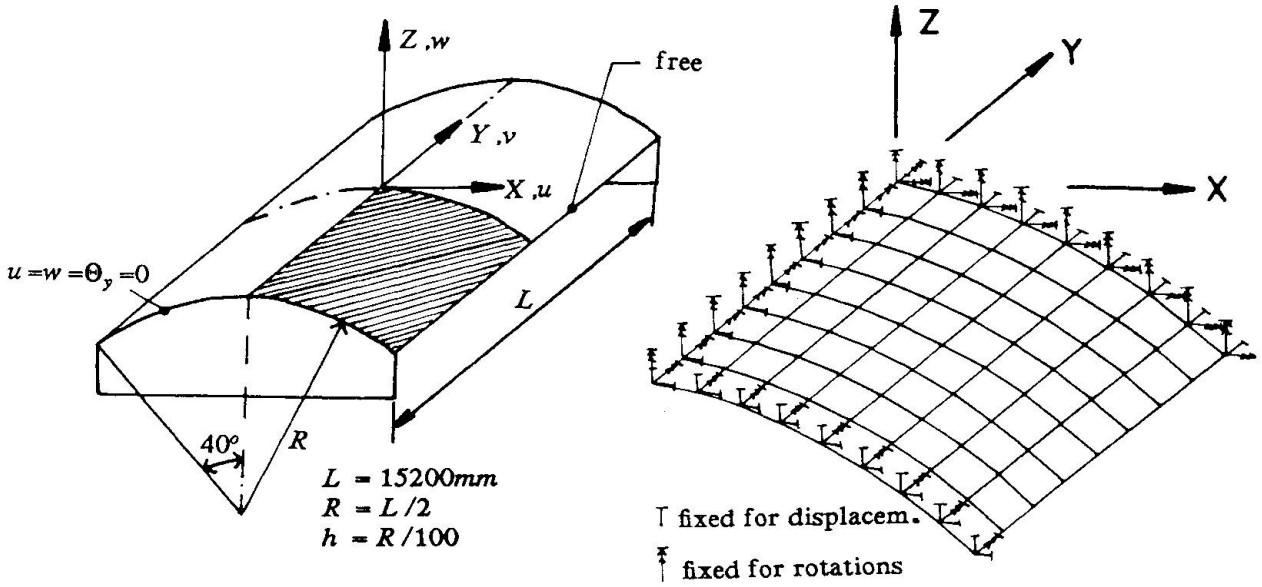

Fig. 5 Cylindrical shell roof

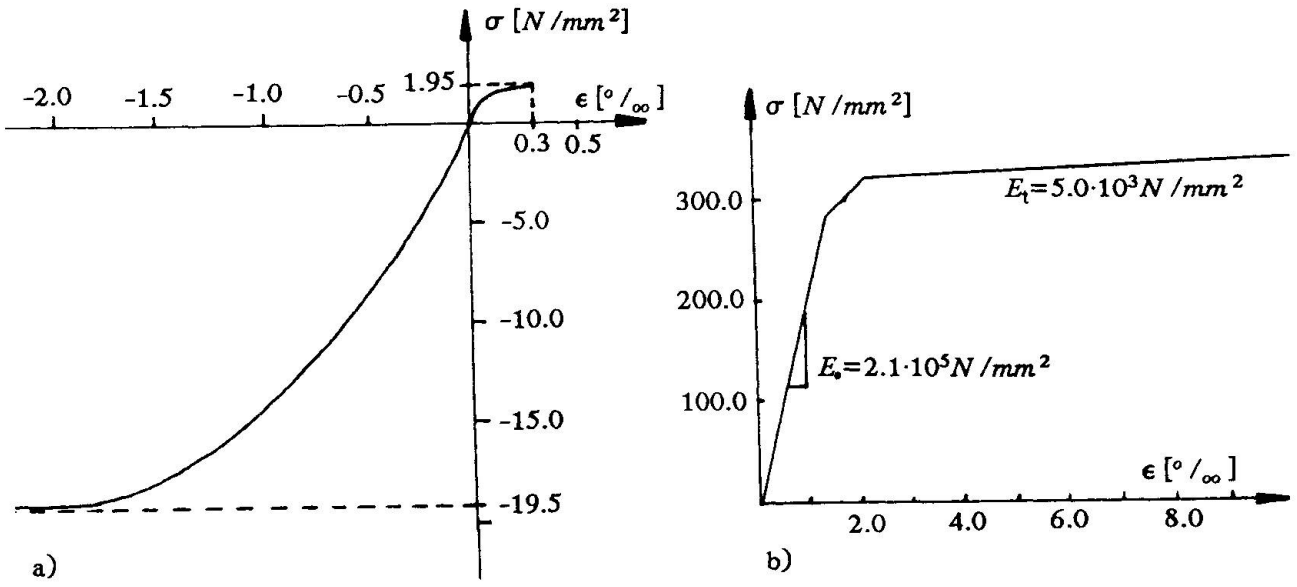

Fig. 6 Equivalent stress/strain relation for a) concrete b) reinforcement

The Fig. 8a show the crack pattern for the integration points in the layer nearest the inside of the roof for three different loads for the $0^o/90^o$ analysis, while the Fig. 8b show the crack pattern for the same integration points for the $45^o/135^o$ analysis for the same three loads. Both analysis show cracking around the load, and cracking around the midpoint of the free side of the roof. This last cracking area was a result of the motion in the x-direction of the elements along the free side of the roof. For this area the shear stresses gave cracking, while under the external load the cracking was a result of bending tensile stresses. The crack propagation in the $0^o/90^o$ analysis has been a little bit less than for the $45^o/135^o$ analysis. And this show clearly that the difference in the crack area is the reason for the difference in the load-deflection at the midpoint in Fig. 7.

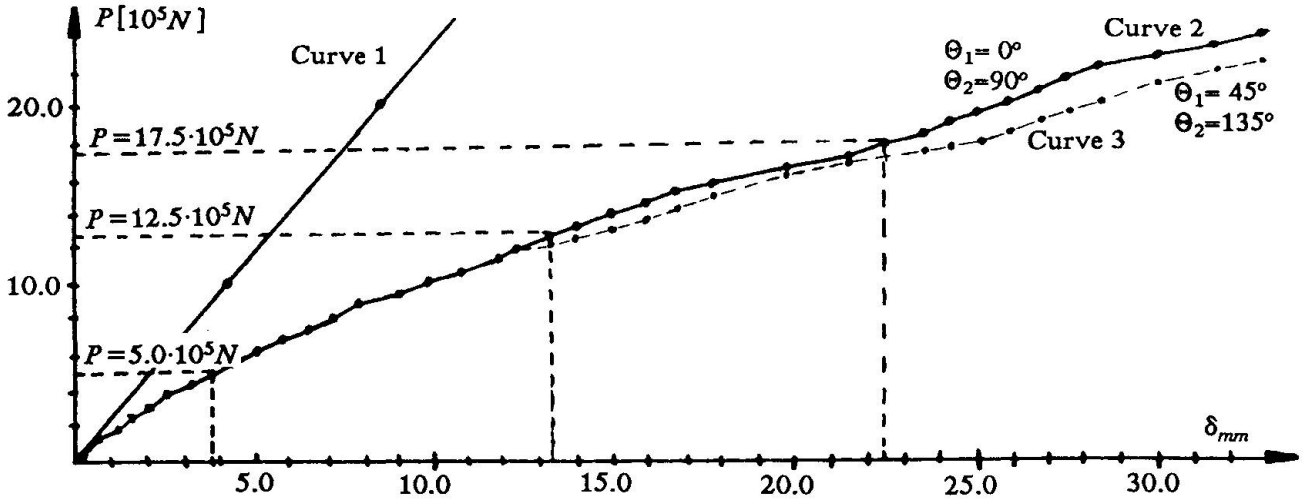

Fig. 7 The load-deflection curve of the midpoint of the roof.

Investigations of the deflection of the roof along the x-axis for $P=5.0\cdot10^5$N showed that the tangent of the deflection curve was horisontal at node 1, while for $P=17.5\cdot10^5$N the deflection curve along the x-axis has no definit tangent at node 1. For this last load the material at node 1 is crushed and cracked, and the stiffness around node 1 is only represented by the reinforcement.

7. CONCLUSIONS

Except for A.C.T.Chen and W.F.Chen's investigations not much experience has previously been gained with their flow theory for large structures. However, the present study shows that the theory is well suited for numerical implementation in shell elements. The greatest weakness of the theory is the assumptions concerning to the coupling between the equivalent stress-strain in tension and compression. Though the strain criteria, in which straining in the opposite direction as loaded is included, does the modell well suited for modelling concrete.

The numerical example demonstrate the applicability and accuracy of the present approaches. The important factors for failure are in many cases cracking and crushing of concrete, yielding of reinforcement, geometric nonlinearities and the size of the load. The accuracy of the results obtained indicates that these factors are well represented in the present approach.

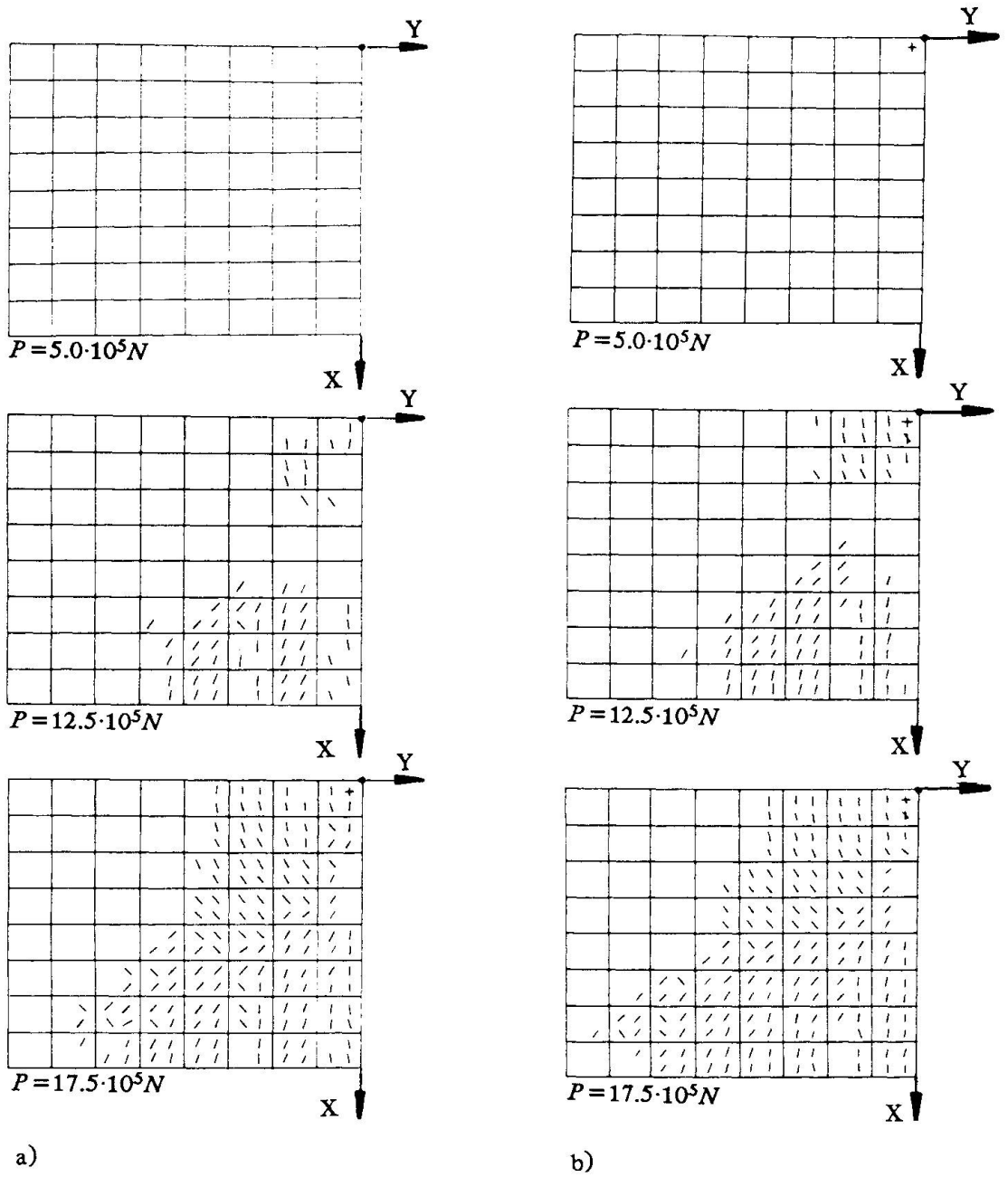

Fig. 8 The crack pattern for a) the $0^o/90^o$ analysis b) the $45^o/135^o$ analysis

7. REFERENCES

1. NYGÅRD, M.K.: "The Free Formulation for Nonlinear Finite Elements with Applications to Shells", Doctoral Thesis, Report no. 86-2, Div. of Struct. Mech., Norwegian Institute of Technology, Norway 1986
2. BERGAN, P.G. and NYGÅRD, M.K.: "Nonlinear Shell Analysis Using Free Formulation Finite Elements", Europe - US Symposium : Finite Element Methods for Nonlinear Problems, Vol. 2, Norway 1985

3. CHEN, A.C.T. and CHEN, W.F.: "Constitutive Relations For Concrete", Journal of the Engineering Mechanics Division, Vol. 101, 1975
4. CHEN, A.C.T. and CHEN, W.F.: "Constitutive Equations and Punch-Indentation of Concrete", Journal of the Engineering Mechanics Division, Vol. 101, 1975
5. CHEN, W.F.: "Plasticity in Reinforced Concrete", McGraw-Hill Book Company, U.S.A. 1982
6. BERGAN, P.G.: "FENRIS-System, Theory-Program Outline-Data Input", NTH-SINTEF-VERITEC, Norway 1986
7. STRØM, O.: "Nonlinear Analysis of Reinforced Concrete Structures Using Beam and Membrane Elements", Doctoral Thesis, Report no. 86-1, Div. of Struct. Mech., Norwegian Institute of Technology, Norway 1986
8. SCORDELIS, A.C. and LO, K.S.: "Computer Analysis of Cylindrical Shells", Journ. of American Concrete Institute, Vol. 61, pp 539-561, 1969
9. VASBOTTEN, A.: "Shell-Elements for Reinforced Concrete", Diploma work, Div. of Struct. Mech., Norwegian Institute of Technology, Norway 1986
10. The norwegian code NS3473 : "Prosjektering av betongkonstruksjoner. Beregning og dimensjonering", NBR, Norway 1982

Ultimate Shear Design from Non-Linear Finite Element Analysis

Calcul à l'effort tranchant ultime à partir de méthodes non-linéaires aux éléments finis

Schubfestigkeitsberechnung mittels nicht-linearer Finiter Elemente

Graham CROSS
Senior Lecturer
Univ. of the
Witwatersrand
Johannesburg,
South Africa

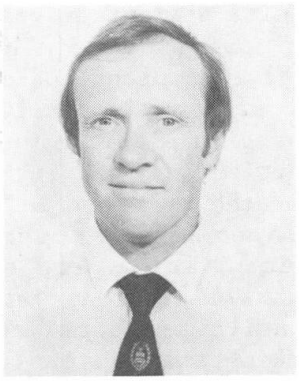

Graham Cross, born 1950, graduated at Witwatersrand University (BSc MSc PhD). He worked in industry a number of years in reinforced and prestressed construction and design. Is currently engaged in research, teaching and specialist consulting in concrete at the University of the Witwatersrand.

SUMMARY
This paper briefly describes certain aspects of ultimate shear evaluation with respect to current non-linear finite element codes. Consideration is given to apparent pitfalls in the direct application of the finite element results to a general design approach.

RÉSUMÉ
Cet article décrit succintement quelques aspects de calcul à l'effort tranchant ultime par rapport aux méthodes courantes, non-linéaires, d'éléments-finis. L'accent est mis sur certains cas où l'utilisation de méthodes aux éléments-finis, comme outil général de calcul, n'est pas satisfaisante.

ZUSAMMENFASSUNG
Der folgende Artikel beschreibt gewisse Aspekte der Schubfestigkeitsberechnung mittels der Methode der nicht-linearen Finiten Elemente. Es wird dabei auf offensichtliche Probleme hingewiesen, die bei der Anwendung der Resultate in allgemeinen Entwurfsberechnungen auftreten können.

1 INTRODUCTION

Finite element analysis in its early form was based primarily on a linear-elastic stiffness approach. As such it was recognised by reinforced concrete designers as defining certain service conditions fairly well but not defining ultimate limit states satisfactorily. However, it can be used successfully in ultimate design applications because of maintenance of overall equilibrium of the structure and suitable use of code resistance models.

A number of current non-linear finite element programs are making significant progress in addressing this short-coming, and are being used with increasing frequency in research and design in reinforced and prestressed concrete, even in evaluation of ultimate limit states. Typically, steel reinforcement is represented by truss elements having an elastic-plastic material model, or a rebar option, with similar properties, can be incorporated in the concrete elements. The concrete is represented by 2- or 3-dimensional solid elements having a material model with a non-linear compressive stress-strain relationship resulting ultimately in crushing, and cracking in tension at a suitably low level of tensile strain. Various techniques, such as tension stiffening, are used to aid the modelling of localised effects. The composite material is thus modelled by linking the two basic material models in the formation of the finite element mesh.

It would appear that the flexural ultimate limit state is well defined by this form of combination of the material models, but the shear ultimate limit state, most usually associated with abrupt strain-weakening, appears to be difficult to predict in terms of this approach. Indeed, detailing for shear from all types of finite element analysis results appears to present persistent difficulties for reinforced concrete designers.

A reason for the difficulties experienced with existing material models in non-linear finite element codes is that cracking *per se* does not necessarily indicate an ultimate limit state in reinforced concrete, even for structural elements unreinforced for shear. The extent of the cracking, however, might be a guide to evaluating a shear ultimate limit state. Some proposals as to possible avenues which could be explored in solving this problem are presented in this paper.

2 ASPECTS OF SHEAR BEHAVIOUR

Shear failure should not precede flexural failure in reinforced concrete in general, and particularly where ductility is necessary in terms of the design concept of the structure. It is thus important to be able to monitor the ultimate shear capacity of the structure (in terms of general non-linear finite element code results) relative to the ultimate flexural capacity, especially for structural members unreinforced for shear or lightly reinforced for shear. Structures of this type are relatively common in reinforced concrete construction, and are well within the scope of current codes of practice[1,2,3].

The likelihood of shear failure preceding flexural failure is dependent on geometric and material properties of the structural member. This concept is

elegantly portrayed by Kani's[4] valley of diagonal failure, for mild steel, 300mm deep beams unreinforced for shear, subjected to 2-point loading, as shown in Figure 1. These valleys can be considerably larger for other structural situations, such as punching shear in flat plates or use of high yield flexural reinforcement, and also continue to increase in size with the depth scale of the member, which is a major cause for concern in structures of large scale. The valleys are eliminated by the inclusion of shear reinforcement as necessary for the required probability of ductile flexural failure.

Special caution is thus required when evaluating non-linear finite element analysis results, as it is possible that shear failure is preceding flexural failure and only the flexural ultimate limit state is being identified automatically.

Some tests for the imminence of shear failure are proposed, and consideration is also given to comparisons between finite element results and observed test behaviour.

3 STRUCTURAL MEMBERS UNREINFORCED FOR SHEAR

Laboratory tests for shear failure have been conducted widely, usually with stiff testing machines, and there is some agreement that these indicate that if average shear stress is the measure of shear performance, then the major parametric trends can be represented by the curves shown in Figure 2, with an average coefficient of variation between 12 and 15%. These curves are in effect an alternate depiction of Kani's valleys. The form of these curves presents difficulties in representing ultimate shear failure in the material model for the finite element code. The problem is unlikely to be fully resolved in terms of the finite element combination of the two materials (concrete and steel) while current models for shear remain empirical and based on a "combination of materials" approach with a combined partial resistance factor. The difficulty in modelling is also caused by the difference in spread of cracks in the general finite element code results and the observed diagonal crack precipitating the shear failure. The shear deformation in the shear sensitive zone (shear arm or "D region" [5]) of the structural member is concentrated to a large extent in the diagonal shear crack the instant before shear failure. This is evident in the photograph of typical diagonal cracking in Figure 3 (in which strain softening has not yet commenced). These observations also apply to members of larger scale.

A number of non-linear finite element analyses[6,7] and a parallel laboratory and field test programme have been undertaken by the writer in a series of parametric, comparative studies on shear resistance. It appears from the finite element code results that the larger distortions caused by cracking are spread over all the cracked elements, straining in a manner consistent with the constitutive model laws and the definition of plane stress for the studies considered. In tests, distortions are concentrated in a discrete diagonal crack just prior to shear failure. Thus while accumulated distortions within the shear arm are reasonably well predicted by the finite element results, specific distortions within the mesh are not representative, as indicated by comparing the distortion at ultimate in Figure 3 with the finite element distortions for comparable loading in Figure 4.

However, without making major changes to the constitutive relationships for existing material models, there is an approach which is proposed as an possible measure in the development of a procedure for assessing the imminence

of diagonal shear failure, for general design from non-linear finite element analysis. If all the finite element distortion is assumed to be concentrated at the geometric centre of the shear arm (or shear sensitive zone), then peak shear resistance is indicated by the attainment of an absolute value for this distortion, measured normal to the observed or envisaged diagonal crack at failure, while bending reinforcement remains elastic, such as shown in Figures 4 and 5. The components of resistance to shear on this crack must be greater than or equal to the applied shear force differential across the crack. This approach results in curves which closely match those in Figure 2. This appears to be applicable for shear arm to effective depth ratios from 0,4 to 2, which is a reasonable range for most practical problems. Shear distortions can be assumed to predominate in this range while bending reinforcement remains elastic. If bending reinforcement becomes plastic during the incremental solution procedure, deformations abruptly become large, and the (desired) flexural ultimate limit state has been attained. The absolute deformation has to be calibrated by test, but preliminary evidence suggests that a cumulative deformation of the order of 1,3 to 1,5mm yields likely values for mean, ultimate shear resistance. It is believed that this value is linked to both a measure of the extent of propagation of the diagonal crack (or splitting energy), and the absolute magnitude of diagonal crack at which mean aggregate interlock is totally destroyed (for most ranges of practical concretes)[8]. Statistical variability and the use of an appropriate partial resistance factor obviously also require consideration before adopting the approach in a design application. This procedural check, although generally iterative, is fairly easily built into a post-processing subroutine (without resorting to writing a dedicated constitutive material model for shear in reinforced concrete).

4 STRUCTURAL MEMBERS REINFORCED FOR SHEAR

The parametric trends shown in Figure 2 for members unreinforced for shear maintain some influence for structural members lightly reinforced for shear, but rapidly disappear as the link reinforcement ratio increases. Once the "transition" phase is passed, the truss analogy becomes fully applicable for vertical link reinforcement[9] and finite element modelling of the truss concept is feasible. In this type of "dedicated" model of the concrete, the ultimate limit state is identified by either plastic yield of the links or flexural steel, or crushing of the concrete in the compression flange or web, and all these modes can be detected by the current "general" material models. However, this approach does not make use of direct modelling of the structure with what could be perceived as the more appropriate solid elements, and is applicable only to members having a reasonably high link reinforcement ratio. Tests indicate that an increase in "spread" or smearing of diagonal cracks across the shear arm is observed with increasing link reinforcement ratio, a trend which is also difficult to simulate with existing combinations of material models.

In the event that plane stress solid elements are used with truss element vertical links and flexural reinforcement, excessive shear distortions of the concrete elements occur between links. The links traversing the shear arm thus appear to be virtually ineffective in the finite element analysis, whereas tests on members lightly reinforced for shear indicate that the vertical links reach yield near the centre of the diagonal shear crack which precipitates ultimate shear failure, prior to peak shear resistance being attained. Horizontal links in members having steeply inclined diagonal shear cracks at ultimate, such as corbels, are better modelled by the general material models,

because the finite element distortions match the observed test behaviour more closely in this case. Axial tension or compression (prestress) affecting shear is also well modelled in this case.

The transition zone for structural members very lightly reinforced for shear with vertical links appears to be an area where modelling is particularly difficult. Either a simulated sloping link can be used or a revised constitutive material model for the composite solid finite element must be derived, as for the layered plate bending elements dedicated to flexural evaluation of reinforced concrete slabs. The advantage of automatic application of a general material model is, however, lost in these approaches.

5 APPLICATIONS

Notwithstanding the manipulation that is required from general finite element codes, the approaches outlined briefly in this paper have been used to aid in the derivation of a design model for shear in reinforced concrete, particularly in deep slab applications. The following are examples of structures for which the writer investigated various shear ultimate limit states:
- 20m high reinforced concrete retaining wall, with wall thicknesses up to 2000mm, for diamond mine washing plant.
- 2000mm deep silo floor slabs for 35m high rock silos for gold mining applications.
- Investigation of alternatives for transfer level of high-rise hotel structure.

6 CONCLUSION

Reinforced concrete designers should exercise some caution in using general non-linear finite element codes, as not all ultimate limit states might be identified automatically. This is attributable to the trend for state-of-the-art non-linear finite element analyses to be "dedicated" in many of their formulations, probably being more aligned to research than general design at present.

7 ACKNOWLEDGEMENTS

The support of the Portland Cement Institute, Johannesburg, for ongoing research in shear in reinforced concrete, is gratefully acknowledged.

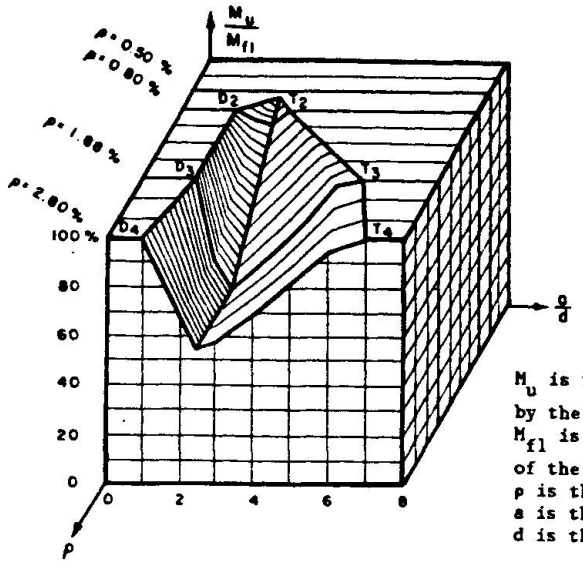

M_u is the ultimate moment carried by the beam at the instant of shear failure.
M_{fl} is the ultimate flexural capacity of the beam.
ρ is the flexural steel ratio of the beam.
a is the shear arm of the beam.
d is the effective depth of the beam.

Figure 1 Kani's valley of diagonal failure for mild steel, 300mm deep, RC beams subjected to two-point loading.

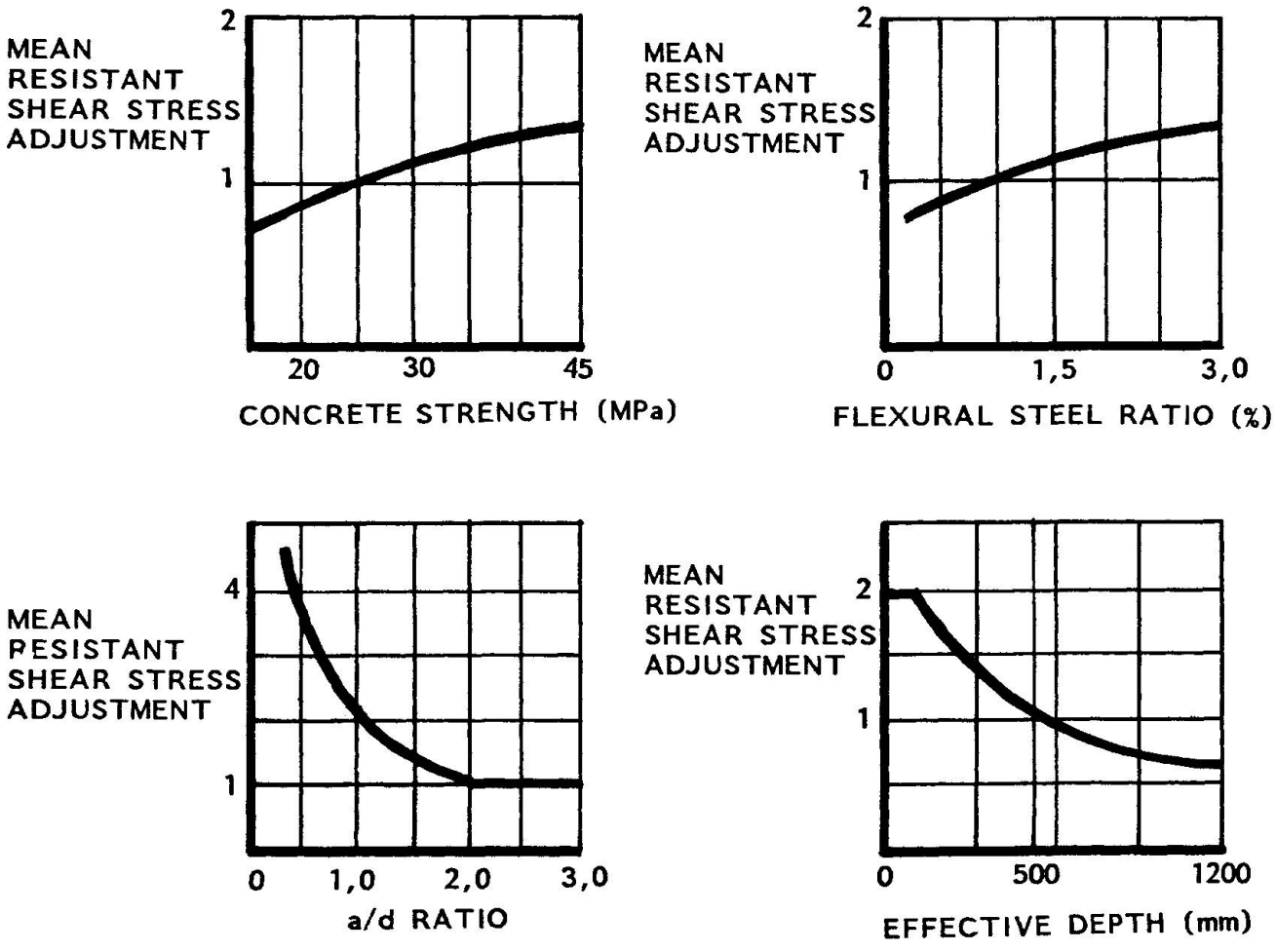

Figure 2 General parametric behaviour for mean resistant shear stress in members unreinforced for shear.

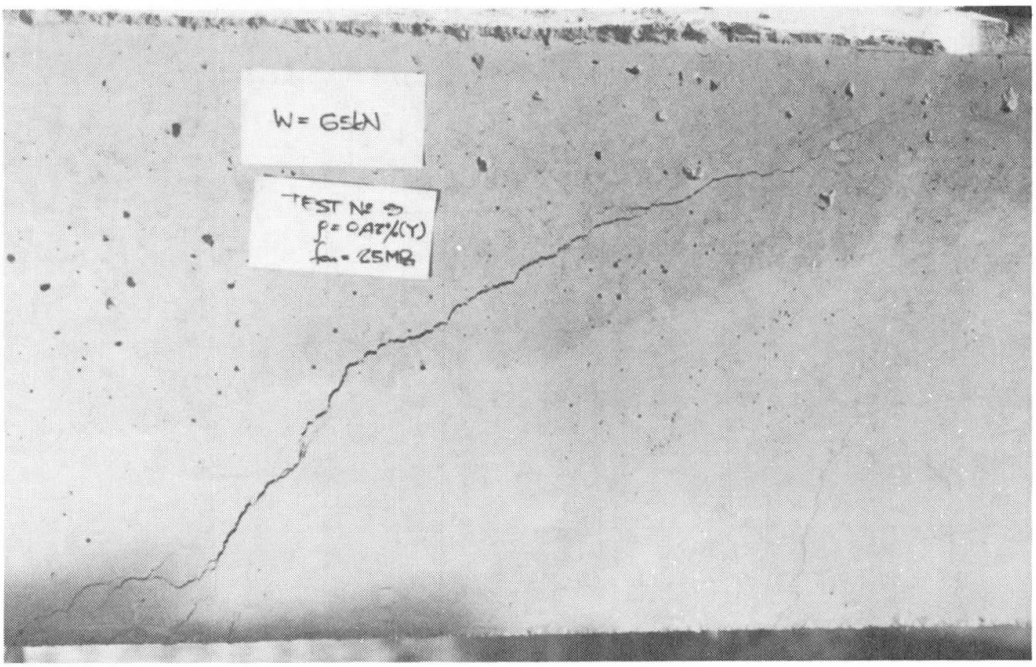

Figure 3 Photograph showing diagonal cracking for beam unreinforced for shear with a/d ratio greater than 2 just prior to ultimate shear collapse.

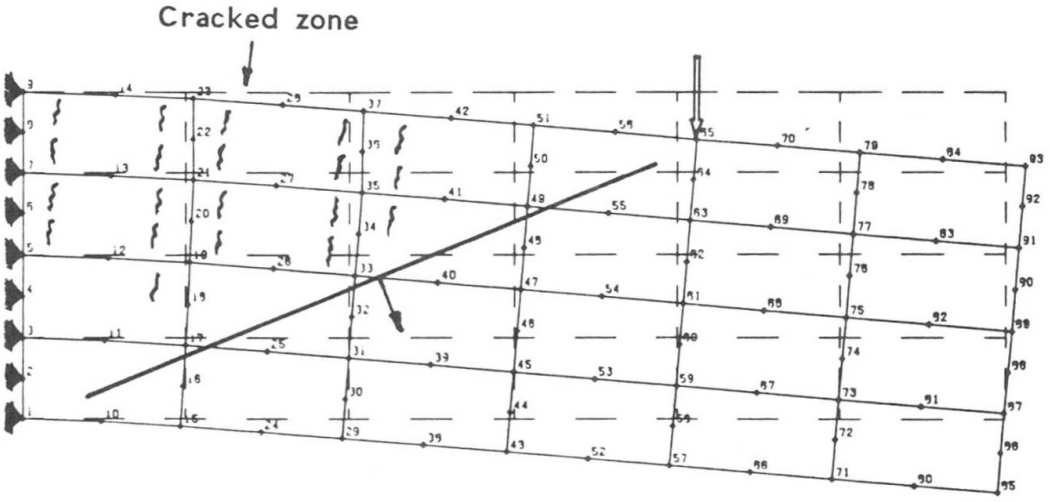

Figure 4 Example of plane stress finite element mesh and distortions for a/d ratio of 2.

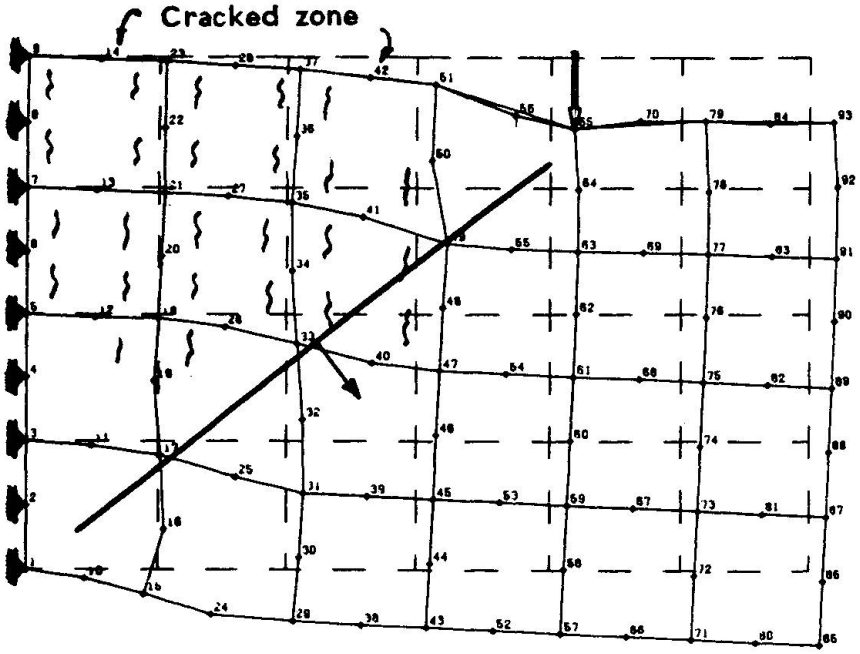

Figure 5 Example of plane stress finite element mesh and distortions for a/d ratio of 1.

REFERENCES

1. ACI Standard, Building Code Requirements for Reinforced Concrete (ACI 318-77), Standard of the American Concrete Institute, October 1977.

2. Code of Practice for the STRUCTURAL USE OF CONCRETE, BS8110, Part 1, British Standards Institution, London, 1985.

3. International System of Unified Standard Codes of Practice for Structures, CEB-FIP Model Code for Concrete Structures 1978, Comite Euro - International du Beton (CEB) 1978.

4. Kani on Shear in Reinforced Concrete, Edited by Kani, Huggins and Wittkopp, Department of Civil Engineering, University of Toronto, 1979.

5. SCHLAICH J. and WEISCHEDE D., Detailing of concrete structures, Bulletin d'Information No 150, Comite Euro-International du Beton, Paris, March 1982.

6. ADINA. A finite element program for automatic dynamic incremental nonlinear analysis, by Klaus-Jurgen Bathe. September 1975. Massachusetts Institute of Technology.

7. ABAQUS. Non-linear finite element programme developed by Hibbitt, Karlsson and Sorensen, Inc. Providence, R.I.

8. Walraven J. C. and Reinhardt H. W., Theory and experiments on the mechanical behaviour of cracks in plain and reinforced concrete subjected to shear loading, Heron Publication, Delft, Vol. 26, No. 1A, 1981.

9. Thürlimann B., Plastic analysis of reinforced concrete beams, Birkhauser Verlag Basel und Stuttgart, Bericht Nr. 86, November 1978.

Behaviour of Reinforced Concrete of Structural Walls: A New Interpretation

Comportement des parois de cisaillement en béton armé: une nouvelle interprétation

Bruchverhalten von Stahlbetonscheiben: eine neue Interpretation

Ioannis D. LEFAS
Research Assistant
Imperial College
London, U.K.

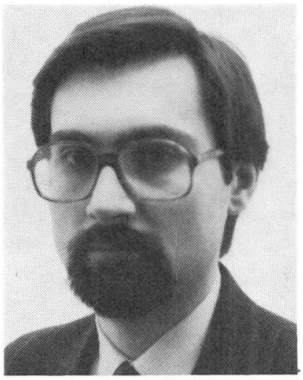

I. Lefas, born 1959, obtained his civil engineering degree at the National Technical University of Athens and his MSc degree at Imperial College, London. He is currently carrying out research at Imperial College investigating the behaviour of R.C. structural walls.

M. Kotsovos, born 1945, obtained his civil engineering degree at the Technical University of Athens and his D.Eng. at Imperial College. His interests cover a wide range of topics related to concrete at both material and structure levels.

Michael D. KOTSOVOS
Lecturer
Imperial College
London, U.K.

SUMMARY

The work forms part of a comprehensive research programme which has been aimed at developing a sound theoretical basis for the design of reinforced concrete structures in shear. Finite element analysis is used to verify that the 'shear' capacity of reinforced concrete structural walls is associated with the strength of the compressive zone. Experimental evidence is presented with indicates that current code provisions are not safe; it is shown that shear capacity can be improved by strengthening the compressive zone rather than the portion of the wall below the neutral axis as specified by these provisions.

RÉSUMÉ

L'étude constitue une partie d'un programme de recherche qui tente de formuler une base théorique solide pour le calcul au cisaillement des structures en béton armé. Des analyses par éléments finis sont utilisées pour vérifier que la résistance au cisaillement des murs en béton armé est associée à la résistance de la zone comprimée. Les résultats expérimentaux présentés montrent que les règlements actuels ne sont pas sûrs. La résistance au cisaillement peut être améliorée par un renforcement de la zone comprimée plutôt que de la zone située sous l'axe neutre comme cela est normalement recommandé.

ZUSAMMENFASSUNG

Die vorliegende Arbeit fasst Teile eines umfassenden Forschungsprogrammes zusammen, das auf die Entwicklung einer soliden theoretischen Basis für die Schubbemessung von Stahlbetonbauteilen hinzielt. Ein Finite Elemente Modell wird angewandt, um den direkten Zusammenhang von Schubspannungskapazität von Stahlbetonscheiden und Festigkeit der Druckzone zu verifizieren. Durch Experimente erhaltene Aussagen werden benutzt, um auf die Unsicherheit aktueller Normen hinzuweisen. Es wird gezeigt, dass die Schubspannungskapazität eher durch Verstärkung der Druckzone als des Bereiches unterhalb der neutralen Faser verbessert werden kann.

1. INTRODUCTION

Reinforced concrete structural walls are widely considered to provide an efficient economic bracing system, not only for high-rise, but also for low-rise buildings in areas of high or moderate seismicity. Such walls are designed as cantilever beams with concrete, above the neutral axis, and longitudinal reinforcement resisting the combined action of gravity loads and bending moment, whereas the region of the wall below the neutral axis provides shear resistance to the action of the horizontal forces, with horizontal reinforcement sustaining the portion of the shear force in excess of that which can be sustained by concrete alone. The horizontal reinforcement is assessed by using one of a number of methods invariably based on the "truss analogy" concept which stipulates that, once inclined cracking occurs, the beam behaves as a truss with concrete between the inclined cracks forming compression struts and the horizontal reinforcement forming the tension ties.

It has been recently found, however, that the above design method is not always safe since the wall shear capacity as predicted on the basis of the "truss analogy" concept often overestimates considerably that established by experiment [1,2]. The reason for this appears to be compatible with recent experimental evidence indicating that the "truss analogy" does not provide a realistic description of the mechanism of shear resistance [3]. In fact, it has been demonstrated that shear resistance is associated with the strength of concrete in the region of the path along which the compressive force is transmitted to the supports, with the portion of the beam below the neutral axis making an insignificant, if any, contribution [4].

It would appear from the above, shear resistance of the wall can only be improved by strengthening the compressive force path, rather than the portion of the wall below the neutral axis. The present work, therefore, has been aimed at verifying the validity of the above concept by means of finite element analysis (FEA). FEA is used to, first indicate that the method yields realistic predictions of R.C. wall behaviour and then, investigate whether strengthening the compression force path does indeed improve the structural behaviour of the walls.

2. NONLINEAR FINITE ELEMENT ANALYSIS

The nonlinear finite element system used in the programme is fully described elsewhere [5] and thus is only discussed briefly here. Essentially it is an iterative procedure which incorporates a linear solution technique. This is based on the Newton-Raphson method and the residual force concept. The procedure has been incorporated into a Choleski linear solution FE system and its application to the analysis of R.C. structures requires the use of "constitutive" laws describing the strength and deformation properties of concrete and steel as well as the interaction between concrete and steel.

The constitutive laws are fully described elsewhere [6,7] and their discussion is beyond the scope of this paper. It should be noted, however, that these laws for concrete include a description of the cracking process of concrete based on the smeared crack approach.

The finite elements used to model concrete and steel have been 8-node isoparametric and 3-node bar (possessing axial stiffness only) elements, respectively, with a steel element always coinciding with the boundaries of the adjacent concrete elements.

3. STRUCTURAL FORMS INVESTIGATED

The NLFEA system has ben validated by comparing analytical predictions with published information obtained experimentally for a wide range of R.C. structural walls [1,2,8,9]. The walls investigated represent the critical storey element of a structural wall system with rectangular, barbell or flanged cross-section. The height to width ratio of the elements analysed varied from 0.5 to 2.4, whereas their thickness to width ratio varied from 0.04 to 0.10. Vertical and horizontal reinforcement was distributed over the whole width of the wall. The ultimate strength of the reinforcement varied from 510 to 765 MPa, while the uniaxial compressive strength of concrete varied from 28 to 50 MPa.

The full design details of a typical wall are given in Figure 1, whereas Figure 2 shows the finite element mesh adopted for the analysis. The latter figure also indicates the boundary conditions and loading history of the wall.

Of the walls investigated, those which failed below the predicted design level were re-analysed after modification of their reinforcement details. The modification involved strengthening the compressive zone, by increasing the amount of the compression reinforcement, as well as weakening the region below the neutral axis, by reducing the horizontal reinforcement by more than half the original amount. These modifications have been made in order to demonstrate, not only that the compressive zone makes a significant contribution to shear capacity, but also that, in contrast to widely held views, the wall does not have to behave as a truss in order to sustain shear forces after inclined cracking occurs.

An indication of the modification to the reinforcement details of the typical wall shown in Figure 1, is given in Figure 3. It is interesting to note that the compressive zone at the critical section has a significantly smaller size than that of the overall wall cross-section.

4. RESULTS

The main results of the investigation are shown in Figures 4 to 8. Figure 4 shows the correlation between predicted and experimental values of the load-carrying capacity for a wide range of R.C. structural walls subjected to various combinations of vertical and horizontal loading, whereas Figure 5 illustrates the predicted and experimental load-displacement curves for the typical wall of Figure 1.

Figure 6 shows a typical mode of failure established by experiment [2] together with that predicted by analysis in the present work, whereas Figure 7 shows the predicted crack pattern and deformed shape of the wall at characteristic load stages corresponding to (i) crack initiation, (ii) significant inclined crack formation and (iii) maximum load-carrying capacity.

Finally, Figure 8 shows the relationship between shear capacity and amount of horizontal reinforcement predicted by current Code provisions for walls investigated into two different experimental programmes. The Figure also shows for comparison the values predicted by the analysis and those from experiments.

5. DISCUSSION OF THE RESULTS

Figures 4 to 7 demonstrate a satisfactory correlation between prediction and experiment for all aspects of structural behaviour investigated in the present work i.e., load-carrying capacity, deformational characteristics and mode of failure. Similar correlations have also been obtained for a wide range of R.C. structural forms [10,11]. The apparent successful application of the FEA system to all cases investigated to date, is attributed to the constitutive model of concrete behaviour which the system incorporates.

From Figures 6 and 7, it may be noted that the predicted mode of failure is characterised by longitudinal cracking within the compressive zone near the base of the wall where the flexural moment attains its maximum value. The modes of failure of R.C. beams in both flexure and combined flexure and shear have also been found to be characterised by similar cracking [12]. Such behaviour is considered to indicate a common underlying cause of failure, fully described by the concept of the compressive force path [13]. It is interesting to note in Figure 6 that the mode of failure established experimentally is also characterised by longitudinal cracking of the compressive zone near the base of the wall.

Figure 8 indicates, that the Code provisions [14] predict a linear increase in shear capacity with increasing percentage of horizontal reinforcement, from a lower level representing the contribution of concrete to shear resistance, to an upper level corresponding to "crushing" of the concrete struts of the "truss" model. Beyond this level, it predicts that shear capacity remains constant. From the Figure, it is apparent that while the Code predictions are conservative for the lower range of values of the percentage of horizontal reinforcement, they overestimate considerably the wall capacity, for the upper range of these values. On the basis of the "truss analogy", predictions can only improve by adjusting current design methods so as to provide a lower bound failure envelope to published experimental data such as those included in Figure 8.

In contrast to the "truss" analogy, the concept of the compressive force path suggests that shear capacity can increase by strengthening the compressive zone of the concrete in the region of the critical section. Vertical and horizontal reinforcement is considered to have no purpose other than safeguarding against out-of-plane instability due to the heterogeneity of concrete.

The validity of the above view is supported by the analytical evidence obtained in the present work. Figure 8 shows that the inclusion, near the extreme compression and tension fibres, of additional reinforcement in both the compression and tension zones of the wall, results in a significant increase of load-carrying capacity; this happens in spite of the considerable reduction of horizontal reinforcement to near nominal levels. An experimental verification of the above predictions forms part of an on-going experimental programme, and the results obtained to date have been found to correlate closely with the predictions [15].

6. CONCLUSIONS

(1) The results obtained in the present work indicate that "truss analogy" does not form a suitable basis for the design of R.C. structural walls.

(2) It is shown that the shear capacity of the walls is associated with the strength of concrete in the compressive zone in the region where the maximum bending moment develops and not, as widely believed, in the region of the wall below the neutral axis.

(3) It has been demonstrated that strengthening of the compressive zone can lead to a significant increase in load-carrying capacity, in spite of the considerable reduction of horizontal reinforcement.

(4) The above evidence is compatible with the concept of the compressive force path and it appears that this concept can form the basis for the development of a method suitable for the design of walls.

REFERENCES

1. CARDENAS, A.E., RUSSELL, H.G. and CORLEY, W.G.; "Strength of Low Rise Structural Walls", Reinforced Concrete Structures Subjected to Wind and Earthquake Forces, SP-63, American Concrete Institute, Detroit, 1980, pp. 221-241.

2. MAIER, J. and THURLIMANN, B.; "Bruchversuche an Stahlbetonscheiben", Institut fur Baustatic und Konstuction, Eifgenossishe Technische Hochschule Zurich, Januar, 1985, 130 pp.

3. KOTSOVOS, M.D.; "Shear Failure of R.C. Beams: A Reappraisal of Current Concepts", to appear in CEB Bulletin, 1987.

4. KOTSOVOS, M.D.; "Mechanics of 'Shear' Failure", Magazine of Concrete Research, Vol. 35, No. 123, June 1983, pp. 99-106.

5. KOTSOVOS, M.D. and PAVLOVIĆ, M.N.; "Non-linear Finite Element Modelling of Concrete Structures: Basic Analysis, Phenomenological Insight and Design Implications", Engineering Computations, Vol. 3, No. 3, September 1986, pp. 243-250.

6. KOTSOVOS, M.D.; "Concrete - A Brittle Fracturing Material", Materials and Structures, RILEM, Vol. 17, No. 98, March-April 1984, pp. 105-115.

7. BÉDARD, C. and KOTSOVOS, M.D.; "Fracture Processes of Concrete for NLFEA Methods", Journal of Structural Engineering, ASCE, Vol. 112, No. 3, March 1986, pp. 573-587.

8. OESTERLE, R.G.; FIORATO, A.E.; ARISTIZABAL-OCHOA, J.D. and CORLEY, W.G.; "Hysteretic Response of Reinforced Concrete Structural Walls", Reinforced Concrete Structures Subjected to Wind and Earthquake Forces, SP-63, American Concrete Institute, Detroit, 1980, pp. 243-273.

9. BARDA, F.; HANSON, J.M. and CORLEY, W.G.; "Shear Strength of Low-Rise Walls with Boundary Elements", Reinforced Concrete Structures in Seismic Zones, SP-53, American Concrete Institute, Detroit 1977, pp. 149-202.

10. KOTSOVOS, M.D.; "Behaviour of Reinforced Concrete Beams with a Shear Span to Depth Ratio Between 1.0 and 2.5", ACI Journal, Proceedings, Vol. 81, No. 3, May-June 1984, pp. 279-286.

11. KOTSOVOS, M.D.; "Behaviour of Reinforced Concrete Beams with a Shear Span to Depth Ratios Greater Than 2.5", ACI Journal, Proceedings, Vol. 83, No. 6, November-December 1986, pp. 1026-1034.

12. KOTSOVOS, M.D.; "Consideration of Triaxial Stress Conditions in Design: A Necessity", to appear in ACI Journal, 1987.

13. KOTSOVOS, M.D.; "Shear Considerations", to appear in Design of Cast-in-Place Concrete (Topical Volume), Council of Tall Buildings and Urban Habitat, 1987.

14. ACI Committee 318, "Building Code Requirements for Reinforced Concrete (ACI 318-83)", American Concrete Institute, Detroit, 1983, 111 pp.

15. LEFAS, I.D.; "Behaviour of Reinforced Concrete Structural Walls", PhD Thesis, University of London, to be submitted in 1987.

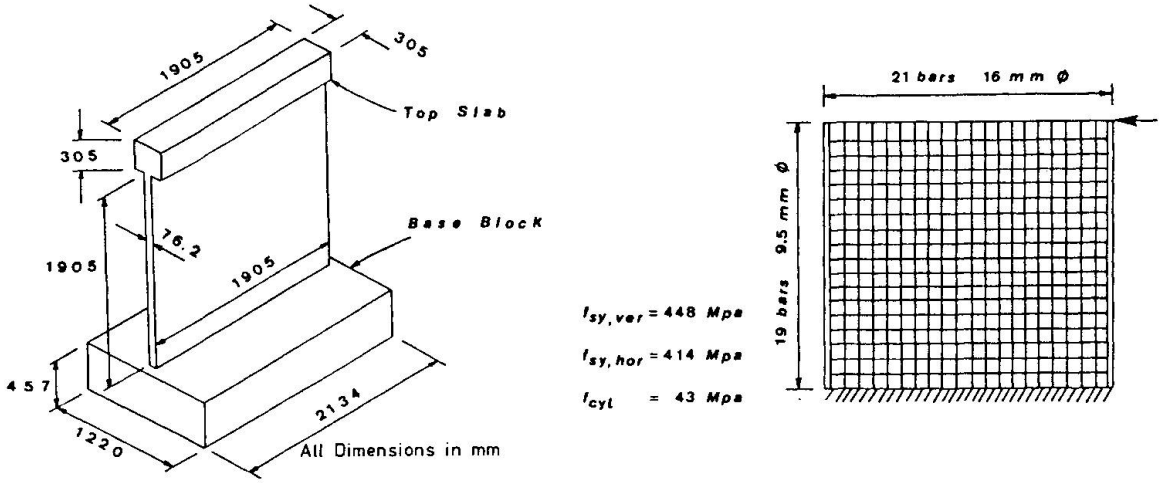

Fig. 1 Design details of a wall typical of those investigated (ref. [1])

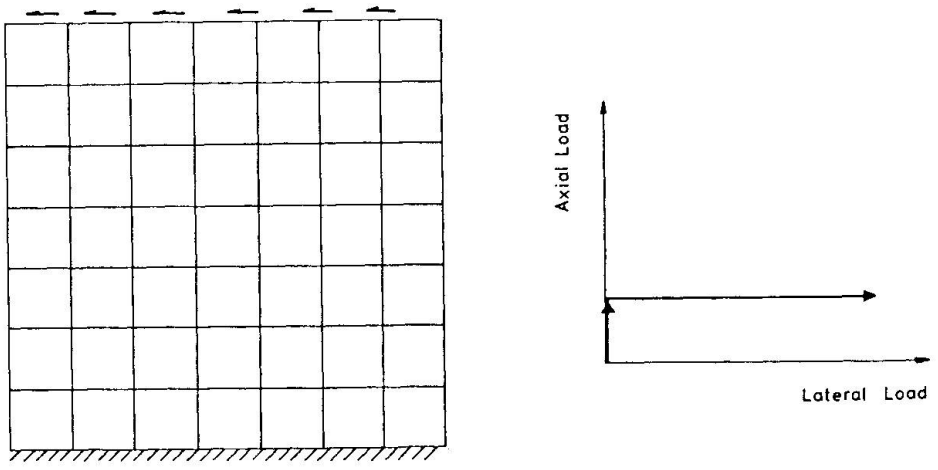

Fig. 2 Finite element mesh adopted for the wall shown in Fig. 1

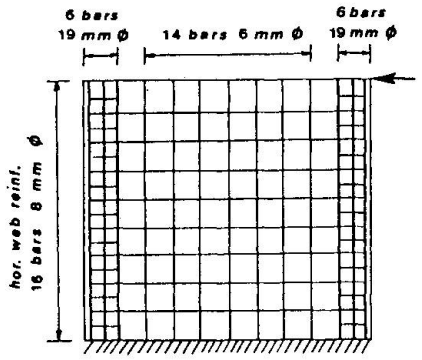

Fig. 3 Reinforcement details of wall with strengthened compressive zone

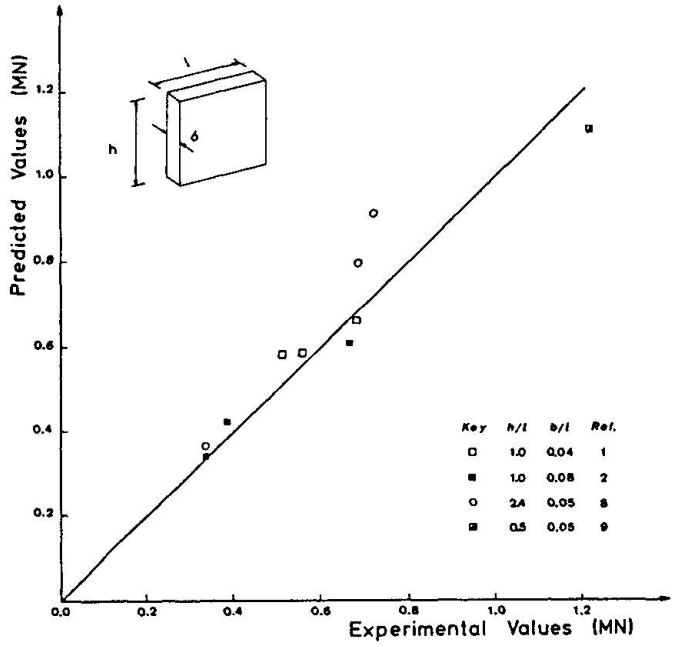

Fig. 4 Correlation of predicted load-carrying capacity of walls with experimental values

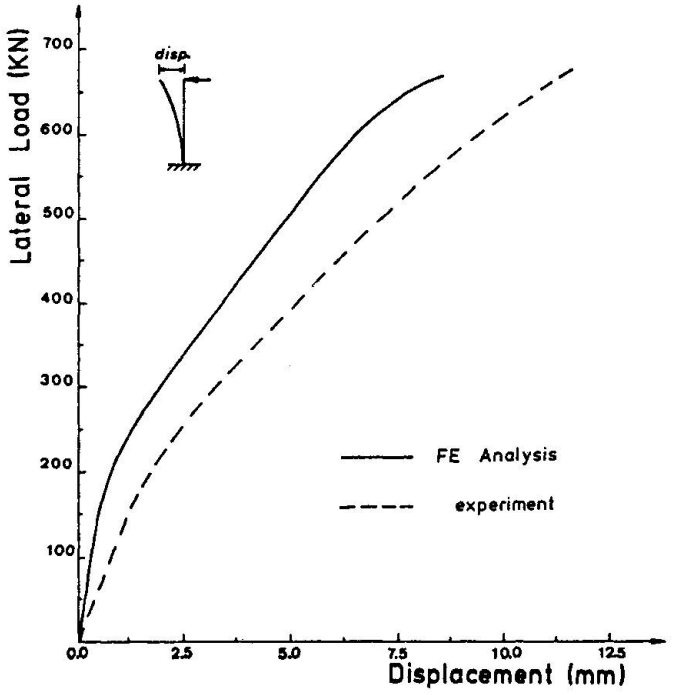

Fig. 5 Typical load-displacement curve of wall

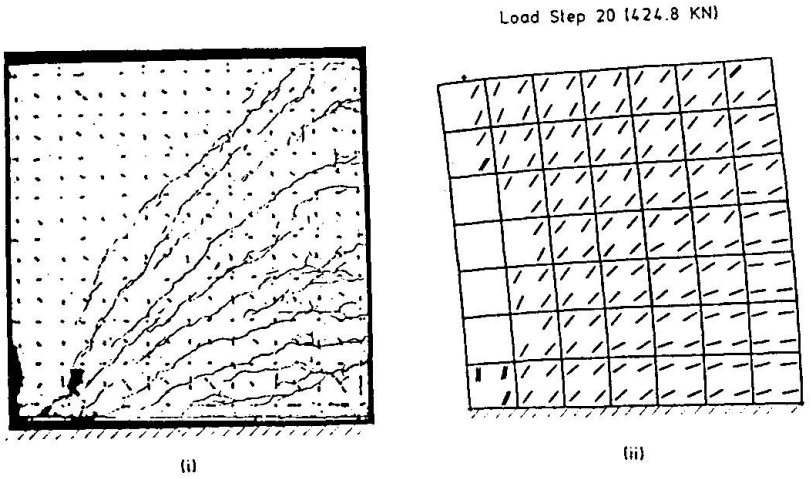

Fig. 6 Typical mode of failure (i) established by experiment (ii) predicted by analysis

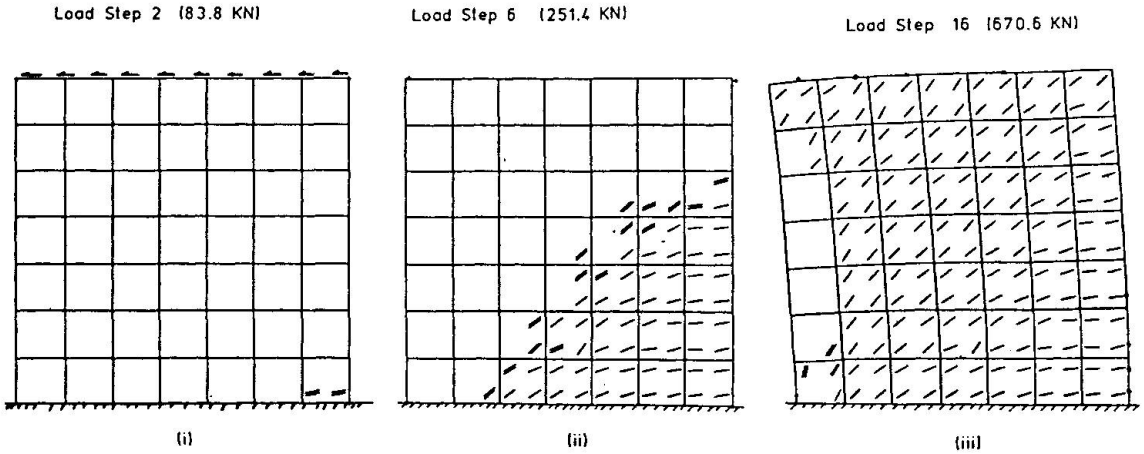

Fig. 7 Crack pattern and deformed shape of a typical wall at load stages corresponding to (i) crack initiation (ii) significant inclined crack formation and (iii) maximum lateral load capacity

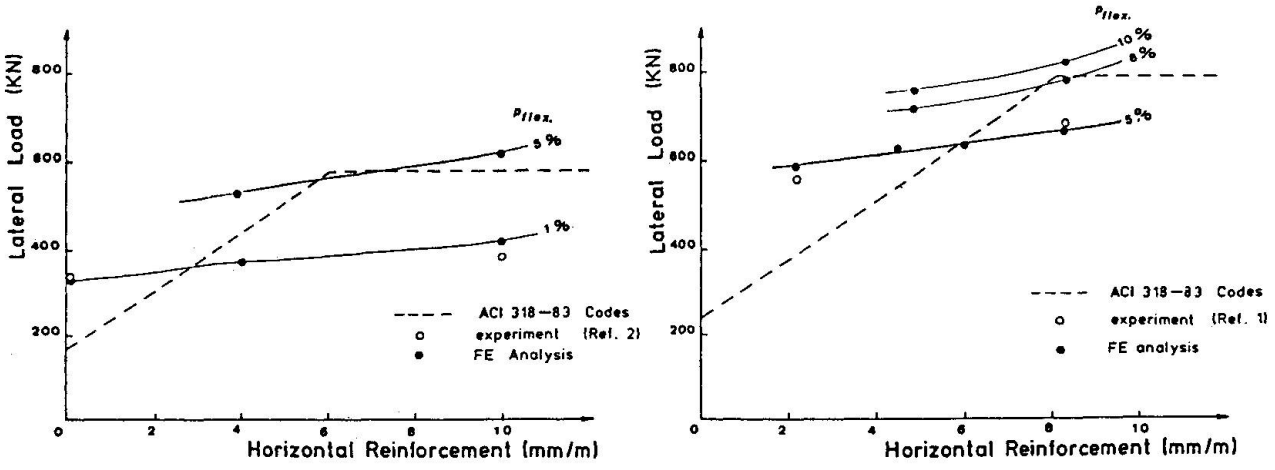

Fig. 8 Relation between shear capacity and amount of horizontal reinforcement predicted for two different experimental programmes

Design Techniques for Continuous Deep Beams Using Finite Element Modelling

Projet de poutres continues de grande hauteur au moyen d'un modèle des éléments finis

Entwurfstechniken für hohe Durchlaufträger mit Hilfe von Finite Element Modellen

D.V. PHILLIPS
Lecturer
University of Glasgow
Glasgow, U.K.

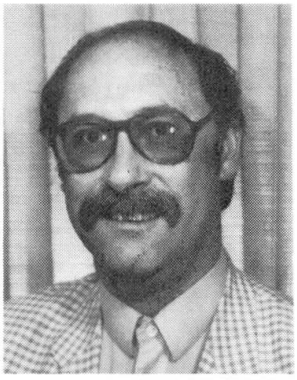

Dr. D.V. Phillips obtained his Ph.D. from the University of Swansea, Wales in 1972 and then worked at the University of Nairobi, Kenya until taking up his present appointment in 1976. His major research interests are in the analysis and design of structural concrete, and in computing methods, particularly finite element techniques.

D.R. GREEN
Head of Department
University of Glasgow
Glasgow, U.K.

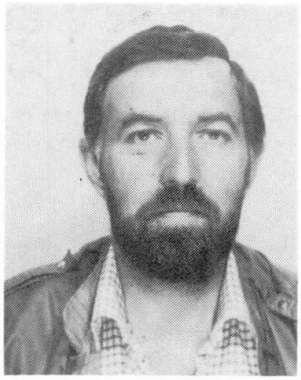

Dr. D.R. Green has been active in research since 1966, working on shearwalls, deep beams and slab structures. He is the author of many papers in these fields and is the co-author of a finite element analysis and design package which has been commercially successful throughout Europe.

G.B. KHASKHELI
Research Student
University of Glasgow
Glasgow, U.K.

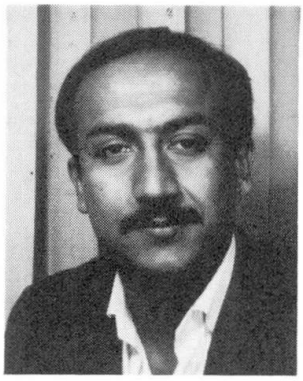

Ghous Khaskeli graduated from M.U.E.T., Jamshoro, Pakistan in 1983 and received an M.Eng. Degree from Sheffield University, U.K. in 1984. Since 1985 he has been a research student in the Department of Civil Engineering, Glasgow University where he has been working on the design and analysis of reinforced concrete continuous deep beams for his Ph.D. degree.

SUMMARY

A lower bound direct design method for the design of reinforcement in continuous deep beams is described. A linear-elastic finite element plane stress model is used to determine a stress field in equilibrium with the applied design load. This stress field is employed to calculate orthogonal reinforcement ratios throughout the beam. The resulting design is checked at serviceability and ultimate limit states using non-linear finite element techniques for structural concrete and by large scale experimental tests.

RÉSUMÉ

Une méthode directe de projet pour le calcul de l'armature dans des poutres continues de grande hauteur est décrite. Un modèle linéaire et élastique à l'aide des éléments finis est utilisé pour déterminer un champ de contraintes en équilibre avec la charge de projet appliqué. Ce champ de contraintes est employé pour calculer les ratios d'armature orthogonales tout au long de la poutre. Le projet résultant est contrôlé pour l'aptitude au service et à l'état ultime en utilisant des techniques non-linéaires d'éléments finis pour le béton armé, et à l'aide d'essais expérimentaux à grande échelle.

ZUSAMMENFASSUNG

Eine Untergrenzenberechnungsmethode für hohe Stahlbetondurchlaufträger wird beschrieben. Lineare FE-Berechnungen bestimmen den Gleichgewichtsspannungszustand. Hieraus werden orthogonale Bewehrungen berechnet. Der Entwurf wird für den Gebrauchs- und Versagenszustand mit Hilfe nichtlinearer FE-Berechnungen überprüft.

1. INTRODUCTION

In recent years various proposals have been made for the design of reinforcement for in-plane forces based on the lower bound limit state approach where a stress field in equilibrium with the ultimate load is used in conjunction with an appropriate yield criterion. Such a stress field can be obtained by any suitable procedure such as a linear elastic finite element analysis. Reinforcement is then provided so that the combined resistance of the steel and concrete at every point is equal to or greater than the applied stress.

In theory, by satisfying equilibrium and yield exactly at every point simultaneously, the entire structure will become a mechanism at ultimate load. Practical considerations, such as reinforcement being provided as discrete bars, make it impossible to achieve this idealised behaviour. Also the theory gives no guarantee that serviceability behaviour will be satisfactory. However, if verified as an acceptable design process, the following advantages ensue:
- analysis and design becomes one continuous process which is suited to automatic computation,
- steel is used economically as the design equations are based on minimising steel requirements, although this will be affected by the convenience of fabrication,
- excessive ductility demands are minimised by aiming for most parts of the structure to yield simultaneously at a particular ultimate load. The difference between the load at which yielding starts and the ultimate load is kept at a reasonable level which should prevent excessive cracking at working load.

Verification for practical reinforcement details can be provided by non-linear finite element modelling of the resulting designs, backed up by large experimental tests. Although the direct design philosophy is applicable to a wide range of continuum structures, this paper is concerned with its application to the design of continuous deep beams.

2. DIRECT DESIGN EQUATIONS FOR IN-PLANE FORCES

The design equations adopted here for in-plane actions were originally presented by Neilsen [1] using the yield criterion for orthogonal tension reinforcement,

$$(N_x^* - N_x)(N_y^* - N_y) - N_{xy}^2 = 0 \qquad (1)$$

where N_x^* and N_y^* are yield ultimate strengths, and N_x, N_y and N_{xy} are the in-plane stress resultants in the concrete at any point. Clark [2] later developed this approach to cover compression steel and skew reinforcement. The design equations are derived assuming:
1) the reinforcement is placed symmetrically about the middle surface of the section and is in two non-orthogonal directions (Fig.1) and carries only uniaxial stress in the original bar directions so that kinking and dowel actions are neglected,
2) bar spacing is small in comparison with the overall structure dimensions so that reinforcement can be considered in terms of area per unit length rather than as individual bars,
3) concrete has zero tensile strength, exhibits the square yield criterion shown in Fig.2(a) and is perfectly plastic, whilst reinforcement exhibits perfect elastic-plastic behaviour with a yield stress of f_s in tension and f_s' in compression, as shown in Fig.2(b),
4) that proper detailing and choice of section prevents instability and bond failures,
5) in-plane stresses are resisted by a combination of concrete and steel stresses (Fig.3).

These assumptions lead to design equations for nine possible combinations of reinforcement which are shown schematically in Fig.4. In each direction tension, compression or no reinforcement may be required. When tension reinforcement is provided $\sigma_1 = 0$ because the concrete is cracked and when compression reinforcement is provided $\sigma_2 = f_c$ in order to make optimum use of concrete. Direct solutions are possible in all cases except when tension-tension or compression-compression reinforcement is provided. In these cases an additional equation is available by minimising the total reinforcement, i.e.

$$\frac{\partial(\rho_x + \rho_y)}{\partial(\tan\theta)} = 0 \qquad (2)$$

It is also necessary that $\tau_{xy} < 0.5 f_c$ in order to prevent shear failure.

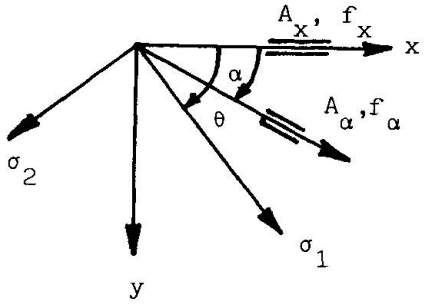

Fig.1 Principal concrete stress and directions of reinforcement

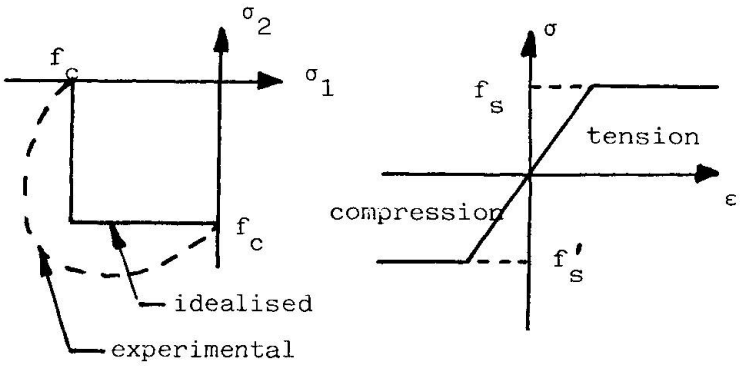

(a) concrete (b) steel

Fig.2 Design yield criteria for concrete and steel

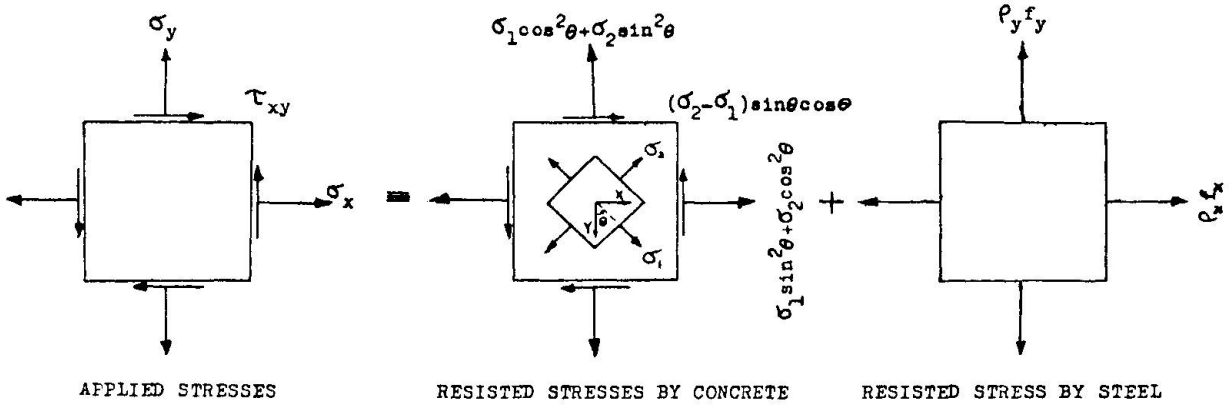

Fig.3 Combination of resistant stresses

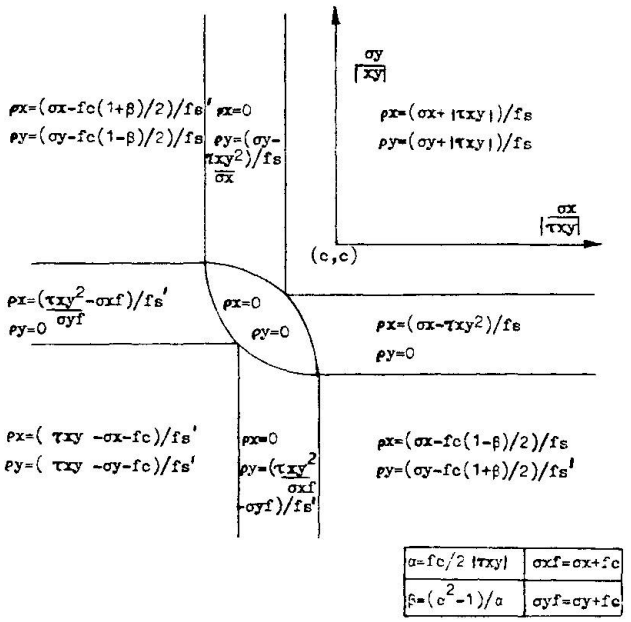

Fig.4 Design equations for reinforcement

3. DIRECT DESIGN OF CONTINUOUS DEEP BEAMS

Rogowsky and MacGregor [3] and Ricketts and MacGregor [4] have carried out a number of tests on continuous deep beams which has provided useful information on their behaviour. They used plastic truss analogies to predict the ultimate loads of their beams and used a concrete efficiency factor to achieve satisfactory agreement between the analytical and experimental behaviour. Little other experimental data has been reported and so design rules are mainly based on a knowledge of single span deep beam behaviour.

The CIRIA Guide [5], in common with many Codes of Practice, base deep beam reinforcement design on indirect methods which use moment and shear envelopes and internal lever arms which are assumed functions of beam dimensions. Appropriate distribution rules are then used for positioning the reinforcement in sagging and hogging zones, and for resisting shear. This approach, although simple to use, does not make the most effective use of the reinforcement due to the varying nature of the stress distribution in the beams. The direct design philosophy attempts to overcome this by using an actual equilibrium stress field.

The following procedure is adopted here.
1. An internal stress field in equilibrium with the design ultimate load is obtained from a linear– elastic finite element analysis of the unreinforced beam using elastic material data for concrete.
2. Reinforcement ratios are calculated using the design equations (Fig.4) with intended values of f_s, f_s' and f_c.
3. Discrete reinforcing bars are selected by taking arbitrary levels across and along the beam and calculating the average reinforcement ratios at each level. Reinforcing bars are then selected and distributed using specified bar diameters and limits on cover and spacing.

This procedure was used to design the two–span continuous beam shown in Fig.6. The beam was designed to carry a total ultimate load of 850kN as two concentrated loads acting at the centres of each span. The overall depth and length of the beam was 900 mm and 2000 mm respectively with a thickness of 100 mm. The span between the centres of support bearings was 960 mm. Hot rolled deformed high tensile reinforcing bars with a 0.2% proof stress of 501 N/mm^2 and concrete with a cube strength of 45 N/mm^2 were specified. Isometric views of the envelopes of the resulting reinforcement ratios in the horizontal and vertical directions are shown in Fig.5. The final designed beam with discrete reinforcing bars is shown in Fig.6.

4. LARGE SCALE TEST OF CONTINUOUS DEEP BEAM

The full size designed beam was experimentally tested to failure in increments of 50 kN under displacement control. Applied loads and support reactions, deflections on the underside of the beam and steel strains at each reinforcement level were automatically measured using data logging facilities. Concrete strains, crack propagation and crack widths were also monitored. Material properties were measured as follows: concrete – cube strength = 63 N/mm^2, cylinder splitting strength = 3.22 N/mm^2, modulus of elasticity = 19.5 kN/mm^2: steel – 0.2% proof stress for 6 mm and 8 mm bar = 513 N/mm^2 and 501 N/mm^2 respectively, modulus of elasticity for 6 mm and 8 mm bar = 200 kN/mm^2 and 195 kN/mm^2.

The beam failed in shear at a load of 1333 kN, over 50% higher than the design load. The serviceability load corresponding to a 0.3 mm crack width was 900 kN. Measurements indicated that most of the steel had yielded prior to ultimate conditions. Load–displacement and steel strain curves are shown in Figs.11 and 12 whilst Fig.13(b) illustrates the cracks in the beam at failure. The high experimental load can be attributed to several causes:
– the actual concrete strength was 63 N/mm^2 compared to the design value of 45 N/mm^2,
– the steel exhibited strain hardening which was not accounted for in the design equations,
– significant displacement along shear cracks was observed at higher loads causing dowel action and interface shear transfer effects which were not accounted for in the design equations,
– the reinforcement provided, particularly the shear reinforcement, was more than the design values because of practical requirements such as minimum bar size.

Notwithstanding, the design procedure produced an acceptable design with an adequate reserve of strength and satisfactory behaviour at serviceability load.

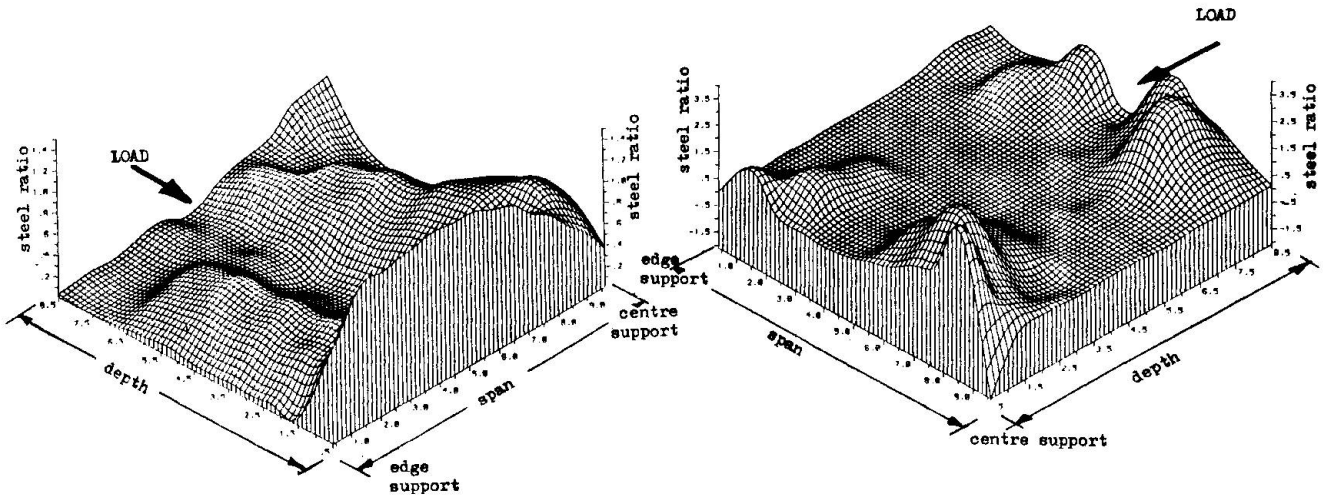

(a) horizontal steel (b) vertical steel

Fig.5 Isometric views of envelopes of reinforcement ratios (1/2 beam)

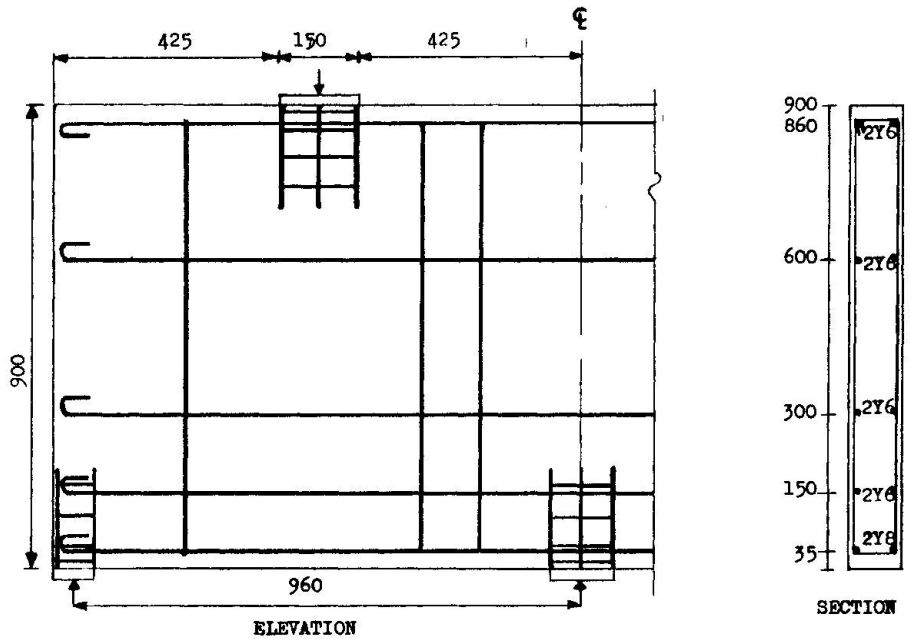

Fig.6 Dimensions and reinforcing details of designed beam (one span)

5. NON– LINEAR FINITE ELEMENT ANALYSIS

The beam was analysed using a plane stress non– linear finite element model [6] which is one of several developed at Glasgow University for analysing the non– linear behaviour of structural concrete. A brief description of the analysis follows.

5.1 Discretisation and non– linear solution procedure

Concrete was modelled by 8– noded isoparametric elements using standard Serendipity shape functions and a 3 x 3 Gaussian integration rule. Reinforcement was modelled by bars embedded anywhere within the element along lines of constant local curvilinear co– ordinates [7]. This

representation assumes the bars carry uniaxial stress only and that perfect bond exists between the steel and concrete.

A modified Newton–Raphson incremental–iterative solution scheme was used where the stiffnesses were upgraded at the first iteration within a load increment. Load control was applied and no line searches were employed. Convergence was checked by a residual force norm and was assumed to have occured when the convergence factor was less than 2%.

5.2 Material models

Cracking was simulated by a smeared orthotropic fixed crack approach. A crack was assumed to occur in a plane perpendicular to the maximum principal stress when this exceeded the tensile strength criterion for concrete. After crack formation, the material matrix was modified to reflect the change from an isotropic to an orthotropic material and to account for the partial loss of stiffness normal and parallel to the crack planes. A second crack could occur at right angles to the first crack if the tensile strength was exceeded in this direction also. A crack was assumed to close if the strain across the crack became compressive. Post cracking behaviour was represented by laws defining a variable shear retention factor and a variable tension stiffening and strain softening factor, as shown in Fig.7. These laws were used to modify the modulii in the material matrix for subsequent stiffness and stress calculations.

Concrete behaviour under biaxial stress states was modelled by a short–term hyperelastic constitutive law which uses tangential bulk and shear modulii which vary according to the stress invariants I_1 and J_2. The relationships are shown in Fig.8. A linear form of the octahedral stress failure criterion was used to predict the biaxial ultimate strength of concrete (Fig.9).

For reinforcing steel a bi–linear uniaxial stress/strain relationship allowing for isotropic strain hardening and elastic unloading was used as shown in Fig.10.

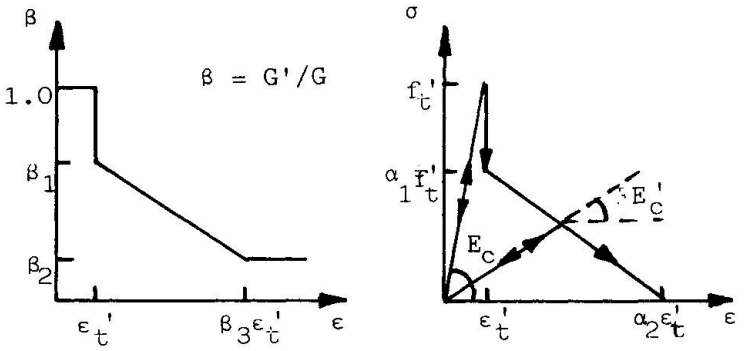

(a) Shear retention (b) tension stiffening

Fig.7 Post–cracking laws

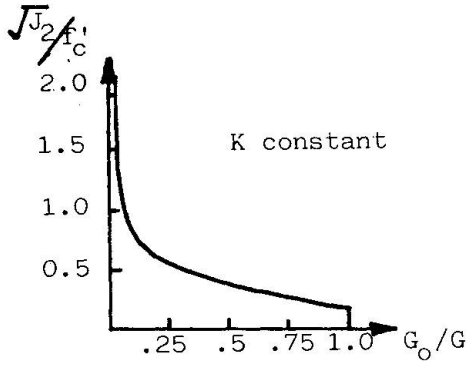

Fig.8 Hyperelastic invariant law for concrete in biaxial compression

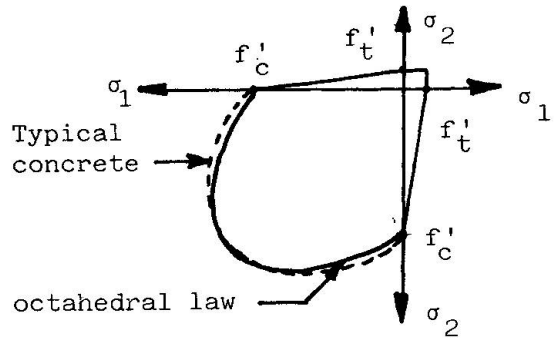

Fig.9 Failure criterion for concrete

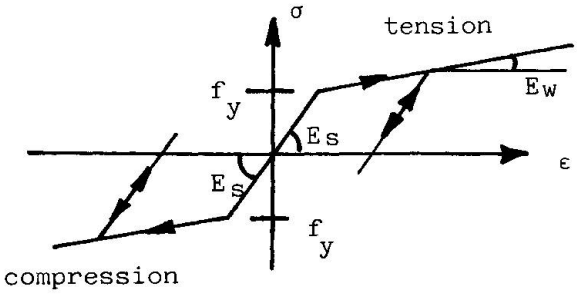

Fig.10 Stress–strain law for reinforcement

5.3 Results for the continuous deep beam

The load– deflection and load– steel strain curves are compared with the experimental results in Figs.11 and 12 where satisfactory agreement is evident. Fig.13 shows crack propagation at various load levels and compares them with the experimental crack pattern at failure. Flexural cracks first initiate at the bottom of the beam at about 300 kN, followed later by flexural cracking at the top of the beam over the central support at a load of 750 kN. At about 825 kN, shear cracks start to develop which eventually spread from the load point to the central support. Failure was by shear and crushing of concrete in the central shear span and close to the applied load. This description compares well with the experimental observations. The ultimate load predicted by the finite element analysis was 1275 kN which was 4% below the test value. A truss analogy approach [8] predicted an ultimate load of 934 kN, some 30% lower than the actual value.

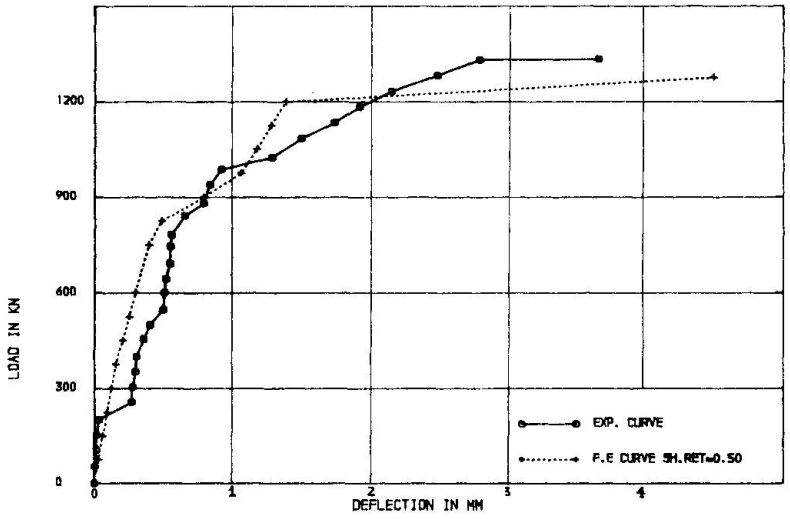

Fig.11 Comparison of experimental and finite element load– displacement curves

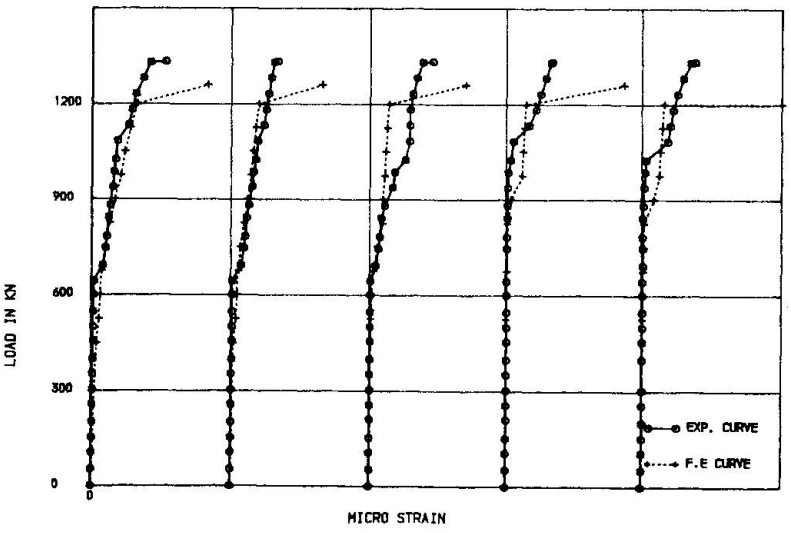

Fig.12 Comparison between experimental and finite element load– steel strain curves

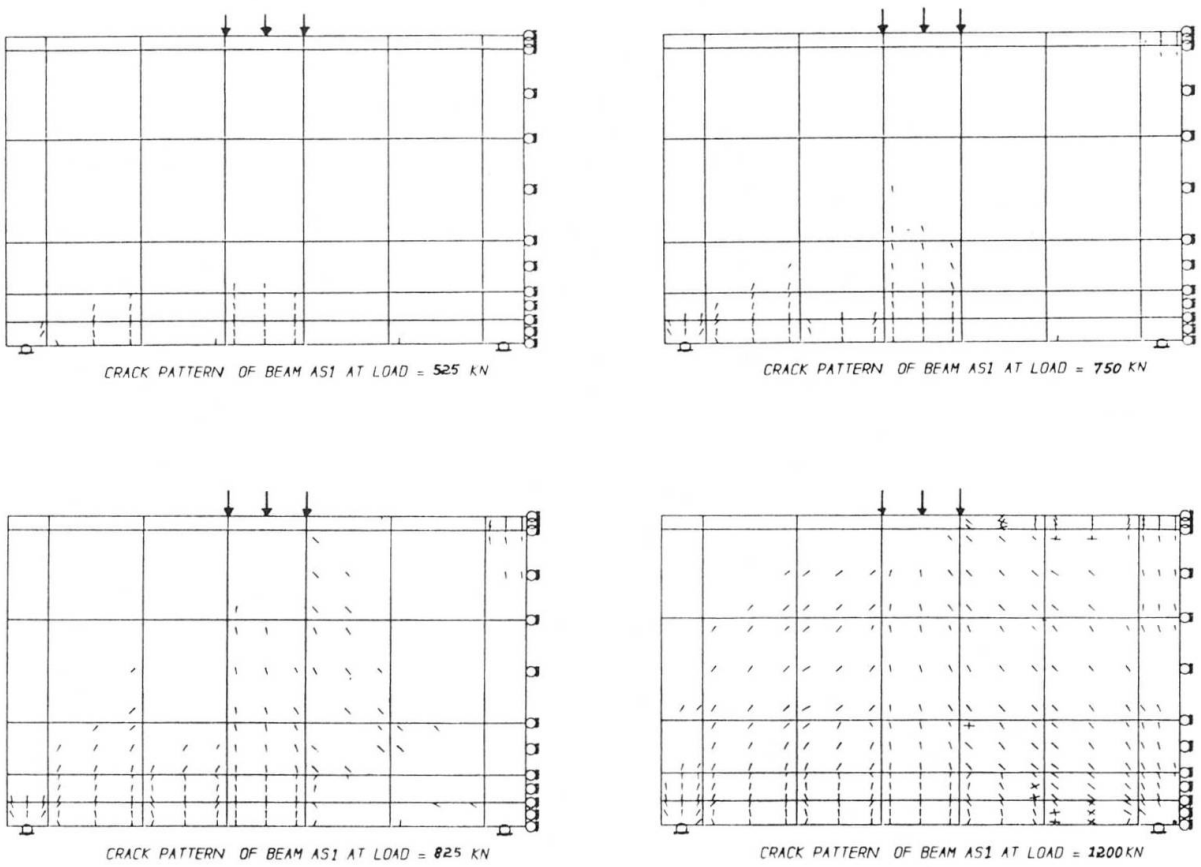

(a) Finite element analysis (1/2 beam)

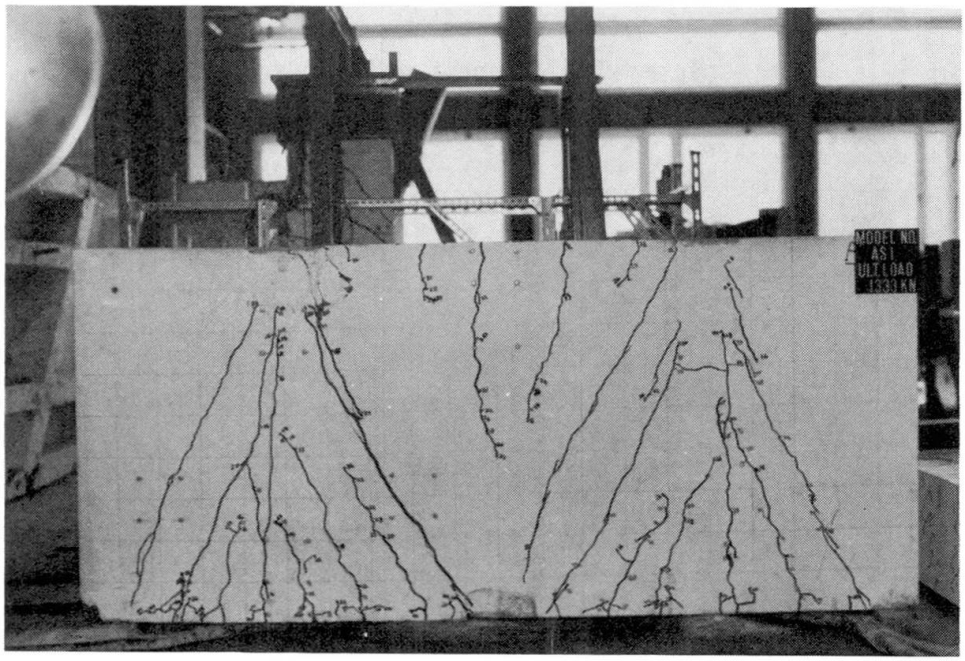

(b) Experimental crack pattern at failure

Fig.13 Crack propagation in the continuous deep beam

6. CONCLUDING REMARKS

By using the elastic stress field produced by a finite element analysis a procedure has been developed whereby reinforcement in continuous deep beams can be directly designed to resist in–plane forces. The serviceability and ultimate load behaviour of the resulting design was verified by a non–linear finite element analysis and by a large scale experimental test.

Other theoretical and experimental work is continuing on designs with different span to depth ratios, and with other features such as skew reinforcement, prestressing and holes within the shear spans [9]. Although the procedure described uses a linear elastic stress field for obtaining the reinforcement ratios, any suitable equilibrium field could be used and studies are also being made using elasto–plastic finite element models with appropriate yield and flow rules.

The non–linear finite element models which have been developed are providing a better appreciation of structural behaviour at various stages of loading which has proved very useful in developing the most effective design procedures. The finite element modelling is being continuously developed and is backed up by separate experimental tests for verifying the models developed and for providing information on material behaviour.

The direct design procedures are being applied to other structural forms, including combined torsion and bending of reinforced and prestressed concrete beams [10], perforated deep beams [11], and reinforced concrete right– and skew–slabs [12],[13]. The method is proving satisfactory in these areas also. Ultimately, the objective of this work is to produce automated techniques which can be used in computer–aided design software.

REFERENCES

1. NIELSEN, M.P. "Yield conditions for reinforced concrete shells in the membrane state". Non–classical shell problems, IASS Symposium, Warsaw, 1963, pp.1030–1038
2. CLARK, L.A. "The provision of tension and compression reinforcement to resist in–plane forces", Mag. Conc.Res., Vol.28, No.94, 1976, pp.3–12
3. ROGOWSKY, D.M. & MACGREGOR, J.G. "Shear strength of deep reinforced concrete continuous beams", Structural Engineering Report No.110, Department of Civil Engineering, University of Alberta, Canada, 1985
4. RICKETTS, D.R. & MACGREGOR, J.G. "Ultimate behaviour of continuous deep reinforced concrete beams", Structural Engineering Report No.126, Department of Civil Engineering, University of Alberta, Canada, 1983
5. CIRIA, "The design of deep beams in reinforced concrete", Guide 2, Construction Industry Research and Information Association, London, 1977
6. PHILLIPS, D.V. "FECON: Nonlinear finite lement programs for structural concrete", FECON Manual, Mark 2, University of Glasgow, 1986
7. PHILLIPS, D.V. & ZIENKIEWICZ, O.C. "Finite element non–linear analysis of concrete structures", Proc.Instit,Civ.Engnrs, Part 2, Vol.61, 1976, pp.59–88
8. KUMAR, P. "Collapse load of deep reinforced concrete beams", Mag.Conc.Research, Vol.28, No.94, 1976, pp.30–36
9. KHASKHELI, G.B. "The direct design of reinforced concrete transfer girders", Ph.D Thesis, University of Glasgow, to be submitted.
10. EBIRERI, J.O. "Direct design of beams under combined bending and torsion", Ph.D. Thesis, University of Glasgow, 1985
11. MEMON, G.H. "Ultimate strength of perforated deep beams", M.Sc. Thesis, University of Glasgow, 1982
12. HAGO, A.W. "Direct design of reinforced concrete slabs", Ph.D. Thesis, University of Glasgow, 1982
13. ABDEL–HAFEZ, L.M. "Direct design of reinforced concrete skew slabs", Ph.D. Thesis, University of Glasgow, 1986